ANKLE MORPHOLOGY: INTERFACE OF GENETICS, ONTOGENY, AND USE

by

KEVIN TURLEY

A DISSERTATION

Presented to the Department of Anthropology
and the Graduate School of the University of Oregon
in partial fulfillment of the requirements
for the degree of
Doctor of Philosophy

June 2013

DISSERTATION APPROVAL PAGE

Student: Kevin Turley

Title: Ankle Morphology: Interface of Genetics, Ontogeny, and Use

This dissertation has been accepted and approved in partial fulfillment of the
requirements for the Doctor of Philosophy degree in the Department of Anthropology by:

Dr. Stephen Frost   Chair
Dr. John Lukacs   Member
Dr. Frances White   Member
Dr. Gregory Retallack   Outside Member

and

Kimberly Andrews Espy   Vice President for Research & Innovation/Dean of the
                           Graduate School

Original approval signatures are on file with the University of Oregon Graduate School.

Degree awarded June 2013

ii

DISSERTATION ABSTRACT

Kevin Turley

Doctor of Philosophy

Department of Anthropology

June 2013

Title: Ankle Morphology: Interface of Genetics, Ontogeny, and Use

A central concept in Evolutionary theory is the character trait. It provides a context in which to explore differences and similarities among taxa, both extant and extinct. It is expanded in scope in Evolutionary Developmental theory to functional units with a biological role, "evolutionarily stable configurations." The talo-crural joint is such a configuration, a highly canalized structural unit in primates forming the interface between organism, and foot and substrate. It is a microcosm in which to examine the relationship of shape with environment and function and the interplay of genetics, ontogeny, and use.

Geometric Morphometric analysis of landmark data was employed in studying the articular surfaces of the talus in a diverse sample of adult specimens in nine catarrhine taxa. The influence of four factors on talar shape was examined: superfamily, a proxy for phylogeny; size and mass, a proxy for physical attributes; and substrate preference, a proxy for behavior. All significantly affected shape, and substrate preference was unrelated to the others. Appositional articular morphology, the shape of the subchondral bone surfaces of the talo-crural joints in an expanded sample of 12 taxa, showed a

significant effect of the four proxies on the tibial and talar components, and substrate preference was weakly related to the other proxies in each. Singular Warp analysis of the cross-covariance matrices of the joints demonstrated sorting of taxa by substrate use and signals of convergent and divergent evolution among hominoids and cercopithecoids in joint shape. The ontogeny of the appositional articular shape was examined using adult and subadult specimens grouped by molar eruption. Singular Warp analysis demonstrated a genetic signal in the subadults, strongest in the slowly maturing African hominoids, and an epigenetic signal across taxa to substrate use in the adults.

The talo-crural joint, a highly canalized, modular, and integrated "evolutionarily stable configuration," provides a model for the study of the evolution of shape. The epigenetic signal observed is consistent with plasticity or developmental plasticity in response to the interaction of the joint complex with the environment due to a behavioral effect, substrate use.

This dissertation includes previously unpublished, co-authored material.

CURRICULUM VITAE

NAME OF AUTHOR: Kevin Turley

GRADUATE AND UNDERGRADUATE SCHOOLS ATTENDED:

University of Oregon, Eugene
University of California, San Francisco
University of South Florida, Tampa
The Ohio State University, Columbus
Medical College of Wisconsin, Milwaukee
Fordham University, New York

DEGREES AWARDED:

Doctor of Philosophy, Anthropology, 2013, University of Oregon
Master of Science, Anthropology, 2008, University of Oregon
Graduate Medical Education, Cardiothoracic Surgery, 1978, University of
    California, San Francisco,
Graduate Medical Education, General Surgery, 1976, University of South Florida
Graduate Medical Education, Surgery, 1973, The Ohio State University
Doctor of Medicine, 1972, Medical College of Wisconsin
Bachelor of Arts, Biology, 1968, Fordham University

AREAS OF SPECIAL INTEREST:

Primate Evolution
Evolutionary Developmental Theory
Human Origins

PROFESSIONAL EXPERIENCE:

Chief Pediatric and Congenital Heart Surgeon, California Pacific Medical
    Center, San Francisco, 1990-2000

Research Staff, Heart Research Institute, Medical Research Institute of San
    Francisco, 1990-2000

Professor of Surgery and Pediatrics, University of California, San Francisco, 1988-1990

Associate Professor of Surgery, University of California, San Francisco, 1984-1988

Assistant Professor of Surgery, University of California, San Francisco, 1979-1984

Instructor in Surgery, University of California, San Francisco, 1978-1979

Fellow, Cardiac Fetal Physiology, Cardiovascular Research Institute, University of California, San Francisco, 1978-1979

GRANTS, AWARDS, AND HONORS:

Luther S. and Dorothy C. Cressman Fellowship, 2012

University of Oregon Department of Anthropology Student Travel Award, 2011

University of Oregon Graduate School Doctoral Student Research Award, 2010

University of Oregon Department of Anthropology Student Travel Award, 2007

University of Oregon Department of Anthropology Student Travel Award, 2006

"Best Heart Doctors in America," Good Housekeeping, March 1996

Consultant, National Institute of Health, Congenital Heart Disease, 1992

US-USSR Symposium, National Institute of Health, 1986

US-USSR Traveling Fellowship, National Institute of Health, 1980

University of California, President's Recognition for Outstanding Research, 1978

PUBLICATIONS:

Turley K, Guthrie EH, Frost SR. 2011. Geometric morphometric analysis of tibial shape and presentation among catarrhine taxa. Anat Rec 294: 217-230.

ACKNOWLEDGMENTS

To my wife, Kerry M. Turley

TABLE OF CONTENTS

LIST OF TABLES

LIST OF FIGURES

CHAPTER I

INTRODUCTION

Chapters II, III, and IV have been submitted for publication and are co-authored by my advisor, Stephen Frost, who provided direction in designing the statistical analysis of the data and the programs used, as well as assistance with the figures. The intellectual content is mine, and I performed all specimen acquisition, processing, and analysis.

Morphology, life's form, reflects evolution (the Bauplan-genome), development (the process-genetic regulatory networks), and environment (the feedback-epigenetic/plasticity; West-Eberhard, 2003; Carroll, 2008; Davidson, 2005).

In this dissertation, I explore the broad evolutionary concepts of homology (related species having similar traits due to their inheritance from a common ancestor), convergent evolution (species with different ancestry having similar traits) and divergent evolution (species with common ancestry with different traits) within the microcosm of ankle joint shape. Genetic, developmental and environmental influences are examined using the comparative method (Hall, 2007; West-Eberhard, 2003). This exploration is set within the theoretical framework of evolutionary developmental theory (Müller, 2005). The terms which define this theoretical framework are critical to understanding the place of the subject of this dissertation, talo-crural joint, within evolutionary developmental theory.

Concepts of Evolutionary Developmental Theory

Central to this theoretical framework is the concept of the character trait. Wagner (2001) defines a character in this way: "biological character can be thought of as a part of

an organism that exhibits coherence and [has] a well defined identity and plays a (causal) role in some biological processes."

Within the context of this definition, such characters are important as the subject of adaptation since they interact with the environment and respond to adaptive challenges (Wagner, 2001). Schwenk (2001) contends that these should be viewed as character complexes rather than the "atomistic individual characters" or the "structuralist's interactions" within the Bauplan.

Since character complexes are interrelated, they fit within the definition of biological role proposed by Bock and von Wahlert (1965): the actual ways that an organism uses a character throughout its life history. Schwenk takes this definition further to include structural units that are morphological units, mechanical units that have the properties of character complexes, as well as structural units and evolutionarily stable configurations, which are character complexes, that are both structural and mechanical units.

This last idea is central to this dissertation's approach to the joint complex, whose coordinated function is intimately related to shape. Schwenk (2001) points out those units embody an evolutionary paradox providing evolutionary stability, but through those interactions, variation, which provides for evolvability.

The evolutionary developmental theory of macroevolution and the phenotypic expression of the adult form pose a number of important ideas. These define the landscape the framework explores. The genotype results from natural selection and the effect of microevolutionary processes on the organism. Canalization, as defined by

Hallgrimsson et al. (2002), is the tendency for development of a specific genotype to follow the same trajectory despite different conditions, such as environmental change. They define developmental stability as the tendency for development of a specific genotype to follow the same trajectory under the same conditions (Hallgrimsson et al., 2002).

Modularity is defined by Wagner as the concept that phenotypes are composed of many hierarchal and semi-independent units, organismal parts with local and independent (dissociated) genetic and developmental control (Wagner, 2001). As observed above, it is a prerequisite to evolvability and adaptation. The phenotype of a module can be modified during the course of evolution without producing major side effects to other modules, and within this context, increasing the chance of adaptation. By separating developmental control, functionally unrelated systems may have an increased potential to evolve along separate pathways. Conversely, an integrated system for the module itself will allow for the evolution of functionally dependent traits. Modules can be identified among skeletal elements from developmental sequence data with events such as development of ossification centers proceeding in a specific order in a module (Blomquist, 2009; Poe, 2004).

Morphological integration is defined by Hallgrimsson et al. (2002) as the tendency for structures to show correlated variation because they develop in response to shared developmental processes or function in concert with other structures.

Blomquist (2009) observes that such integration among modules, and complimentary disassociation of structures between them, creates "paths of least resistance" along which size and size-related variation tend to evolve (Blomquist, 2009).

Heterochrony is the theory that, during evolution, changes can occur to the relative timing and rates of developmental processes due to changes in the regulation of developmental pathways. These changes have been demonstrated to be associated with different life history strategy and changes in genotype (Müller, 2005).

Plasticity is the property of responding to use with a permanent change in form. This differs from elasticity, which is a temporary response, because plastic changes remain despite a change in the precipitating factor (Schaeffer and Bookstein, 2009). Plasticity is closely related to environmental variances and fluctuating asymmetries, which are deviations in symmetry among individuals and within populations (Hallgrimsson et al., 2002). Of relevance to this study is that fluctuating asymmetry has also been shown to increase distally in primate limbs (Hallgrimsson et al., 2002). Young and Hallgrimsson (2005) have shown that constraints imposed by covariance are reduced in nonquadruped species, allowing divergence in structure correlated with function (i.e., hind limb), and more distally on the extremity.

Phenotypic plasticity, which Pigliucci (2001) defines as a developmental process in which the reaction norms that we usually measure in the adult stage at reproductive maturity are, in fact, the result of the positive feedback between environment and genes throughout ontogeny of an organism. West-Eberhard (2003) expands this concept to the ability of an organism to react to an environmental input with a change in form state,

4

movement or rate of activity. This is synonymous with developmental plasticity. It is observed to be present in the response of bone to "condition sensitivity" molding bone shape.

Finally, epigenetics in its broadest sense refers to those factors that together produce a phenotype, including genetics, development and environmental influences (West-Eberhard, 2003).

Talo-Crural or Upper Ankle Joint

The talo-crural joint was chosen for this study because it is an evolutionarily stable configuration, which is a highly canalized character trait reflecting modularity and integration at the ankle. It is the interface between organism and substrate, and a lens for observing both epigenetic variation and plasticity of form due to differences in biological morphology.

The structural morphology of the adult talo-crural joint is the result of complex sequencing of limb bud ontogenic gene activity (Hox, Shh and Wnt gene), transcription factors, and regulatory sequences (Carroll, 2008; Chiang et al., 2001; Dobbs et al., 2006; Hornstein, 2005; Kmita et al., 2002; Wagner, 2001; Zakany et al., 2004). These result in specific surface shapes. These shapes are formed at the ankle at the interface of two modules, the zeugopodium proximally, and the autopodium distally (Cachel, 2006). They are the result of integration, which in the ankle is manifest by a complex pattern of correlation and covariance that demonstrates a lack of independence among variables at the appositional articular surface (Mitteroecker and Bookstein, 2007; Wagner, 2001). The ankle is the region of greatest developmental modularity in the postcranium, as defined by

5

co-evolving regions of ossification centers (Blomquist, 2009; Mitteroecker, 2009; Mitteroecker and Bookstein, 2008; Poe, 2004). Variation in presentation and articular morphology in the adult reflect natural selection for this genetically canalized state, the response of the organism to ontogenetic signaling, the biomechanical stresses encountered during ontogeny, and mechanical or developmental plasticity in response to the environment (Anapol et al., 2004; Baker, 2005; Chiu and Hamrick, 2002; Gilbert, 2000; Hallgrimsson et al., 2002; Pearson and Lieberman, 2004; Schaefer and Bookstein, 2009; Scheuer, 2004; West-Eberhard, 2003; Young and Hallgrimsson, 2005). All these factors may produce the end-point morphology encountered in the individual (Hall, 2007; Jonsson et al., 1984; Jungers, 1988; Lieberman et al., 2001; Lovejoy et al., 2000; Pearson and Lieberman, 2004; Ruff, 1988). Variation in this end-point morphology allows for the differences in functional morphology of this joint complex among taxa, as well as their phylogenetic histories, physical attributes, modes of locomotion, and substrate preferences (Hall, 2005; Lieberman et al., 2001; Lovejoy et al., 2000; Pearson and Lieberman, 2004; Turley et al., 2011). Finally, the anatomy of the talo-crural joint and its appositional articular morphology form the interface between the proximal organism and the distal foot and substrate, as well as an interface between the organism's phylogeny, physical attributes and habitat.

The talo-crural or upper ankle joint is classically described as a mortise and tenon joint with tibial plafond (trochlear and medial malleolar facets) and fibular facet forming the mortise, or malleolar fork, holding the three sides of the proximal talus (trochlear, medial and lateral facets) to the tenon (Fig. 1). The synovial membrane with synovial
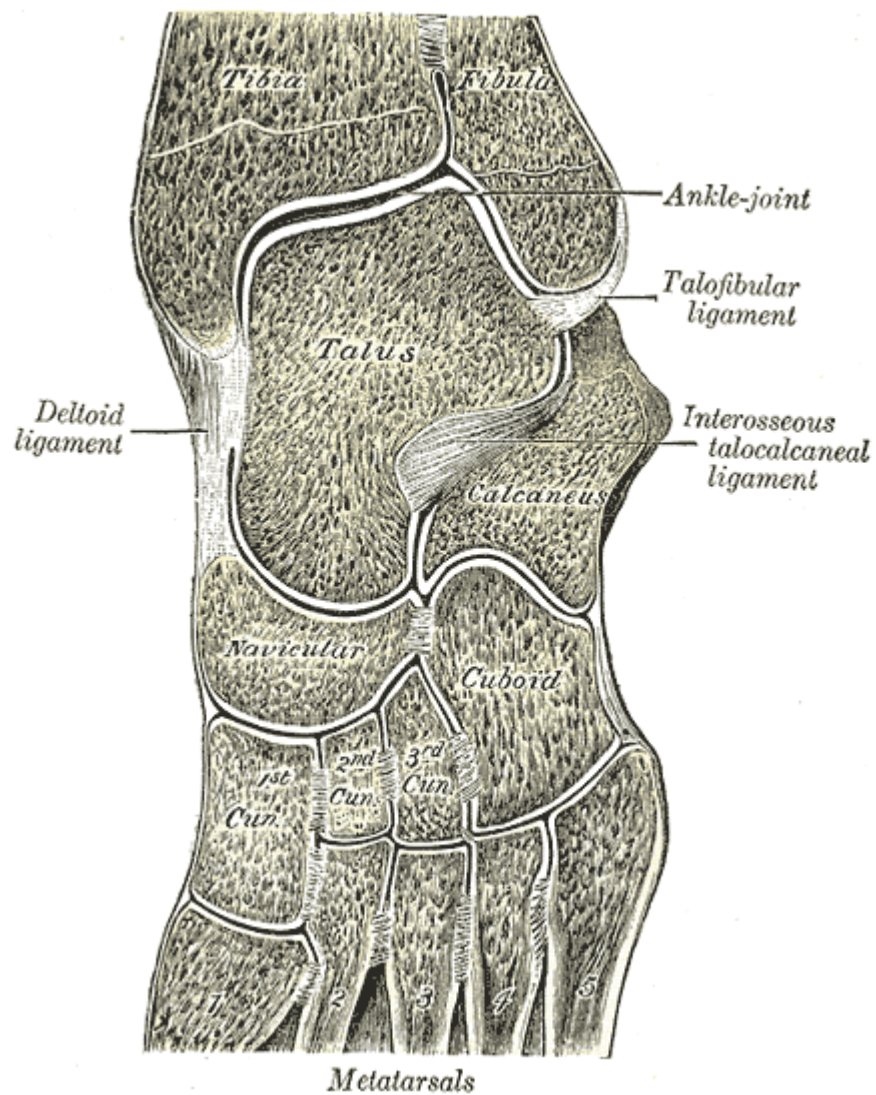
FIGURE 1. Talo-crural joint anatomy demonstrating the mortise and tenon, tibial/fibular "fork" and talus. Downloaded 5-28-2013 from Wikimedia, *Gray's Anatomy*, 20th ed., non-copyright Public Domain.

fluid is contained within the fibrous capsule, and articular cartilage covers the articular surfaces, with the joint supported by medial (deltoid) ligament and lateral ligaments. The distal tibiofibular ligament binds the distal tibia and fibula, although motion between them is possible.

The distal end of the tibia has five surfaces, the inferior surface or plafond with trochlear and medial malleolar facets, anterior, posterior and lateral margins, and the medial surface with the medial malleolus as an extension. The inferior surface forms the frustum of a cone, with an average medial conical angle of 22 degrees +/- 4 degrees in humans, and a range of 0 to 35 degrees (Sarrafian and Kelikian, 2011). An angle of 0 degrees would correspond to a cylinder. The tibial trochlear facet covers two-thirds of the talar trochlear surface in any position, with one-third exposed in humans. The medial malleolus has two segments or colliculi with the anterior and posterior separated by the intercollicular groove formed by the insertion site of the deltoid ligament. The posterior border of the medial malleolus is the groove formed by the fibrous tunnel of the tendon of tibialis posterior. The long axis of the ankle mortise is rotated 23 degrees laterally to the transverse axis of the tibial plafond (tibial torsion) (Sarrafian and Kelikian, 2011).

The talus lies between the malleolar fork and the tarsal bones. It has no tendon or muscular component, only the ligamentous attachments to tibia and tarsal bones. The talus is divided into three components: the body or *corpus tali*, the neck or *collum tali*, and the head or *caput tali*. The body is the component located behind an imaginary plane passing through the anterior border of the trochlea posterior to the calcaneal surface. The neck is the component anterior to this plane, but between the body and the head. The head is the articular surface covering the neck and is rotated on its longitudinal axis while relative to the body (Sarrafian and Kelikian, 2011).

Multiple measurements and angles have been devised to provide information as to talar shape. The angle of declination of the talar neck relative to the body is the angle

between the long axis of the neck and the long axis of the body. In humans it ranges from 10 to 44 degrees with an average of 24 degrees. The angle of inclination of the talar neck relative to the body is formed by a line from the apex of the navicular articular surface of the head to a line perpendicular to a line centering on the lateral trochlear arc. In humans a maximum of 50 degrees, minimum of 5 degrees, and average of 24 degrees are observed. The length is determined by a line joining the apex of the navicular surface to the flexor hallucis longus groove and the width from the middle of the medial trochlear line to the tip of the lateral process with maximum 60, minimum 40, and average 48 mm in the former, and maximum 45, minimum 30, average 37 mm in the latter in humans. The angle of lateral projection of the lateral process yields values of maximum 55 degrees, minimum 15 degrees, and average 32 degrees. The angle of inclination of the sulcus of the flexor hallucis longus tendon ranges from maximum 85 degrees, minimum 55 degrees, average 68 degrees, and the angle formed by the long axis of the posterior calcaneal facet and a line parallel to the anterior trochlear border, a maximum 50 degrees, minimum 26 degrees, average 37 degrees. The length of the talar neck is determined from the midpoint of an imaginary line, across the anterior trochlea and the midpoint where the articular surface is encountered on the navicular facet, a maximum 23 mm, minimum 12 mm and average 17 mm. Finally, the angle of rotation of the talar head is described by a line parallel to the trochlear surface and one parallel to the long axis of the head. It is maximum 65 degrees, minimum 30 degrees, with an average of 49 degrees in humans (Sarrafian and Kelikian, 2011).

The number and complexity of such measurements and the variation observed in a single species (*Homo sapiens*) is compounded when comparisons are undertaken across multiple taxa (Aiello and Dean, 2002; Gebo, 1992; Latimer et al., 1987; Lisowski, 1967; Lisowski et al., 1974; Lisowski et al., 1976) or applied to fossil taxa, as in the case of *Homo habilis* OH 8 (Day and Wood, 1968; Harcourt-Smith and Aiello, 2004; Kidd et al., 1996; Lisowski et al., 1974; Lisowski et al., 1976; Oxnard, 1972).

Issues of size and scaling confounded prior examinations of the talo-crural joint complex using standard measurements and angles, which fail to appreciate important components of appositional articular shape due to examination limited to the proximal and distal bones (DeSilva, 2009).

In this dissertation, landmarks are placed on digitally reconstructed laser scans of the articular surfaces of specimens. Geometric morphometrics, the statistical analysis of form based on Cartesian landmark coordinates, is used. After separating shape from overall size, position, and orientation of the landmark configurations, the Procrustes shape coordinates that result are used for statistical analysis. Geometric morphometrics has been used to study integration (singular warps analysis), modularity, and plasticity in prior osteological studies (Baab et al., 2012; Bookstein et al., 2003; Frelat and Mitteroecker, 2011; Mitteroecker and Bookstein, 2007, Mitteroecker and Bookstein, 2008; Schaefer and Bookstein, 2009).

Kendall's shape space, the mathematical space induced by the shape coordinates, is a metric space that can be approximated locally by a Euclidean tangent space. The differences between Kendall's shape space, GPA space ("Slice's shape space"), and

tangent space are outlined by Baab et al. (2012), with Kendall's space a spherical surface, GPA space a hemisphere, and Euclidean tangent space a plane. Procrustes distances, differences in shape, in Kendall's space are the angle (p), in radians, while in GPA (between specimens and mean) it is the Procrustes chord distance (Δ). Projections from Kendall's space to Euclidean tangent space result in a "shape distance which is a simple Euclidean distance (d)" (Baab et al., 2012). Using these techniques' similarities and differences between shapes can be assessed. The results of statistical techniques such as Relative Warp analysis, multivariate regression and Singular Warps analysis can be visualized as actual shapes or shape deformation. These visualization tools allow for identification and quantification of previously unknown shape features (Mitteroecker and Gunz, 2009; Turley et al., 2011).

Statistical analysis also allowed the assessment of the relationship between factors studied, such as superfamily, size, mass and substrate preference, and the relatedness of species.

Superfamily was used in this dissertation as a proxy for phylogeny, size and mass as a proxy for physical attributes, and substrate preference as a proxy for behavior. These same four factors were examined in our prior study of tibial shape (Turley et al., 2011). In that study, substrate preference was observed to be largely unrelated to the proxies for phylogeny and physical attributes and was an important factor in the variability of the distal tibia. In the current dissertation, the whole talus, the appositional articular morphology (tibial plafond plus talar trochlear, medial and lateral facets) of the talo-crural joint itself and the ontogeny of that appositional articular morphology are

11

examined. The appositional articular morphology corresponds to the subchondral bone

surfaces of the cleaned osteological specimens. The taxa, as in the original tibial study,

are obtained from osteological collections where noninvasive laser scanning of the

specimen was performed and the specimens were digitally reconstructed for landmark

placement (see Acknowledgements for specific institutions). The ontogenetic series were

constructed using dental eruption of the first and second molars in subadults and third

molar in adults.

These are the objectives of the dissertation and questions examined:

1. Identify the adult morphology of the talus among the taxa studied and the

relation of shape to superfamily, size and mass, and substrate as proxies for phylogeny,

physical attributes, and behavior. What is the effect of the factors studied on whole talar

shape, as well as proximal and distal talar shape, and is substrate preference unrelated to

the other factors studied as observed in the distal tibia? These are the subjects of Chapter

II.

2. Identify the adult appositional articular morphology among taxa studied,

evidence of integration, and the relation of shape to superfamily, size and mass, and

substrate preference. What is the effect of the factors on the appositional articular

morphology of the joint's subchondral surfaces and is substrate preference unrelated to

the other factors studied? These are the subjects of Chapter III.

3. Identify if subadult appositional articular subchondral morphology is consistent

with adult appositional articular subchondral morphology, suggesting a genetically

programmed effect, or does it suggest an epigenetic effect? Identify the relationship of the

proxies for phylogeny, physical attributes and behavior to adult appositional articular subchondral shape, and if shape does change from subadult to adult, does substrate preference influence the ontogeny of appositional articular subchondral shape, demonstrating an epigenetic behavioral effect and evidence of plasticity? These are the subjects of Chapter IV.

Null hypotheses tested:

H-1: Adult talar shape is not related to superfamily, size, mass, or substrate preference.

H-2: If H-1 is rejected, all factors are strongly correlated with each other.

These are the subjects of Chapter II.

H-3: Adult appositional articular morphology is not related to superfamily, size, mass, and substrate preference.

H-4: If H-3 is rejected, adult appositional articular morphology is not related to any specific factor studied.

These are the subjects of Chapter III.

H-5: Subadult appositional articular shape is the same as the adult appositional articular shape.

H-6: If H-5 is rejected, change in appositional articular shape is not related to any specific factor studied.

These are the subjects of Chapter IV.

Criteria for rejecting the null hypothesis:

H-1: Will be rejected if adult talar shape has a significant relationship to the factors studied ($p < 0.05$). Relative importance equated to percent variance in the total sample.

H-2: Will be rejected if any factor is weakly related to the other factors (angular difference of the vectors > 40 degrees).

H-3: Will be rejected if adult appositional articular morphology has a significant relationship to the factors studied ($p < 0.05$). Relevant importance equated to percent variance of the total sample.

H-4: Will be rejected if adult appositional morphology is related to any specific factor studied.

H-5: Will be rejected if adult and subadult joint shapes are not identical.

H-6: Will be rejected if shape differences are related to any specific factor studied.

Chapter II will examine the talus, the shape of its articular surfaces and hypotheses H1 and H2.

CHAPTER II

THE SHAPE AND PRESENTATION OF THE CATARRHINE TALUS

This chapter has been submitted for publication and is co-authored by my advisor Stephen Frost, who provided direction in designing the statistical analysis of the data and the programs used, as well as assistance with the figures. The intellectual content is mine, and I performed all specimen acquisition, processing, and analysis.

The talo-crural joint is the structural unit at the interface of substrate (the foot) and organism (Langdon, 1986; Lewis, 1989: Schwenk, 2001). It is a highly conserved trait among Catarrhine taxa, but variation in its morphology provides for differences in joint function among taxa in both extant and fossil assemblages (Hall, 1998; Langdon, 1986; Lieberman et al., 2001; Schwenk, 2001; Turley et al., 2011; Vancata, 1991). It is characterized by three components, the tibia with its presentation, the joint surface configuration or appositional articular morphology, and the talus with its presentation. Presentation is defined as "the joint surfaces orientation in space relative to the substrate and the organism proper" (Turley et al., 2011). Presentation is differentiated from alignment by independence of adjacent structures, except to constrain their potential shape. In the case of the talo-crural joint, presentation of the proximal and distal bones, the tibia and talus respectively, constrain appositional articular variation influencing joint functional morphology (Turley et al., 2011).

In this the second in a series of papers examining the talo-crural joint, the presentation of the distal component of the talo-crural joint, the talus, is explored. It includes talar shape and angulation, and the plane and shape of its proximal (the trochlea,

15

medial and lateral facets), as well as the orientation and shape of its distal (posterior

calcaneal and navicular facets) surfaces. These are described in relation to the upper ankle

joint interface rather than standard anatomical nomenclature. The end-point morphology

encountered among the taxa examined reflect multiple factors related to the joint's

biological role (sensu Bock and von Wahlert, 1965), including phylogeny, physical

attributes, and behavior, which have been related to articular shape (Hall, 2005;

Lieberman et al., 2001; Lovejoy et al., 2000; Pearson and Lieberman, 2004; Turley et al.,

2011). The influence of each on shape and their interdependence were assessed in the

current study (Hall, 2005; Lieberman et al., 2001; Lovejoy et al., 2000; Pearson and

Lieberman, 2004; Turley et al., 2011).

Geometric morphometric analysis was used to examine the differences in talar

shape among catarrhine taxa, avoiding the drawbacks of metric analysis (Aiello and

Dean, 2002; DeSilva, 2009; Gebo and Schwartz, 2006; Jungers, 1988; Latimer et al.,

1987; Turley et al., 2011). It explored the relationship of those differences in the same

factors studied in the tibia which relate to the biological role of the joint, superfamily

(hominoid and cercopithecoid), a proxy for phylogeny, body mass and size, proxies for

physical attributes, and substrate preference (terrestrial and arboreal), a proxy for

behavior. These gross categories provided a lens, as in the tibia, to assess their influence

on talar shape and presentation, as well as both their interrelation and lack thereof.

Likewise, an evolutionary and developmental (Evo-Devo) influence, an epigenetic or

genetic signal, may be evidenced, if a behavioral effect is observed in talo-crural form

(Müller, 2005; Turley et al., 2011). Finally, the differences and similarities of talar shape among the individual taxa are documented (Harcourt-Smith, 2002; Turley et al., 2011).

Materials and Methods

Sample

The tali of 219 specimens from 9 catarrhine taxa formed the study sample. All were adult, without pathology, and among the nonhuman specimens, wild-shot with provenience documented. The 65 human specimens derived from six populations: 16 European American (19th century), 13 African American (19th century), 10 Inuit (19th century), 7 Egyptian (4th century), 6 Southwest Paleoamericans, and 13 California Paleoamericans. Nonhuman primate specimens included 123 Apes and 31 Old World monkeys (see acknowledgements for specific institutions) (Table 1). The latter were chosen to represent both subfamilies (Xing et al., 2007) with a range in size and substrate use to the extent possible. Estimated mass and substrate preference for males and females of each taxon were obtained from the literature (Auger et al., 1980; Delson et al., 2000a; Fleagle, 1999; Katzmarzyk and Leonard, 1998; Kraus, 1961; Smith and Jungers, 1997). Substrate preference was estimated from 0 (most arboreal) to 10 (most terrestrial) (Table 1).

Data Collection

Laser surface scans were made from each specimen using a Konica Minolta Vivid 910 Noncontact 3-D Digitizer and were processed using Geomagic Studio 8 software. Thirty landmarks were collected by one observer (KT) using Landmark Editor software (Wiley, 2006). These covered the proximal and distal articular surfaces (Fig. 2). The

template included the 29 landmarks described by Harcourt-Smith plus a 30th, number 14,

the most proximal point on the lateral malleolar facet edge (Harcourt-Smith, 2002) (Table

2). Nine were Type II landmarks and 21 were Type III landmarks (Table 2) chosen to

TABLE 1. Number of Specimens in Each Taxon Included in This Analysis,
Along with Their Sex, Mass and Substrate Preference

Taxon	N	M	F	Mass (kg) M / F	Substrate (0-10) M / F
Homo sapiens	65	36	26	59.3 / 53.2	9.99/9.99
Pan troglodytes	57	27	28	56.6 / 44.0	4 / 3
Gorilla spp.	45	27	11	169.8 / 73.5	7 / 4
Pongo spp.	15	8	7	78.1 / 35.7	2 / 0.2
Hylobatidae	6	1	4	8.6 / 8.0	0.1/ 0.1
Macaca fascicularis	5	2	1	5.3 / 3.6	1 / 1
Macaca thibetana	9	7	1	15.2 / 9.5	8 / 8
Papio hamadryas	12	5	5	25.1 / 13.3	9 / 9
Nasalis larvatus	5	3	2	20.4 / 9.8	0.1/ 0.1

Mass values obtained from Delson et al. (2000a) and Smith and Jungers (1997). Substrate
preference obtained from Fleagle (1999).

reflect both function and the overall size of the bone (Bookstein, 1991; Harcourt-Smith,

2002; Turley et al., 2009). Three landmark subsets were used: the whole talus, proximal

talar facets (trochlea, medial and lateral facets), and distal talar facets (proximal calcaneal

and navicular facet). Separate analyses were performed on each subset to determine shape

differences in each region without the confounding effects of the whole talar morphology.

One specimen of *Homo sapiens* was landmarked ten times in order to evaluate

observational error. The 90 individual landmark coordinates demonstrated an average

standard deviation of 0.4 mm (range 0-1.5 mm, with 88 coordinates < 0.08 mm). The

18

distance from the centroid to each of the 30 landmarks had a standard deviation of 0.48

mm (range 0.20-0.76 mm). Principal Components Analysis revealed tight clustering of

these repeated measures compared to variation within and among taxa used in this

analysis. Since this study focused on variation above the species level, precision was

deemed satisfactory.
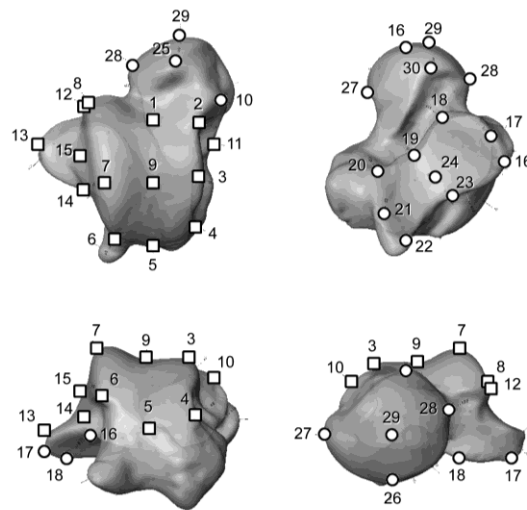
FIGURE 2. Thirty landmarks on the talus articular surfaces, 15 on the proximal facets □, and 15 on the distal facets ○, used in this study illustrated using a talus of male *Pan troglodytes*. The talus is visualized in a dorsal, plantar, anterior and posterior view (clockwise from upper left) (White and Folkens, 2000). *Caput tali* landmarks 25-30, *corpus tali* including the articular surfaces including landmarks 1-24, *collum tali* between 1-2, and 25-28 dorsal and 18 and 30 plantar, trochlea 1-8, medial facet 2, 3, 3, 10 and 11, lateral facet 6, 7, 8, 12, 13 and 14, and calcaneal facet 19-23.

Generalized Procrustes Analysis

Generalized Procrustes Analysis (GPA) was performed using *Morpheus* (Slice,

1998). GPA superimposes landmark configurations and removes variance due to position

and rotation, and scales each to unit centroid size (Rohlf and Slice, 1990). Centroid size is

19

the square root of the sum of the squared distances of each landmark to the centroid

(Rohlf and Slice, 1990) and is stored as a separate variable during GPA. Centroid size

TABLE 2. Landmarks Used in This Study

No.	Type	Description
1	III	Most distal point of the trochlear groove
2	II	Most distal point of contact between the medial malleolar facet and the trochlear surface
3	III	Most dorsal point on the medial malleolar facet margin
4	II	Most proximal point of contact between the medial malleolar facet and the trochlear surface
5	III	Most proximal point of the trochlear groove
6	II	Most proximal point of contact between the lateral malleolar facet and the trochlear surface
7	III	Most dorsal point on the lateral facet margin
8	II	Most distal point of contact between the lateral malleolar facet and the trochlear surface
9	III	Most dorsal point on the trochlear groove
10	III	Most distal point on the medial malleolar facet
11	III	Most plantar point on the medial malleolar facet
12	III	Most distal point on the lateral malleolar facet
13	II	Most plantar point on the lateral malleolar facet
14	III	Most proximal point of the base of the lateral malleolar facet
15	III	Deepest (most medial) point on the lateral malleolar facet
16	III	Most disto-lateral point on the proximal calcaneal facet
17	III	Most lateral point on the proximal calcaneal facet
18	III	Most proximo-lateral point on the proximal calcaneal facet
19	II	Deepest (most dorsal) point on the proximal facet margin
20	II	Most proximo-medial point on the proximal calcaneal facet
21	III	Most medial point on the proximal calcaneal facet
22	II	Most disto-medial point on the proximal calcaneal facet
23	III	Deepest (most dorsal) point on the distal facet margin of the proximal calcaneal facet
24	III	Deepest (most dorsal) point on the proximal calcaneal facet
25	III	Most dorsal point on the head/navicular facet
26	III	Most plantar point on the head/navicular facet
27	III	Most medial point on the head/navicular facet
28	III	Most lateral point on the head/navicular facet
29	III	Most distal point on the head/navicular facet
30	II	Most lateral point of contact between the head/navicular facet and the distal calcaneal facet

was transformed to its natural logarithm for subsequent analysis. GPA was done with reflection allowed, since our data set included both the right and left specimens. Separate GPAs were performed for each of the three landmark subsets. All subsequent statistical analyses were performed using SAS 9.1 (SAS, 2006). As GPA-aligned coordinates have a very high correspondence with their Euclidean tangent space projections, unprojected aligned coordinates were used. Shape differences among landmark configurations were measured by Procrustes distance, the Pythagorean distance between the two Procrustes superimposed landmark configurations (Bookstein, 1991; Turley et al., 2011).

Principal Component Analysis

Principal component analysis (PCA) was performed on the covariance matrix of the GPA-superimposed landmark coordinates as a data reduction and exploration technique (Neff and Marcus, 1980). Initial visualization of the effect on shape described by each Principal Component (PC), both within and among superfamilies, was performed using *Morphologika* software (O'Higgins, 2006; O'Higgins and Jones, 1998).

Permutation Test

Differences in shape between individual taxa were assessed using pair-wise permutation tests with 1,000 replicates performed for each landmark subset. Individuals, with equal random samples drawn, were randomly permuted across the two taxa and Procrustes distance was calculated between the permuted groups' means. The α was the fraction of permuted values that were greater than the actual Procrustes distance between group means (Good, 2000). Results were reported with a Bonferroni-adjusted significance level of $p < 0.002$ (Turley et al., 2011).

Regression Analysis

The relationship between shape and the different variables was assessed using multivariate regression analysis (Bookstein, 1996b; Frost et al., 2003). Substrate preference, body mass, log centroid size, and superfamily (Hominoidea and Cercopithecoidea) were used as independent variables and GPA-aligned coordinates as dependent variables.

The proportion of the total variance accounted for by each independent variable (mass, log centroid size, superfamily, and substrate preference) was calculated for each of the subsets by subtracting the residual variance after regression from the total variance and dividing the difference by the total variance (multivariate multiple regressions) (Frost et al., 2003). The sample size did not allow for a robust test of the interaction of all four variables together, or combinations of three. However, pair-wise analysis of the interactions among all four variables was possible. The angles among the shape vectors for each factor were calculated as the arccosine of their vector correlation (dot product) to evaluate the closeness of the relationship among the independent variables (Cobb and O'Higgins, 2004). Relatively parallel angulation (0°-30°) demonstrated a strong correlation, the closer to 0°, the tighter the relation, while relatively orthogonal angulation (60°-90°) demonstrated a weak relation, the closer to 90°, the less related (Turley et al., 2011).

Visualization

Visualization of shape differences was accomplished by comparing landmark configurations directly in *Morpheus* and by warping an exemplar surface to fit those

landmark configurations using *Landmark Editor*. Mean landmark configurations were

computed for each taxon. Shape differences associated with substrate preference, mass,

log centroid size, and superfamily were visualized by adding the vector of regression

coefficients from multivariate regression to the consensus landmark configuration for

each of the landmark subsets. Features used in the resulting descriptions are explained in

Table 3.

TABLE 3. Aspects of Talar Shape Examined in Each Data Set

Whole Talus Data Set

- Relative height, width, and length
- Plane of trochlea (Aiello and Dean, 2002)
- Horizontal angle (Aiello and Dean, 2002)
- Neck length (Landmark 1 to 24)
- Relative distances between the three components proximal facets, head and calcaneal facet

Proximal Facets Data Set

- Trochlea shape
- Central groove relative depth
- Anterior trochlear margin (plane and lateral to medial shape)
- Posterior trochlear margin (plane and lateral to medial shape)
- Medial trochlear margin shape
- Lateral trochlear margin shape
- Medial crest angle, shape and position of the apex
- Lateral crest angle, shape and position of the apex

Distal Facets Data Set

- Relative head size, shape and convexity (subtalar axis) (Aiello and Dean, 2002)
- Relative posterior calcaneal facet shape depth and concavity (talo-navicular axis) (Aiello and Dean, 2002)
- Proximal calcaneal facet distal, medial, proximal and lateral shape, and relative length
- Proximal calcaneal facet relative orientation

Results

Principal Component Analysis

Table 4 shows the eigenvalues of the principal components 1 to 5 in each subset. A scatter plot of PC1-PC2 of the whole talus sample demonstrates separation of the nine taxa studied (Fig. 3). Analysis of the mean male and female values for each taxon was consistent with the analysis of the individual values. Talus log centroid size and substrate preference correlation coefficients with PC-1 were ($r = 0.71$) and ($r = 0.70$), respectively. PC-1 reflected differences in length, width and height, neck length, horizontal angle, head

TABLE 4. The First Five Eigenvalues of the Covariance Matrix on Procrustes Aligned Coordinates for Principal Component Analyses on the Three Different Data Sets with the Proportion and the Cumulative Values of the Total Variance Provided

	Rank	Eigenvalue	Proportion	Cumulative
Whole Talus Data Set				
	1	0.00579342	0.2153	0.2153
	2	0.00247613	0.0920	0.3073
	3	0.00194976	0.0725	0.3797
	4	0.00177248	0.0659	0.4456
	5	0.00123816	0.0460	0.4916
Proximal Talus Data Set				
	1	0.00466378	0.1826	0.1826
	2	0.00317782	0.1244	0.3070
	3	0.00271988	0.1065	0.4135
	4	0.00238939	0.0935	0.5070
	5	0.00166666	0.0653	0.5723
	1	0.00466378	0.1826	0.1826
Distal Talus Data Set				
	1	0.00537270	0.2380	0.2380
	2	0.00295568	0.1309	0.3689
	3	0.00210629	0.0933	0.4622
	4	0.00146706	0.0650	0.5272
	5	0.00135145	0.0599	0.5871

size, and posterior calcaneal facet size and concavity, while PC-2 reflected trochlea

shape, medial and lateral crest shape and apical displacement, and medial and lateral facet

size. PC-1 of the proximal talar data set reflected trochlea facet shape (rectangular to

wedge to square) and plane, while PC-2 reflected medial and lateral crest angle, shape

and apex position (symmetrical and central to distally displaced), and medial and lateral

facet size. Finally, PC-1 of the distal talar data set reflected the size of the head and

calcaneal facets, while PC-2 reflected rotation of the distal calcaneal facet medially and

laterally.
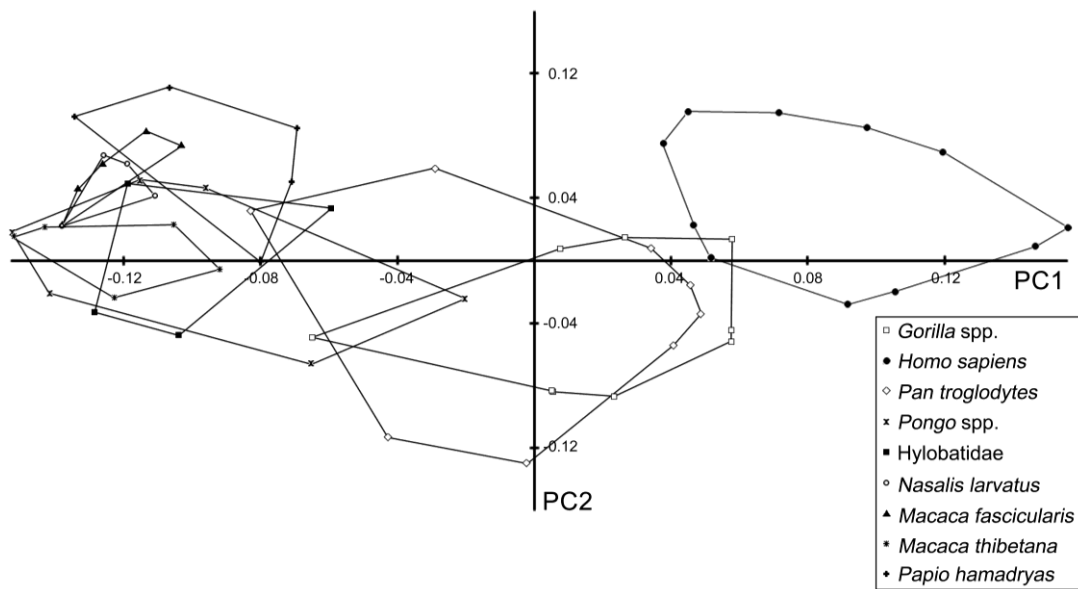
FIGURE 3. Scatter plot showing principal component scores for individual tali based on PCA of Procrustes aligned coordinates, with PC1 on the X-axis and PC 2 on the Y-axis. Convex polygons are used to show the range of scatter with individual points hidden for clarity.

Linear regression with scores from first principal component of the talus data and

log talar size demonstrated separation among the constituent individuals (Fig. 4). *Gorilla*

25

and *Homo* clustered demonstrating the greatest log centroid size, and *Pan* and *Pongo*

clustering below (Fig. 4).

Table 4 provides the percent variance of principal components 1-5 of the three

subsets, talus 49%, proximal 57%, and distal 59%.

Shape Effects Due to Biological Role

In this study we observed that all four factors had a significant effect on shape

($p <$ 0.0001). Percent variance for the whole talar subset was 12.5%, 12.3%, and 10.3%

for substrate preference, log centroid size and superfamily, respectively (Table 5).
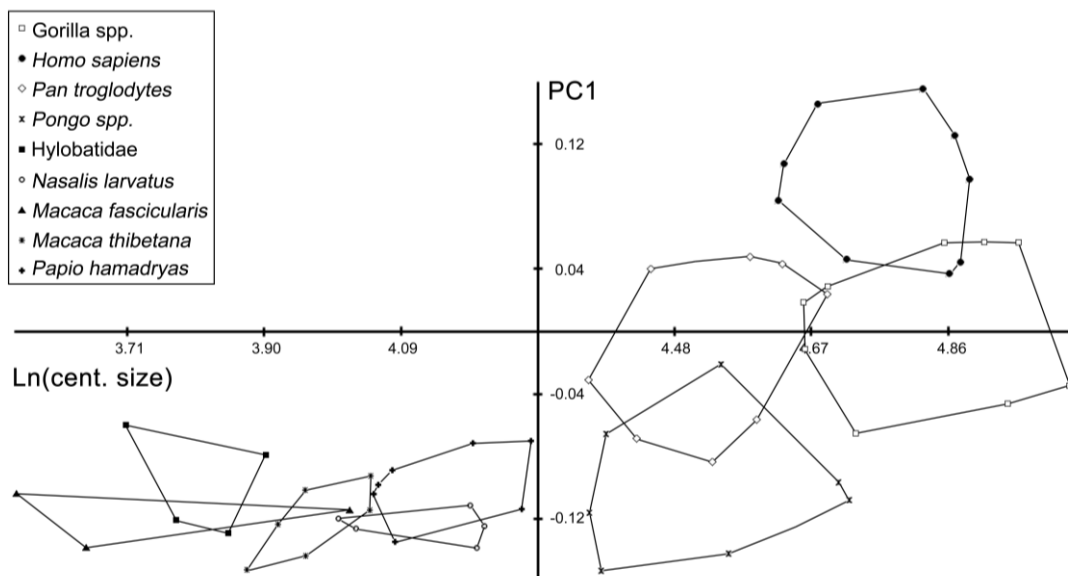
FIGURE 4. Scatter plot showing principal component scores for individual tali based on PCA of Procrustes aligned coordinates, with PC1 on the X-axis and log talus centroid size on the Y-axis. Convex polygons are used to show the range of scatter with individual points hidden for clarity.

TABLE 5. Percent of Total Variance Explained by Different Factors
Within Different Landmark Subsets

Data Set	Substrate %	Mass %	L Centroid Size %	Superfamily %
Whole Talus	12.5	5.5	12.3	10.3
Proximal Talus	12.1	5.8	9.2	6.5
Distal Talus	10.0	4.0	9.8	9.7

Mass accounted for only 5.5%, consistent with our findings in the distal tibia (Turley et al., 2011). All the pair-wise interactions among the independent variables were highly significant ($p < 0.0001$). The magnitude of the interactions was calculated from angles among the shape vectors for each factor. The angular difference between the vectors showed a weak relation of substrate preference from the other factors, whereas size and superfamily were strongly related (Table 6).

TABLE 6. Angular Differences Between the Vectors for Different Factors
Presented in Degrees

	Substrate	Mass	Log Centroid Size	Superfamily
Whole talus				
Substrate	x	80.0	40.9	53.8
Mass	80.0	x	42.8	40.3
Log centroid size	40.9	42.8	x	18.1
Superfamily	53.8	40.3	18.1	X
Proximal talus				
Substrate	x	93.0	50.0	65.1
Mass	87.0	x	50.0	50.2
Log centroid size	50.0	50.0	x	21.7
Superfamily	65.1	50.2	21.7	X
Distal talus				
Substrate	x	80.3	43.1	55.6
Mass	80.3	x	41.6	39.3
Log centroid size	43.1	41.6	x	17.7
Superfamily	55.6	39.3	17.7	x

In the proximal talar data set, substrate preference accounted for a greater percentage of the total variance (12.1%), with superfamily (6.5%), mass (5.8%), and

centroid size (2.4%) accounting for smaller percentages of the total variance (Table 5). As with the distal tibia, mass was again less related to substrate preference (Turley et al., 2011). Superfamily was unrelated to substrate preference, in the total proximal subset, and related to centroid size (Table 6).

In the distal talar data set, substrate preference (10%), centroid size (9.8%) and superfamily (9.7%) accounted for the most variance, with mass accounting for only 4%. In the distal talar data set, substrate preference was again unrelated to mass. It was mildly unrelated to superfamily but mildly related to size. However, size was strongly related to superfamily (Tables 5 and 6).

Visualization

Morpheus and *Landmark Editor* were used to visualize the shape effects (Fig. 5), with the finding summarized below.

Substrate preference. The terrestrial form of the talus was relatively greater in height, dorsal-plantar, and width, medial (M)-lateral (L), and shorter in length, proximal (P)-distal (D).

The shape of the proximal facets of the terrestrial form includes a trapezoidal trochlea with equal P-D and M-L dimensions, flat plane, square lateral and medial crest angles, smaller, flatter, distally wedge-shaped lateral and medial facets, a shallower central groove, and the trochlea was higher and distally displaced along its crests.

The arboreal form includes a slightly oval trochlea with increased P-D and decreased M-L dimensions, angular lateral-medial plane, acute lateral trochlear crest

28

angle, obtuse medial trochlear crest angle, concave lateral and medial facets, a deeper

central groove, and the trochlea was symmetrically curved along its crests.
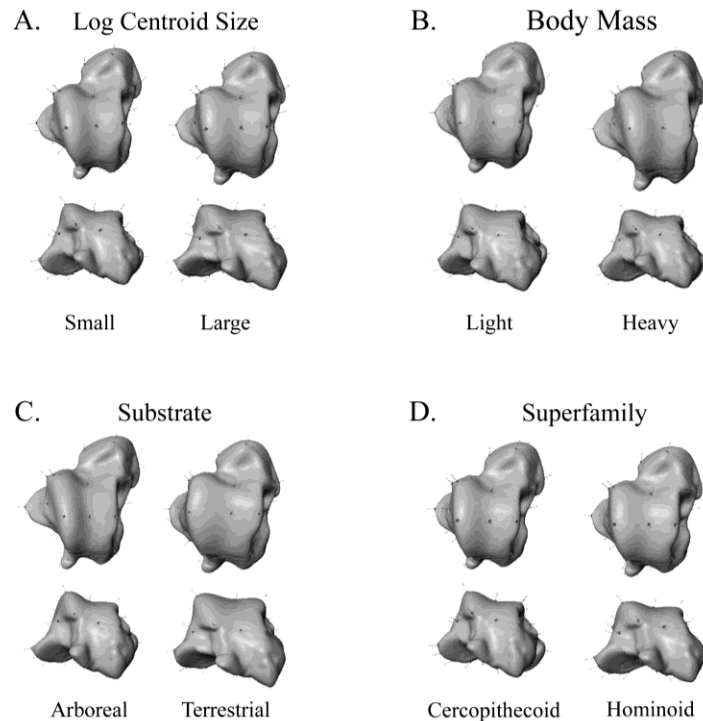
FIGURE 5. Visualization for the whole talus data set of four primary variables analyzed: log of centroid size (A), body mass (B), substrate preference (C), and superfamily (D). Landmark configurations estimated by adding and subtracting regression coefficients to the consensus configuration, these were magnified X5 for the purpose of visualization for mass, and substrate preference. An exemplar surface (male *Pan troglodytes*) was then warped to fit the estimated configuration. See methods for details.

The shape of the distal facets of the terrestrial form includes a larger less concave

rectangular calcaneal facet with the posterior rotated laterally, a relatively shorter neck

with more acute horizontal angle, and a flatter, less convex navicular facet.

The arboreal form includes a smaller, kidney-shaped, more concave and more medially placed calcaneal facet, a longer neck with less acute horizontal angle, and rounder, more convex navicular facet.

Body mass. The larger mass form of the talus was relatively lower in height, shorter in length, but little different in width.

The proximal facets of the large mass form includes an increased P-D and reduced M-L trochlea trapezoid shape, angular lateral-medial plane, acute lateral and obtuse medial crest angles, deep central groove, and curved lateral and medial facets with a distal wedge shape. The smaller mass form includes more equal P-D and M-L trochlea dimensions with curved posterior margin, flatter plane and groove, square crest angles, and flat wide lateral and medial facets.

The distal facets of the heavier form includes a wider, oval, and less concave calcaneal facet, slightly shorter neck with a more acute horizontal angle, and a slightly less convex navicular facet. The smaller mass calcaneal facet was oval, but smaller and more concave. The neck was slightly longer with a less acute horizontal angle, and a slightly more convex navicular facet.

Log centroid size. The larger size form of the talus was relatively shorter and wider, but little different in height.

The proximal facets of the larger size form include equal P-D and M-L trochlear dimensions, angular lateral-medial plane, acute lateral and medial crest angles, higher and distally displaced trochlear crests, shallower central groove, and curved lateral and medial facets. The smaller size form includes increased P-D and decreased M-L trochlear

dimensions, angular lateral-medial plane, square crests with low symmetrical crest shape, deeper central groove and larger and distally displaced lateral and medial facets.

The distal facets of the larger form include a larger, less concave, rectangular calcaneal facet, relatively shorter neck with more acute horizontal angle, and larger, less convex navicular facet. The smaller form includes a smaller, more concave calcaneal oval facet, longer neck and less acute horizontal angle, and a smaller, more convex navicular facet.

Superfamily. Hominoid tali include increased height and width, and decreased length when compared to those of cercopithecoids.

The proximal facets of the hominoid form includes greater P-D and M-L trochlea dimensions, a flatter lateral-medial plane, flattening and slight distal displacement of the trochlear crests, shallower central groove, and widening of the lateral and medial facets.

Cercopithecoid tali include shorter P-D and M-L trochlear dimensions, angular lateral-medial plane, acute lateral and obtuse medial crests, deeper central groove, and narrower, less concave medial and lateral facets.

The distal facets of cercopithecoids include a smaller, more concave calcaneal facet, which was kidney shaped rather than oval, longer neck with increased horizontal angle, and a smaller, less convex navicular facet than in the hominoid form.

Shape Differences Between Taxa

Table 7 shows the differences in shape manifest in the pair-wise permutation tests of the talus, proximal facets and distal facets subsets. As in the tibia, shape in the talus is highly conserved within catarrhine taxa (Turley et al., 2011).

31

The pair-wise permutation tests showed that in the whole talus data set there were significant differences among all pairs except Hylobatidae vs. *Macaca fascicularis* and Hylobatidae vs. *Nasalis* (applying the Bonferroni correction) (Table 7). *Homo* differed from all other taxa in all subsets. Among the apes, all were significantly different excepting *Pan* vs. Hylobatidae in the proximal subset. Comparisons between apes and old world monkeys revealed significant differences excepting Hylobatidae vs. *Nasalis* and Hylobatidae vs. *Macaca fascicularis* in all subsets, *Pan* vs. *Nasalis* and *Pan* vs.

Hylobatidae. Among old world monkeys, *Papio* was significantly different from all Asian cercopithecoids excepting vs. *Macaca fascicularis* and vs. *Nasalis* in the proximal subset. *Macaca thibetana* differed from all excepting vs. *Macaca fascicularis* and vs. *Nasalis* in the distal subset. Finally, *Macaca fascicularis* differed vs. *Nasalis* in the distal subset.

The analysis of mean shape was examined in *Morpheus*, with visualization of each taxon (Fig. 6), and the shape differences described below.

Gorilla spp. demonstrated a decreased relative length and increased relative width from all other taxa, and increased relative height from all except *Homo*. The proximal talar facets showed an angled trochlear plane most marked laterally, with a flatter component medially. The trochlea was trapezoid and markedly wedge-shaped with its greatest width distally. The distal margin was wide and concave extending further distally along the medial aspect towards the head. The medial margin was slightly concave, proximal margin short and slightly convex and lateral margin slightly concave. The central groove was moderate at the distal and proximal margins but reduced in the

32

TABLE 7. Shape Differences Observed Among Taxa Examined

	Homo	Pan	Gorilla	Pongo	Hylobatidae	Papio	M. thib.	M. fasc.	Nasalis
Talus									
Homo	x	0.129477	0.125006	0.20883	0.208489	0.205844	0.223608	0.233012	0.239844
Pan	0	x	0.06171	0.14799	0.1271	0.156835	0.155613	0.177673	0.181889
Gorilla	0	0	x	0.151164	0.145315	0.172007	0.16922	0.193475	0.195424
Pongo	0	0	0	x	0.120445	0.160569	0.122908	0.167954	0.150243
Hylobatidae	0	0	0	0.002	x	0.128119	0.127961	0.124938	0.141024
Papio	0	0	0	0	0	x	0.138511	0.112499	0.147132
M. thibetana	0	0	0	0	0	0	x	0.121002	0.148672
M. fasc.	0	0	0	0	0.007	0	0.002	x	0.121002
Nasalis	0	0	0	0	0.005	0	0	0	x
Proximal									
Homo	x	0.137115	0.136548	0.156386	0.204552	0.167691	0.151357	0.204146	0.186819
Pan	0	x	0.084385	0.130374	0.100791	0.102417	0.127201	0.148629	0.102618
Gorilla	0	0	x	0.14062	0.152339	0.147671	0.152507	0.190341	0.14496
Pongo	0	0	0	x	0.158159	0.129435	0.151732	0.181428	0.134596
Hylobatidae	0	0.009	0	0	x	0.110435	0.150339	0.124401	0.107166
Papio	0	0	0	0	0.012	x	0.100957	0.103418	0.09713
M. thibetana	0	0	0	0	0	0	x	0.110555	0.125301
M. fasc.	0	0	0	0	0.062	0.048	0.018	x	0.138091
Nasalis	0	0.018	0	0	0.148	0.046	0.004	0.01	x
Distal									
Homo	x	0.107349	0.105579	0.193382	0.1653	0.187279	0.210217	0.189655	0.215082
Pan	0	x	0.044228	0.131338	0.100608	0.148236	0.151114	0.138692	0.174787
Gorilla	0	0	x	0.132352	0.110539	0.158482	0.15967	0.15165	0.178611
Pongo	0	0	0	x	0.086478	0.162783	0.089758	0.122742	0.130405
Hylobatidae	0	0.001	0	0.035	x	0.135119	0.102375	0.114549	0.125173
Papio	0	0	0	0	0	x	0.130849	0.116354	0.168046
M. thibetana	0	0	0	0.001	0.001	0	x	0.08598	0.123754
M. fasc.	0	0	0	0	0.025	0	0.021	x	0.126493
Nasalis	0	0	0	0	0.18	0	0.006	0.09	x

Procrustes distance between taxon means are shown above the diagonal and P values below the diagonal (1,000 permutations).

33
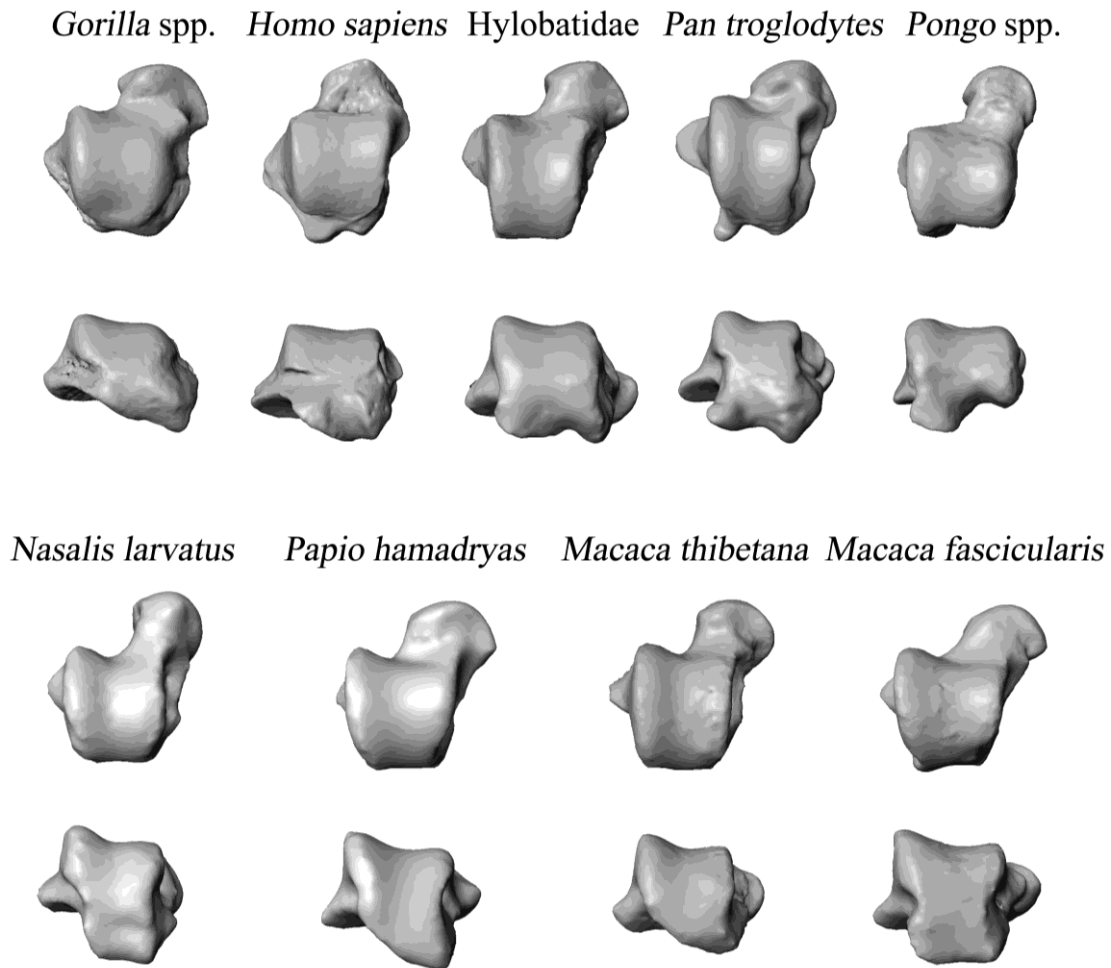
FIGURE 6. Visualization of representative tali of the nine taxa sampled.

mid-facet. The lateral crest was acutely angled with a distally displaced apex, and the

lateral facet was large and flat superiorly, becoming concave inferiorly with its apex mid-

facet and closely related to the disto-lateral corner of the calcaneal facet. The medial crest

was obtusely angled, lower, but with the apex similarly distally displaced, and the medial

facet was large concave, with the apex of the facet distally displaced with the facet

extending toward the head. The distal facets head was medially displaced with an acute

horizontal angle, increased M-L and I-S dimensions, a reduced convex shape, and a short

neck. The posterior calcaneal facet was rectangular with a slightly convex proximal, distal and lateral edge, a flat medial edge, and decreased convexity and depth.

Pan troglodytes revealed a decreased width, and increased length, but a slight increase in height from *Gorilla*. The proximal talar facets had a comparably angled trochlea plane to *Gorilla*, but it was uniform across the facet L-M. The trochlea was more rounded, narrower along the distal more concave margin with a shorter but more superior antero-medial extension towards the head, expanded mid-facet with a concave medial margin, a wider and more convex posterior, and slightly concave lateral margin. The central groove was deeper at the mid-facet. The lateral crest was acutely angled with a central apex and symmetrical curvature, and the lateral facet was large and flat superiorly, becoming concave inferiorly with its apex mid-facet but slightly distal to the disto-lateral corner of the calcaneal facet. The medial crest was obtusely angled with its apex central and symmetrical. The medial facet was larger and flatter, with the apex distally displaced. The head was medially displaced like that of *Gorilla* but with a less acute horizontal angle, slightly increased I-S dimensions, a more convex facet, and a slightly longer neck. The posterior calcaneal facet was slightly shorter, narrower distally and in the mid-facet and wider proximally, with convex distal and proximal edges but a flat lateral and concave medial edge (kidney shaped), and there was increased concavity compared to *Gorilla*.

Homo sapiens demonstrated in the whole talus relatively greater height and slightly greater width (mid-trochlea) and shorter relative length than *Gorilla*. The proximal talar facets had a flatter trochlea plane with a more rectangular trochlea,

narrower distally and wider mid- and posterior facet. The distal margin showed minimal

angulation laterally and was flat, with the medial margin slightly concave, the posterior

flat and the lateral slightly convex. The central groove was shallow. The lateral crest was

more acutely angled (square) with greater anterior displacement of the apex and the

lateral facet was larger flatter and less concave inferiorly, with the apex slightly distal.

The medial crest was acutely angled with its apex more distally displaced than *Gorilla.*

The medial facet was smaller flatter and less concave inferiorly with more proximally

positioned distal edge and apex. The distal facets demonstrated a head with a decreased

horizontal angle, a greater I-S dimension, which was more concave and domed, with a

slightly longer neck. The posterior calcaneal facet was larger, with slightly convex medial

and flat medial edges, narrower and convex distally, and expanded and medially rotated

proximally with a convex edge, and less concavity than *Gorilla*.

Pongo spp. demonstrated in the whole talus a shorter height, narrower width and

longer length compared to *Gorilla*. The proximal talar facets demonstrated an angled

trochlea plane comparable to *Gorilla.* The trochlea was square with a slightly concave

and slightly longer distal margin but without distal extension as in *Gorilla*, flat medial,

posterior and lateral margin. The central groove was deeper than *Gorilla*, *Pan*, and *Homo.*

The lateral crest was acutely angled with a central apex and symmetrical, and the lateral

facet was smaller, flat superiorly, less concave inferiorly, with a central apex. The medial

crest was obtuse, but less than *Gorilla* and *Pan*, with the central apex, lower and

symmetrical, and the medial facet was smaller, less concave with the apex distally

displaced like *Gorilla*, but without the distal displacement of the facet observed in

Gorilla. The distal facets demonstrated a head with comparable horizontal angle to

Gorilla, a smaller, more convex facet, and longer neck. The posterior calcaneal facet was

smaller and kidney shaped with a slightly convex medial and concave lateral edge, and

more concave than in *Gorilla* with medial rotation of the distal edge and lateral rotation

of the posterior edge.

Hylobatidae revealed in the whole talus a shorter height, much narrower width

and longer length compared to *Gorilla*. The proximal talar facets demonstrated a

comparable angled trochlea plane to *Pongo*. The trochlea was rectangular with slightly

concave distal and medial margins, and slightly convex posterior and lateral margins. The

central groove was deeper than any of the hominoids studied. The lateral crest was

acutely angled with a slightly distally displaced apex, and the lateral facet was flat,

smaller and more distally displaced than *Pongo*, including the apex. The medial crest was

more acutely angled and the apex distally displaced, and the medial facet was slightly

larger than Pongo and distally displaced. The distal facets demonstrated a head with an

increased horizontal angle, smaller and less convex than *Pongo* with a longer neck. The

posterior calcaneal facet was smaller and kidney shaped with a concave medial and

convex distal, lateral, and posterior edges, with the latter wider and rotated medially from

Pongo, but of equal concavity.

Papio hamadryas showed in the whole talus a slightly lower height, narrow width

and longer length than all hominoids excepting Hylobatidae, which was lower, narrower

and shorter. The proximal talar facets had an angled plane greater than all hominoids,

including Hylobatidae. The trochlea was rectangular with a concave distal margin without

distal extension, flat medial and lateral margins with a flat posterior margin with increased plane. The central groove was deeper than Hylobatidae. The lateral crest was acutely angled with the apex distally displaced. The lateral facet was flatter than Hylobatidae with the apex mid-facet. The medial crest was more acutely angled than Hylobatidae and lower with the apex distally displaced. The medial facet was flatter and smaller than Hylobatidae with the apex mid-facet. The distal facets demonstrated a head with greater horizontal angle than Hylobatidae, but equal size and convexity, with a longer neck. The posterior calcaneal facet was smaller, rectangular and less concave with the posterior edge rotated medially from Hylobatidae.

Macaca thibetana demonstrated in the whole talus a slightly greater height, greater width and shorter relative length than *Papio*. The proximal talar facets demonstrated reduced plane from *Papio*, but greater than all hominoids. The trochlea was slightly more wedge shaped than *Papio,* with the distal and posterior margins flat with a flat plane, and the medial and lateral slightly convex. The central groove was shallower than *Papio.* The lateral crest was acutely angled with the apex more distally displaced than *Papio*, and the lateral facet was acutely angled flat superiorly with inferior concavity, smaller and proximally displaced with its apex. The medial crest was less acutely angled than *Papio* with the apex more distally displaced. The medial facet was slightly concave, enlarged distally but with a mid-facet apex. The distal facets demonstrated a head with a horizontal angle approximating that of *Papio*, smaller size and increased convexity, but with an equal relative neck length. The posterior calcaneal facet was rectangular, less

concave, with enlargement and lateral rotation of the posterior edge greater than Hylobatidae.

Macaca fascicularis showed in the whole talus a slightly narrower width and longer relative length than *M. thibetana*. The proximal talar facets had increased plane from *M. thibetana* most markedly distally and proximally, but reduced from *Papio*. The trochlea was longer and less wedge shaped with only slightly concave distal, medial and lateral margins, but convex posterior margin. The central groove was deeper than *M. thibetana*. The lateral crest was acutely angled, and the lateral facet was smaller and distally displaced with its apex. The medial crest was more acutely angled, more symmetrical with a proximally displaced apex, and the lateral facet was smaller with a mid-facet apex. The distal facets demonstrate a head with an increased horizontal angle, but equal size and convexity, and neck length. The posterior calcaneal facet was more kidney shaped with equal concavity but medial rotation and expansion of the posterior edge from *M. thibetana*.

Nasalis larvatus revealed in the whole talus equal relative height and width, increased neck length but decreased length of the trochlea compared to *M. fascicularis*, and the proximal talar facets had increased plane. The trochlea was shorter, with concave distal, convex medial and posterior, and flat lateral margins. The central groove was deeper. The lateral crest was acutely angled and symmetrical with a central apex. The lateral facet was comparable in shape to *M. fascicularis*. The medial crest was acutely angled, symmetrical with a central apex, and the medial facet was larger distally with a proximally displaced apex. The distal facets demonstrated a head with the largest

39

horizontal angle, smaller with greater convexity, and a longer neck. Finally, the posterior calcaneal facet was more concave with a convex anterior edge, slightly concave lateral, flat medial, and symmetrically reduced and flat posterior edge.

Discussion

The talus is the distal component of the talo-crural or upper ankle joint, and articulates with the proximal elements, the tibia (medial) and fibula (lateral), forming a mortise and tenon joint, transmitting the weight of the body to the foot and substrate (Fig. 1) (Aiello and Dean, 2002). Among primates, the surface of the talus is covered by a high percentage of articular cartilage, since in addition to the talo-crural joint proximally, it articulates with the calcaneous inferiorly forming the subtalar, or lower ankle joint, and the navicular distally forming the talo-navicular component of the transverse tarsal joint (Polly, 2008). The articular surfaces of the talo-crural joint include the trochlea and malleolar facets, and differences in their shape accommodate plantarflexion and dorsiflexion, but also afford the potential for eversion and inversion during plantarflexion and dorsiflexion, respectively (Aiello and Dean, 2002). The subtalar joint has two components, articulation with the posterior calcaneal facet, which is concave, and the medial and anterior (sustentacular) facets, which are convex, forming an axis of rotation (Aiello and Dean, 2002; Lewis, 1989; Polly, 2008). This axis, the line passing through the posterior and anterior arcs, is the rotational center for inversion and eversion of the foot. Finally, the transverse tarsal joint is the articulation of the head of the talus and proximal articular facet of the navicular bone, as well as the articulation of the calcaneous and cuboid. It is involved in inversion and eversion of the distal pedal elements and

40

transmitting mechanical loads to the foot and substrate, as well as maintaining a rigid

arch in the foot of bipeds.

The structure of the talus includes three main components: the head (caput tali)

with its convex distal articular surface; the body (corpus tali) the "squarish bulk of bone,"

site of the proximal facets and concave posterior calcaneal facet; and the neck connecting

the body to the head, site of the convex medial and anterior calcaneal or subtalar facets

inferiorly (White and Folkens, 2000). Finally, differences in angulation (horizontal,

torsion, and inclination) and length of the neck influence distal presentation of the

articular surface of the head with the navicular and affect total talar presentation to the

foot and substrate (Aiello and Dean, 2002; Day and Wood, 1968; Latimer et al., 1987).

Both presentation and shape influence the ankle joints' functional shape. Their

expression in the talus, however, is mitigated by the complex nature of the interaction

among the three articular complexes in which the talus participates. These interactions

influence the shape, orientation, and curvature of individual facets (Hamrick, 1996;

Harcourt-Smith, 2002; Parr et al., 2011; Sarmiento, 1988).

The Effect of Biological Role on Shape

In this study many aspects of talar shape were detected that differentiate the

various catarrhine taxa. A significant portion of this was probably related to evolutionary

history, as evidenced by the clear differences in talar shape among superfamilies, genera

and species. However, important aspects of talar shape were related to the biological role

of the talus in the various taxa (sensu Aiello and Dean, 2002; Bock and Wahlert, 1965;

DeSilva, 2009; Gebo and Schwartz, 2006; Jungers, 1988; Latimer et al., 1987; Parr et al., 2011; Ruff, 1988; Turley et al., 2011).

The features that differentiate the terrestrial and arboreal forms relate to stability and flexibility on different surface shapes, textures and firmness (Turley et al., 2011). In the tali of more terrestrial catarrhine taxa, the whole talus exhibited increased superioinferior height and mediolateral width and shortened anterioposterior length, providing a stable platform for dorsiflexion and plantarflexion, while the arboreal form exhibited increased length combined with decreased height and width, providing increased flexibility.

The crural articulations of terrestrial forms exhibited features that provide stability in dorsiflexion such as trapezoidal trochlea with equal proximodistal and mediolateral dimensions and a flat plane. They also have square lateral and medial crest angles and a shallow central groove facilitating a stable range of motion. Furthermore, they have smaller, flatter and shallower, distally wedge-shaped lateral and medial facets allowing maximal stability in dorsiflexion. Finally, the trochlea was higher in terrestrial forms, the crest was more anteriorly displaced, and the curvature more convex, consistent with increased "range of joint angular excursion due to sliding translation," correlating with "range of motion" (Hamrick, 1996).

The distal facets exhibited features that provide medial axial stability such as a larger, rectangular, laterally placed posterior calcaneal facet with its posterior margin rotated laterally (Aiello and Dean, 2002). The posterior calcaneal facet was less concave consistent with loads perpendicular to the center of the joint, and negatively correlated

with variation in load orientation (Hamrick, 1996). Likewise, there was a shorter neck and more acute horizontal angle consistent with a more compact presentation distally. The navicular facet of the head was more centrally displaced due to the more acute horizontal angle. Also, it had a less convex shape and the decreased curvature of this "male mating surface" decreased angular excursion and range of motion (Hamrick, 1996).

The tali of more arboreal taxa exhibited features providing flexibility in movement, but stability on unstable substrates. These included a slightly oval trochlea with increased proximodistal and decreased mediolateral dimensions, angular lateral medial plane, acute lateral trochlear crest angle, obtuse medial trochlear crest angle, and concave lateral and medial facets. There was a deeper central groove providing stability, and the trochlea was symmetrically curved along its crests, with the decreased curvature consistent with a decreased "range of joint angular excursion" (Hamrick, 1996).

The shape of the distal facets of arboreal forms includes a smaller, kidney-shaped, and more medially placed posterior calcaneal facet, which was more concave, consistent with directing a component of the load oblique to the center of the joint and increasing joint stability (Hamrick, 1996). The neck was longer with a more acute horizontal angle, and a rounder, more convex navicular facet, consistent with increased range of joint angular excursion.

The features of the talus that differentiate heavier from lighter taxa relate to relative height and length with heavier forms having lower and shorter tali, presenting a more compact shape to the loads experienced. The trochlea was more trapezoidal in the heavier forms, increasing stability with dorsiflexion, with an angular lateral-medial plane,

and acute lateral and obtuse medial crest angles, a deep central groove increasing stability, and curved lateral and medial facets that were more wedge-shaped distally complementing the trochlear configuration (Aiello and Dean, 2002). The distal facets included a less oval, less concave posterior calcaneal facet with a surface directing loads perpendicular to the joint (Aiello and Dean, 2002; Hamrick, 1996). The neck was short with a more acute horizontal angle, placing the less convex navicular facet central, increasing stability and decreasing angular excursion.

Taxa with lower body mass had tali with equal trochlear dimensions with a curved posterior margin, flatter plane and groove, square crest angles, and flat, wide lateral and medial facets, none designed to compensate for load. The posterior calcaneal facet was smaller and more oval with its more concave surface increasing the potential range of angular motion (Hamrick, 1996). Finally, the neck was longer with a less acute angle orienting the more convex head medially, facilitating the increased range of angular excursion.

Talar shape varied in relationship to talar size such that taxa with larger tali also had shorter and wider tali. Furthermore, the crural facets of taxa with larger tali differed in having equal proximodistal and mediolateral dimensions from those with smaller tali, which showed increased proximodistal and decreased mediolateral dimensions, reflecting differences in requirements for mobility and stability. These were also reflected in acute rather than square crest angles in the larger and symmetrically curved crests in the smaller in contrast to higher and distally displaced apices in the larger. There was also a deep

central groove with larger distally displaced lateral and medial facets in the smaller, and a shallower central groove with curved lateral and medial facets in the larger.

The distal facets of taxa with larger tali exhibited a larger, less concave rectangular posterior calcaneal facet with loads directed perpendicular to the joint, as opposed to oblique to it, which might put increased stresses on joint structures, while in the smaller form a more concave oval facet afforded stability to loads directed obliquely to the center of the joint (Hamrick, 1996). The neck of the larger was shorter with a more acute horizontal angle with a larger, less convex head providing stability, while the smaller form had a smaller, more convex navicular facet and longer neck increasing its range of angular excursion.

Shape Variation Among the Taxa Examined

Presentation and articular shape were affected by all the factors examined among the taxa studied. This was not a surprising result, as the same has been demonstrated for the tibia (Turley et al., 2011). Talar presentation was influenced by proximal talo-crural, subtalar, and transverse tarsal joints. In the first it was due to the plane and shape of the trochlea, and in the latter two due to position and rotation of the posterior calcaneal facet, and horizontal angle and length of the neck. Phylogeny, here represented as the superfamily, was also an important factor (Kanamoto et al., 2011). The features that differentiated cercopithecoids from hominoids in talus shape included a square configuration in hominoids with increased height and width, and decreased length and a longer, thinner and shorter configuration in cercopithecoids.

Gorilla was an outlier due to the factors outlined above. The trapezoid trochlea was more wedge shaped than that encountered in the more terrestrial species studied. However, the trochlea plane and its distal facet margin with extension disto-medially onto the superior aspect of the neck was combined with a more acute horizontal angle and a larger, wider, less convex navicular facet. These provided increased stability and decreased mobility in extreme dorsiflexion, with obligatory inversion, accommodating its great mass in safe vertical climbing, while its flat lateral to central component of the distal trochlea margin provides stability and mobility in its terrestrial quadruped, "knuckle walking," gait (DeSilva, 2009). The distal displacement of the crest apices and its reduced curvature, medial and lateral facet shape, and central groove depth contribute to these effects. Finally, the posterior calcaneal facet position, size, and shape were consistent with terrestrial mobility, conferring stability with centrally directed loads as in vertical climbing (DeSilva, 2009; Hamrick, 1996; Sarmiento, 1988).

Pan exhibited increased lateral-medial plane with less distal-medial extension of the trochlea, but a uniform lateral-to-medial elevation of the distal margin, again providing, as in Gorilla, safety in vertical climbing. The trochlea was more rounded, and the crests were symmetrical with the apices central. Combined with larger, flatter medial and lateral facets with a central apex, the proximal facets provide increased mobility. This is consistent with the greater range of motion observed in the talo-crural joint in Pan (55%) than male Gorilla (47%) and Homo (48%) (Latimer et al., 1987). A smaller, deeper, and more concave posterior calcaneal facet would provide stability with loads oblique to the center of the joint, while a smaller, more convex navicular facet would

increase range of motion (Hamrick, 1996). These observations are consistent with the proximal facet paired permutation results for *Pan* and *Nasalis* and those for tibia (Turley et al., 2010). Of note, like the distal tibia, *Gorilla* and *Pan* differed in four of the five PCs in the proximal facet subgroup (Turley et al., 2011; Wunderlich and Jungers, 2009).

Homo differed from all taxa in Table 7. The proximal and distal facet subsets each reflected the unique requirements of terrestrial bipedalism. Mean shape was more consistent with other terrestrial taxa—specifically, the cercopithecoids—than closely related taxa. Among the hominoids, *Pongo* and Hylobatidae, despite size difference, demonstrated similarities in distal facets consistent with some similarities in substrate utilization. These were reflected in the pair-wise permutation tests. Hylobatidae, as in the tibia, clustered with the cercopithecoids, with a phylogeny divergent close to the separation of the superfamilies studied, and with the arboreal taxa specifically, in the whole talus, and proximal and distal facet subgroups. Similarities in posterior calcaneal shape, neck length, horizontal angle, and navicular facet shape are consistent among these, as in other phylogenetically distant, arboreal taxa (Polly, 2008).

The cercopithecoid taxa examined exhibited a common bauplan. These similarities accommodated a common mode of locomotion, palmigrade quadrapedalism, within the context of specific talo-crural, subtalar, and transverse tarsal joint shape constraints (Fleagle, 1999). The most closely related taxa, *Macaca thibetana* and *Macaca fascicularis,* demonstrated differences in shape related to both size and substrate preference. The African cercopithecine, *Papio hamadryas,* had a shorter height than *M. thibetana*, but a rectangular trochlea with more acute, distally displaced crests, deeper

47

central groove, a larger head with less convex navicular facet, and a rectangular, less concave posterior facet combining terrestrial and arboreal patterns of shape. Finally, the Asian colobine, *Nasalis larvatus*, was equal in relative talus dimensions to *M. fascicularis*, but with a maximal arboreal configuration, including a greater plane, deeper central groove, larger medial facet, the greatest horizontal angle, longer neck, and smaller head with greater convexity of the navicular facet, and greater concavity of the posterior calcaneal facet.

Summary and Conclusion

Talar shape correlated with substrate preference among a number of other factors across taxa in the current study. Substrate preference, however, accounted for a significant component of the overall variance in talar shape (Table 5). Further, aspects of talar shape related to substrate use were only weakly related to those associated with the other factors studied (Table 6). When comparisons of the individual taxa were examined, the proximal talar facets tended to reflect the effect of substrate preference (behavior) on articular morphology, while the distal talar facets reflect the effects of superfamily (phylogeny) on modes of locomotion and presentation to the foot and substrate (Turley et al., 2011). Patterns of presentation differed among taxa, but, as in the tibia, were "more constrained within superfamilies" (Turley et al., 2011).

Substrate preference was grossly assessed in this study, as was phylogeny, to identify an epigenetic or genetic signal. Greater insights may be gleaned by examination of phylogeny, modes of locomotion and substrate availability (habitat) to the specimens studied, and subsets of substrate use, such as position in the canopy (Polly, 2008; Rohlf,

2006). Likewise, increasing the number of taxa included (*Pan paniscus*, *Macaca mulatta* and *Colobus guereza*) and sample sizes (*N. larvatus*, *M. fascicularis* and Hylobatidae in particular) of the current sample may define the observed relation, if any, of size and substrate preference. Finally, addressing the appositional joint surfaces (the distal tibia and proximal talus) using Singular Warp analysis would improve the resolution and focus of the investigation of the effect of substrate on joint surface morphology (Harcourt-Smith et al., 2008; Polly, 2008; Turley et al., 2011).

The current data provide insights into the adult morphology among the taxa examined. Our results appear to reflect evolutionary and developmental (Evo-Devo) influences of behavior on talo-crural form, as well as the environmental influences that precipitate them (Müller, 2005; Retallack, 2007). This study centered on the articular component of talar joint morphology, as did our previous study of the tibia (Turley et al., 2011). The influence of substrate preference identified here reinforces the findings in the distal tibia, that in the talo-crural joint, homoplasy of the talar proximal articular morphology may be observed in distantly related taxa (at least between catarrhine superfamilies), and differences in proximal talar form of closely related taxa may reflect variation due to environmentally induced change in substrate use (Begun, 2007; Hall, 2005; Lovejoy et al., 2000; Retallack, 2001; Singleton, 2012; Turley et al., 2011; Wagner, 2001).

Finally, the results demonstrate that Null Hypotheses H-1 and H-2 are rejected since adult talar shape is significantly affected by the factors studied ($p < 0.0001$) and, as in the tibia, the substrate preference influenced shape unrelated to the other factors

examined. The next chapter will explore the relation of adult appositional articular

morphology to the factors previously studied and Null Hypotheses H-3 and H-4.

CHAPTER III

APPOSITIONAL ARTICULAR MORPHOLOGY

OF THE TALO-CRURAL JOINT

This chapter has been submitted for publication and is co-authored by my advisor Stephen Frost, who provided direction in designing the statistical analysis of the data and the programs used, as well as assistance with the figures. The intellectual content is mine, and I performed all specimen acquisition, processing, and analysis.

The concepts of development, modularity and integration are of critical importance in evolutionary studies. The talo-crural joint provides a model for these processes as a functional unit that fulfills the criterion of an evolutionarily stable configuration (Schwenk, 2001). This study aims to evaluate the interaction of the appositional joint surfaces of the talo-crural joint to determine how they covary as a system, exploring their integration and modular structure.

The talo-crural joint or upper ankle joint has three components, the tibia, the talus and the appositional articular morphology. The third component of this joint complex is comprised of the subchondral surfaces of the articular interface encountered in fossil, archaeological and osteological collections (Harcourt-Smith et al., 2008). The presentation, orientation in space relative to the substrate and the organism, and the shape of the proximal (tibia) and distal (talus) components of the complex constrain appositional articular shape (Turley et al., 2011; Turley and Frost, in press). Prior studies of the tibia and talus have demonstrated the effect of multiple factors on the shape of their subchondral articular surfaces. However, substrate preference, in particular, unrelated to

51

the other factors such as size and superfamily, affected the shape of the appositional

articular surfaces of the talo-crural joint, the distal tibial and proximal talar facets (Turley

et al., 2011; Turley and Frost, in press). While these previous studies have examined

distal tibial and proximal talar morphology independently (Turley et al., 2011; Turley and

Frost, in press), here the interaction of the appositional joint surfaces of these two bones

is explored.

The subchondral surfaces were chosen since these are available in museum

collections of the taxa examined, have been used in prior studies suggesting the effect of

substrate preference on shape, and avoid the issues of cartilage, tendon, synovial fluid and

capsule, and soft tissue pathology, as well as the difficulties of scanning living subjects.

Although the importance of the soft tissue elements in joint function is recognized, the

study of the appositional subchondral articular morphology can provide a proxy for the

joint interface shape and provide insights into the response of underlying bone below the

thin layer of cartilage to genetic and epigenetic influences (Hammond et al., 2010;

Hamrick, 1999a; Harcourt-Smith et al., 2008).

The current study examined the subchondral surfaces of this articular interface

using Singular Warp analysis of the cross-covariance matrix of matched talo-crural

landmarked surfaces (Bookstein et al., 2003). When shape coordinates are employed

Singular Warp analysis has been used to assess "morphological integration" among

anatomical structures (Bastir and Rosas, 2005; Bookstein et al., 2003; Mitteroecker and

Gunz, 2009). Using this methodology made matching of such reciprocal surfaces possible

(Harcourt-Smith et al., 2008; McNulty, 2009). The use of matched specimens allows

study of a combined joint interface of the opposing surfaces, which goes beyond the separate analysis of its proximal and distal articular shape, allowing examination of their relationship.

The objective of this study is to evaluate the effect of substrate preference on the talo-crural joint's articular component, a highly modular evolutionary unit (Blomquist, 2009; Schwenk, 2001). Prior studies examined the proximal and distal bones whose presentation constrains articular morphology (Turley et al., 2011; Turley and Frost, in press). Additional specimens and taxa have been included to improve the scope and expand the range of the study. Examining the interaction of the tibial and talar subchondral articular shapes may provide insights into their relation to substrate use and the effects of substrate use on this unit's integration, as well as signals of homoplasy (convergent evolution), and morphological differentiation (divergent evolution) evidenced in the joint morphology among the studied taxa.

Materials and Methods

Sample

The study group consisted of matched distal tibial and proximal talar articular facets from single individuals. Two hundred forty-five specimens from 12 catarrhine taxa were included. All specimens were adults with M3 erupted, and all were without evidence of pathology. Nonhuman specimens had provenience documented, and all were wild-shot or in the case of *Macaca mulatta* from a free-ranging captive population. The nonhuman primate sample included 195 specimens, Hominoids 128 and Cercopithecoids 67. The 50 human specimens were from six populations to provide diversity: California

53

Paleoamericans (13), Southwestern Paleoamericans (6), Inuit (9), 4th-Century Egyptian

(7), 19th-Century European American (7), and 19th-Century African American (8) (see

Acknowledgements for institutional sources) (Table 8).

TABLE 8. The Number of Specimens of the Twelve Taxa Used in This Analysis with
Their Sex, Estimated Mass and Estimated Substrate Preference Documented

Taxon	N	M	F	Mass (kg) M / F	Substrate (0-10) M / F
Homo sapiens	50	26	22	59.3 / 53.2	9.99/9.99
Pan troglodytes	54	26	27	56.6 / 44.0	4 / 3
Gorilla spp.	42	25	11	169.8 / 73.5	7 / 4
Pongo spp.	10	5	5	78.1 / 35.7	2 / 0.2
Hylobatidae	12	6	5	8.6 / 8.0	0.1/ 0.1
Macaca fascicularis	13	6	5	5.3 / 3.6	1 / 1
Macaca thibetana	7	5	1	15.2 / 9.5	8 / 8
Papio hamadryas	12	5	5	25.1 / 13.3	9 / 9
Nasalis larvatus	11	6	5	20.4 / 9.8	0.1/ 0.1
Macaca mulatta	12	6	6	14.0 / 12.0	6.4 / 6.4
Colobus guereza	12	7	4	9.0 / 7.5	0.1 / 0.1
Pan paniscus	10	5	5	45.0 / 33.2	0.5 / 0.5

Mass values obtained from Smith and Jungers (1997) and Delson et al. (2000a). Substrate preference
obtained from Fleagle (1999) and Wells and Turnquist (2001).

The taxa were chosen from each of the superfamilies to provide a spectrum of size

and substrate preference, with comparisons possible of both phylogenetically distantly

and closely related taxa (Xing et al., 2007). The substrate preference estimates were

coded from 0 (most arboreal) to 10 (most terrestrial), and were obtained from the

literature along with taxon mean mass estimates for the taxa examined (Turley et al.,

2011).

Data Collection

Each specimen was laser surface scanned and digitally reconstructed using either a Konica Minolta Vivid 910 Noncontact 3-D Digitizer and Geomagic Studio 8 software, or a NextEngine Desktop 3-D Scanner and ScanStudio HD software. Twenty-seven landmarks were placed by a single observer (KT): 12 on the distal tibial facets, and 15 on the proximal talar facets, using Landmark Editor software. These landmarks were illustrated in Figure 2 and Table 2 for the talus and our prior publication examining the shape of the tibia (Turley et al., 2011, Fig. 1, Table 2).

Observational error was previously assessed in both the tibial and talar subsets using single specimens of *Homo sapiens* landmarked 10 times (Turley et al., 2011; Turley and Frost, in press). Principal component analysis demonstrated tight clustering of the repeated measures compared to variation within and among the taxa studied. This study, like the prior examinations of tibial and talar shape, involves variation above the species level; thus, precision was deemed satisfactory.

Generalized Procrustes Analysis

Generalized Procrustes Analysis (GPA) was performed using *Morpheus* (Slice, 1998). GPA superimposes landmark configurations and removes variance due to position and rotation, and scales each to unit centroid size (Rohlf and Slice, 1990). Centroid size is the square root of the sum of the squared distances of each landmark to the centroid (Rohlf and Slice, 1990), and is stored as a separate variable during GPA. Centroid size was transformed to its natural logarithm for subsequent analysis. GPA was done with reflection allowed, since our data set included both the right and left specimens. Separate

GPAs were performed for the tibial and talar landmark subsets. All subsequent statistical analyses were performed using SAS 9.1 (SAS Institute, Cary NC). As GPA aligned coordinates have a very high correspondence with their Euclidean tangent space projections, unprojected aligned coordinates were used. Shape differences among landmark configurations were measured by Procrustes distance: the Pythagorean distance between the two Procrustes superimposed landmark configurations (Bookstein, 1991; Turley et al., 2011).

Relative Warps Analysis

Relative warps analysis, principal component analysis (PCA) of shape coordinates, was performed on the covariance matrix of the GPA superimposed landmark coordinates and used as a data reduction and exploration technique (Bookstein, 1991; Neff and Marcus, 1980). Here it is used with the components unweighted, although classically it weights the components by bending energy (Bookstein, 1991). Initial visualization of the effect on shape described by each Principal Component (PC) both within and among superfamilies was performed using *Morphologika* software (O'Higgins, 2006; O'Higgins and Jones, 1998).

Permutation Test

Differences in shape between individual taxa were assessed using pair-wise permutation tests with 1,000 replicates performed for each landmark subset. Individuals with equal random samples drawn were randomly permuted across the two taxa and Procrustes distance was calculated between the permuted groups' means. The α was the fraction of permuted values that were greater than the actual Procrustes distance between

group means (Good, 2000). Results were reported with a Bonferroni-adjusted

significance level of $p < 0.00008$ (Turley et al., 2011).

Regression Analysis

The relationship between shape and variables related to biological role was

assessed using multivariate regression analysis (sensu Bock and von Wahlert, 1965;

Bookstein, 1996a; Frost et al., 2003). Substrate preference, body mass, log centroid size,

and superfamily (Hominoidea and Cercopithecoidea) were used as independent variables

and GPA-aligned coordinates as dependent variables.

The proportion of the total variance accounted for by each independent variable

(mass, log centroid size, superfamily, and substrate preference) was calculated for each of

the subsets by subtracting the residual variance after regression from the total variance

and dividing the difference by the total variance (multivariate multiple regressions) (Frost

et al., 2003). The sample size did not allow for a robust test of the interaction of all four

variables together, or combinations of three. However, pair-wise analysis of the

interactions among all four variables was possible. The angles among the shape vectors

for each factor were calculated as the arccosine of their vector correlation (dot product) to

evaluate the closeness of the relationship among the independent variables (Cobb and

O'Higgins, 2004). Relatively parallel angulation (0°-30°) demonstrated a strong

correlation, the closer to 0°, the tighter the relation, while relatively orthogonal angulation

(60°-90°) demonstrated a weak relation, the closer to 90°, the less related (Turley et al.,

2011).

57

Singular Warp Analysis

Singular Warp analysis of the cross-covariance matrix of the appositional articular shape was used in this study to explore the relation of the matched surfaces of the distal tibial facets and proximal talar facets. This is the application of Partial Least Squares within morphometrics that computes two unit vectors such that the covariance is a maximum. It describes how two sets of variables covary with each other, as if it were a "submatrix" of the covariance matrix (McNulty, 2009). In this case, X-variables (shape coordinates) from the tibia form one matrix and Y-variables (shape coordinates) from the talus form the other that have the greatest mutual linear predictive power (Bookstein et al., 2003: Frost et al., 2003; Harcourt-Smith et al., 2008; Rohlf and Corti, 2000). A scatter plot of Singular Warp of the cross-covariance matrix of the appositional articular shapes, as well as a plot of the mean values of the studied taxa, was created, as well as the male/female subgroups of each (Bastir and Rosas, 2005; Bookstein et al., 2003).

Visualization

Visualization of shape differences was accomplished by comparing landmark configurations directly in *Morpheus* and by warping an exemplar surface to fit those landmark configurations using *Landmark Editor*. Mean landmark configurations were computed for each taxon. Shape differences associated with substrate preference were visualized by adding the vector of regression coefficients from multivariate regression to the consensus landmark configuration for the landmark subsets. Features used in the resulting descriptions are explained in Table 9. The exemplar appositional articular surfaces from the Singular Warp analysis were likewise warped using *Landmark Editor*.

TABLE 9. Aspects of Talar Shape Examined in Each Data Set

Distal Tibial Facets Data Set

- Trochlear facet shape-oval/trapezoid
- Anterior trochlear facet margin (plane, lateral to medial)
- Posterior trochlear facet margin (plane, lateral to medial)
- Medial trochlear facet margin (trochlear medial malleolar groove) (axis posterior to anterior)
- Lateral trochlear facet margin (axis posterior to anterior)
- Trochlear-medial malleolar facets angle
- Central trochlear facet concavity (depth)
- Relative medial malleolar height (midline)
- Relative medial malleolar length (base)
- Medial malleolar base shape (concave to convex)
- Medial malleolar central shape (concave to convex)
- Medial malleolar apex shape (position, posterior-central-anterior)

Proximal Talar Facets Data Set

- Trochlea shape
- Central groove relative depth
- Anterior trochlear margin (plane and lateral to medial shape)
- Posterior trochlear margin (plane and lateral to medial shape)
- Medial trochlear margin shape
- Lateral trochlear margin shape
- Medial crest angle, shape and position of the apex
- Lateral crest angle, shape and position of the apex

Results

Relative Warps Analysis

The results of the Relative Warps analysis of the distal tibial and proximal talar matched subsets are provided, with eigenvalues of PC 1-5 and cumulative percentage of variance, in Table 10. These values are consistent with analysis of unmatched distal tibial and proximal talus data previously reported, with 57% of the distal tibial and 58% of the proximal talar variance accounted for by PC 1-5 (Turley et al., 2011; Turley and Frost, in press). Shape differences generated from plots of these PCs likewise separated the studied taxa as in prior analysis (Turley et al., 2011; Turley and Frost, in press).

TABLE 10. The First Five Eigenvalues of the Covariance Matrix on Procrustes Aligned
Coordinates for Principal Component Analyses on the Two Different Data Sets with
the Proportion and the Cumulative Values of the Total Variance Provided

	Rank	Eigenvalue	Proportion	Cumulative
Distal tibia data set				
	1	0.00440300	0.1761	0.1761
	2	0.00342392	0.1369	0.3130
	3	0.00327089	0.0948	0.4078
	4	0.00228114	0.0912	0.4991
	5	0.00186439	0.0746	0.5736
Proximal talus data set				
	1	0.00394096	0.1798	0.1798
	2	0.00284317	0.1297	0.3095
	3	0.00260989	0.1191	0.4285
	4	0.00161724	0.0738	0.5023
	5	0.00160665	0.0733	0.5756

Regression Analysis

Multivariate regression analysis of the shape differences observed between four
variables studied was again significant ($p < 0.0001$) in both the distal tibial and proximal
talar subsets, and are presented in Table 11. Substrate preference accounted for a high
percentage (6.7% distal tibia and 9.7% proximal talus), with mass the least in each subset,
as was the case in previous analyses (Turley et al., 2011; Turley and Frost, in press).
Table 12 presents the arccosine of the vector correlation (dot product) of the four
variables. Substrate preference was unrelated to mass and superfamily, with size
correlating with superfamily.

TABLE 11. Percent of Total Variance Explained by the Different Factors
Within the Proximal Talar and Distal Tibial Landmark Subsets

Adult	Substrate %	Mass %	L centroid size %	Superfamily %
Proximal talus	9.7	6.2	10.3	8.3
Distal tibia	6.7	4.0	6.2	5.2

TABLE 12. Angular Differences (Dot Product) Between the Vectors
for the Different Factors Examined Presented in Degrees

	Substrate	Mass	Size	Superfamily
Adult Tali				
Substrate	x	62.8	41.2	47.3
Mass	62.8	x	30.9	34.8
Size	41.2	30.9	x	14.9
Superfamily	47.3	34.8	14.9	x
Adult Tibiae				
Substrate	x	68.2	54.5	76.8
Mass	68.2	x	27.6	41.8
Size	54.5	27.6	x	29.7
Superfamily	76.8	41.8	29.7	x

The shapes associated with the matched appositional articular subchondral surfaces of the terrestrial and arboreal forms differed in the distal tibial trochlear facet and talar trochlea, with the former being a trapezoid in outline rather than an oval, with a flatter medial-to-lateral plane. The matched central convexity and concavity were greater and the crests were more acute with a more anteriorly displaced apex rather than obtusely angled and symmetrical. Compared with the terrestrial form, the medial malleolus of the arboreal form was longer and had a convex rather than concave base, curved rather than flat facet, and central rather than anterior apex. The talar facets were larger and concave, versus the flatter, smaller and wedge-shaped terrestrial form. Superfamily forms differed with wider and shorter trochlea and trochlear facet dimensions in the hominoids. There was also a flatter plane with flatter crests with anterior displacement of the apex. Compared to hominoids, cercopithecoids had deeper central concavity and convexity, increased medial malleolar surface area relative to trochlear surface area with smaller medial and lateral facets with less concavity. Greater body mass was associated with a trapezoid trochlea and distal tibial trochlear facet with increased length and decreased

width, while lesser mass was associated with more equal dimensions. The latter also had a flatter plane and central groove and convexity, square rather than acute lateral and obtuse medial crest angles, and flat wide facets without distal wedge configurations. The medial malleolus in taxa with greater mass had greater height and width with less convexity and the apex anteriorly displaced than less massive taxa. Finally, larger forms (log centroid size) had equal trochlear and distal tibial trochlear facet dimensions, shallower central groove and lower convexity, greater plane, more acute crest angles, higher, distally displaced crests and grooves compared to smaller forms, and curved lateral and medial facets with central rather than distally displaced apices. The medial malleolus of the larger form had less convexity with apex anterior rather than central.

Permutation Test

The results of the permutation tests for differences in shape of the distal tibial and proximal talar subsets of the individual landmarked taxa are presented in Table 13. All of the great apes and humans were significantly different from each other and all other studied taxa excepting *Pongo* spp. and Hylobatidae in the distal tibia. *P. hamadryas* was significantly different from all other taxa excepting the proximal talus of *M. thibetana* and *M. mulatta* in this study. Hylobatidae were not significantly different from *M. fascicularis* in the distal tibia and proximal talus, *N. larvatus*, *C. guereza*, or *M. thibetana* in the distal tibia, consistent with prior studies (Turley et al., 2011; Turley and Frost, in press). Likewise, *C. guereza* and *N. larvatus*, and *M. fascicularis* and both *M. thibetana* or *M. mulatta* were not significantly different in either subset.

TABLE 13. Shape Differences Observed Among Taxa

	Hs	Pt	Pp	Go	Po	Hy	Ph	Mt	Mm	Mf	Nl	Cg
PTAM3												
Hs	x	0.137169	0.167772	0.136219	0.162395	0.176359	0.165887	0.156942	0.19985	0.181042	0.187819	0.184896
Pt	0	x	0.132431	0.08582	0.135616	0.111888	0.103169	0.138457	0.150009	0.121468	0.112119	0.13477
Pp	0	0	X	0.131379	0.174043	0.131496	0.190634	0.205859	0.161659	0.146405	0.120273	0.127912
Go	0	0	0	x	0.146726	0.139816	0.149287	0.162694	0.167246	0.147005	0.142743	0.150476
Po	0	0	0	0	x	0.179089	0.135621	0.178923	0.159916	0.157528	0.172174	0.180283
Hy	0	0	0	0	0	x	0.13518	0.144598	0.107109	0.084933	0.104387	0.112304
Ph	0	0	0	0	0	0	x	0.11096	0.130911	0.101148	0.140774	0.156833
Mt	0	0	0	0	0	0	0.003	x	0.172245	0.133692	0.172787	0.182571
Mm	0	0	0	0	0	0	0	0	x	0.076496	0.123089	0.129038
Mf	0	0	0	0	0	0.022	0.009	0.003	0.031	x	0.095597	0.11087
Nl	0	0	0	0	0	0	0	0	0	0.008	x	0.07030
Cg	0	0	0	0	0	0	0	0.001	0	0	0.004	x
DTIM3												
Hs	x	0.11280	0.21669	0.11807	0.15405	0.13221	0.12444	0.10522	0.1453	0.11679	0.14690	0.11984
Pt	0	x	0.17535	0.08864	0.12846	0.08993	0.12093	0.12093	0.14174	0.11604	0.11363	0.12146
Pp	0	0	x	0.19586	0.18500	0.15287	0.25908	0.20828	0.21277	0.20578	0.20998	0.21529
Go	0	0	0	x	0.14487	0.10335	0.11099	0.14676	0.14029	0.13124	0.13222	0.13870
Po	0	0	0	0	x	0.10154	0.18938	0.14713	0.17412	0.13690	0.13559	0.12655
Hy	0	0	0	0	0.001	x	0.14740	0.12571	0.10958	0.08751	0.08582	0.09401
Ph	0	0	0	0	0	0	x	0.13887	0.12641	0.12048	0.13135	0.13704
Mt	0	0	0	0	0	0.003	0	x	0.13569	0.10278	0.13994	0.11290
Mm	0	0	0	0	0	0	0	0	x	0.11290	0.09863	0.10590
Mf	0	0	0	0	0	0.019	0	0.015	0.05	x	0.08396	0.06948
Nl	0	0	0	0	0	0.033	0	0	0	0.044	x	0.07666
Cg	0	0	0	0	0	0.007	0	0.002	0	0.133	0.089	X

Procrustes distance between taxon means are shown above the diagonal and P values below the diagonal (1,000 permutations). Legend: *Hs = Homo sapiens*; *Pt = Pan troglodytes*; *Pp = Pan paniscus*; *Go = Gorilla spp.*; *Po = Pongo spp.*; Hy = Hylobatidea; *Ph = Papio hamadryas*; *Mt = Macaca thibetana*; *Mm = Macaca mulatta*; *Mf = Macaca fascicularis*; *Nl = Nasalis larvatus*; *Cg = Colobus guereza.*

The mean shapes of the matched taxa were consistent with the findings in prior studies of the distal tibial and proximal talar facets in *Gorilla* spp*.*, *H. sapiens*, *P. troglodytes*, *Pongo* spp*.,* Hylobytidae, *P. hamadryas*, *M. fascicularis*, *M. thibetana*, *N. larvatus* and the distal tibia of *C. guereza* (Turley et al., 2011; Turley and Frost, in press)*.* The proximal talar facets of *Colobus guereza,* as well as the mean shape of the tali and tibiae of the two additional taxa examined in the current study, *Macaca mulatta* and *Pan paniscus,* are described.

Colobus guereza. The proximal talar facets showed a lesser plane to *Nasalis larvatus.* The trochlea, likewise, was more oval and wider with shorter, less curved proximal margin than *Nasalis larvatus*. There was also a lower lateral crest but more acute angle. The central groove was shallower. The medial and lateral facets were comparable in size and shape to *Nasalis larvatus*.

Macaca mulatta. The proximal talar plane was decreased from that observed in *Macaca fascicularis*, as was the central groove depth and crest height. The crests were symmetrical but angles more acute. There was a smaller medial facet.

The plane of the distal tibial facets was decreased from *M. fascicularis*. The trochlea was wider centrally and narrower distally yielding a more oval lateral margin, but with straight proximal and distal margins and a convex medial groove. The central convexity was decreased as was the trochlear facet medial malleolar angle. The medial malleolus was comparable but with a flatter base and facet, and more distally displaced apex.

Pan paniscus. The proximal talar facet plane was comparable to *Pan troglodytes*. The trochlea was more oval, and longer due to a longer central but shorter medial and lateral, and more curved, proximal margin. There was increased distal-medial extension towards the head. There was a shallower groove centrally but it was deeper distally and proximally. The crests were symmetrical, with the lateral angle more acute. There was a deeper, larger lateral facet with extension proximally.

The distal tibial facets plane was comparable to *Pan troglodytes*. The trochlear facet was oval but with decreased proximal margin and distal medial and lateral widening. There was a more obtuse trochlear facet medial malleolar angle with a shorter but more convex medial malleolar base. The medial malleolus was smaller but with a central apex.

Singular Warp Analysis

The scatter plot of the scores from Singular Warp analysis of the cross-covariance matrix of the appositional articular shape of the talo-crural joints in the current sample was highly significant ($p < 0.0001$) ($r = 0.68$) and revealed sorting by taxa (Fig. 7). This sorting was made more evident by plotting the mean values of each taxon ($r = 0.94$) (Fig. 6). Sorting was consistent with substrate preference or more precisely substrate use, rather than superfamily, mass or size. Likewise, sexual dimorphism had little effect on the sorting, although behavioral differences among the sexes may have influenced results ($r = 0.88$) (Fig. 8). The arboreal taxa clustered toward the Negative including large bodied taxa such as *N. larvatus* and *P. paniscus*, while the remaining taxa sorted toward the

Positive by increasing terrestrial substrate preference, except *Pongo* spp.*,* which clustered

with more terrestrial taxa, and *M. mulatta*, which clustered with the more arboreal taxa.
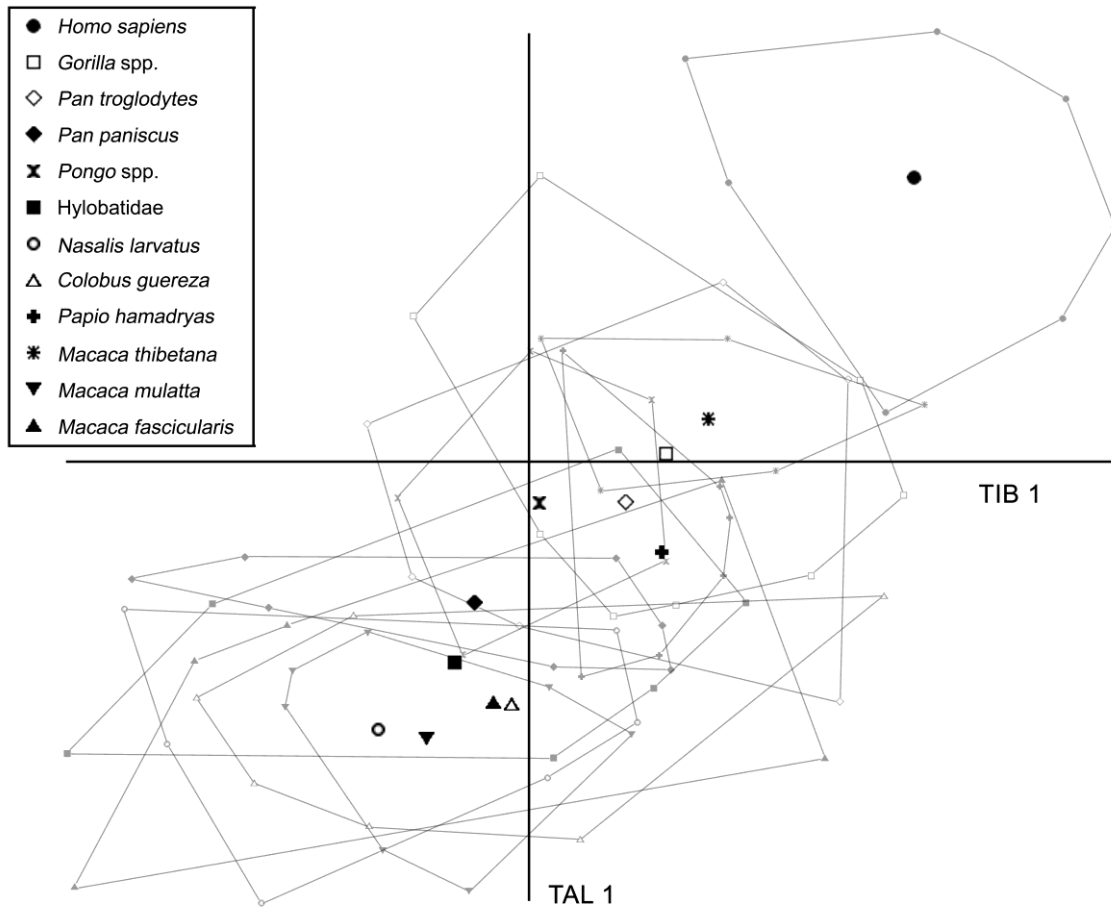
FIGURE 7. Scatter plot showing Singular Warp scores for individual talo-crural joints based on the Singular Warp of Procrustes aligned coordinates. Tibia 1 (TIB 1) is on the X-axis and talus 1 (TAL 1) on the Y-axis. Convex polygons are used to show the range of scatter with individual points hidden for clarity, and the mean values for each taxon recorded.

Visualization

The talo-crural subchondral surfaces were visualized using *Landmark Editor* and

an exemplar surface (*Pan troglodytes*) was warped to fit the estimated configurations.
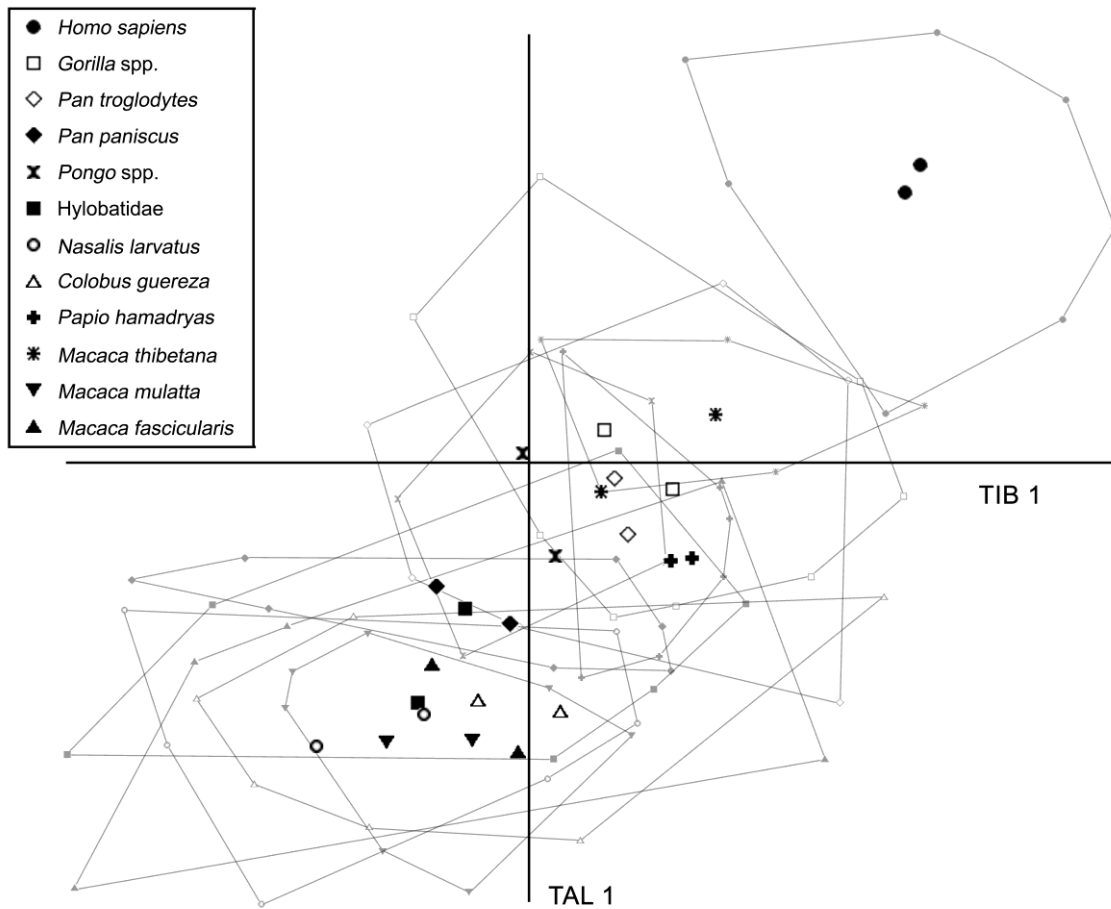
FIGURE 8. Scatter plot using the same method as Figure 6 with the mean male and female values for each taxon recorded.

The shapes related to the arboreal and terrestrial forms are illustrated (Fig. 9). Likewise, the surface (*Pan troglodytes*) was warped to fit the estimated configurations of the Singular Warp vectors (Fig. 10).

Discussion

The talo-crural joint was chosen to examine evidence of homology, homoplasy (convergent evolution), and morphological differentiation (divergent evolution) among catarrhine taxa due to qualities of both its structure and development. It is a well-defined
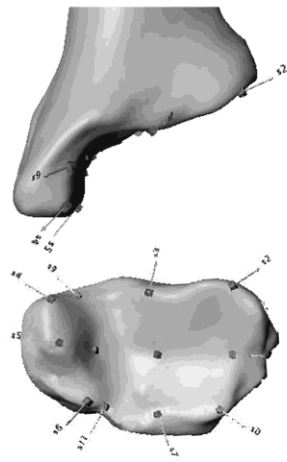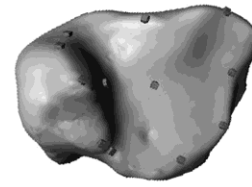
ARBOREAL TERRESTRIAL
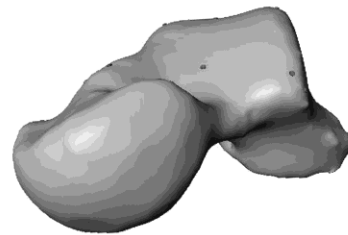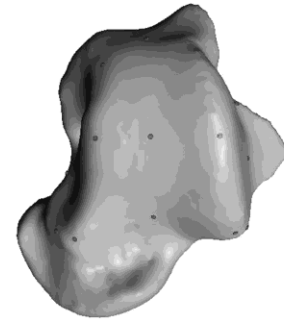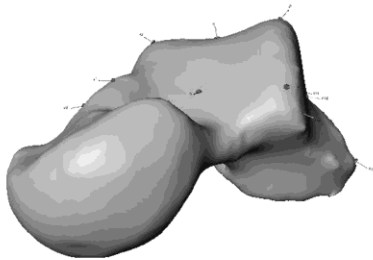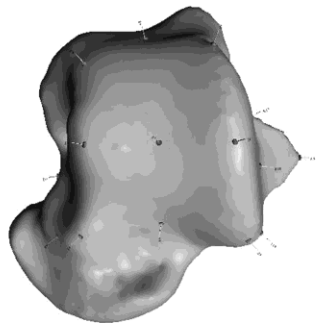
FIGURE 9. Visualization of the appositional articular morphology, the distal tibial and proximal talar surfaces, of the substrate preference variable with the terrestrial and arboreal shapes presented. See methods for details.
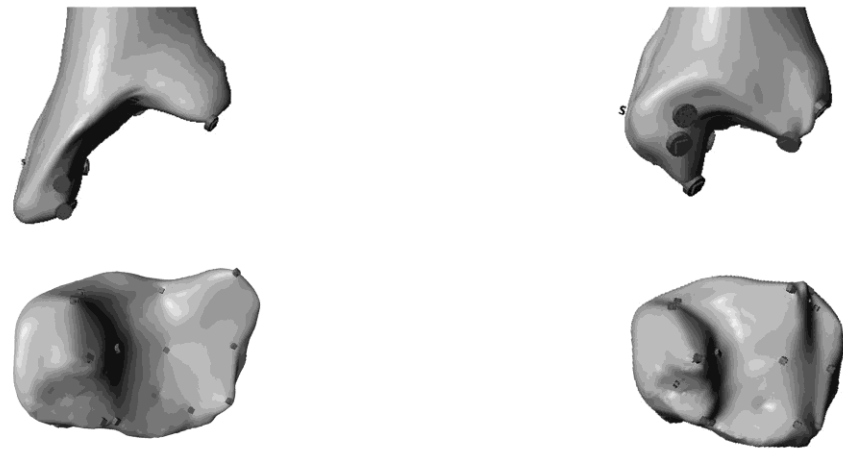
NEGATIVE POSITIVE
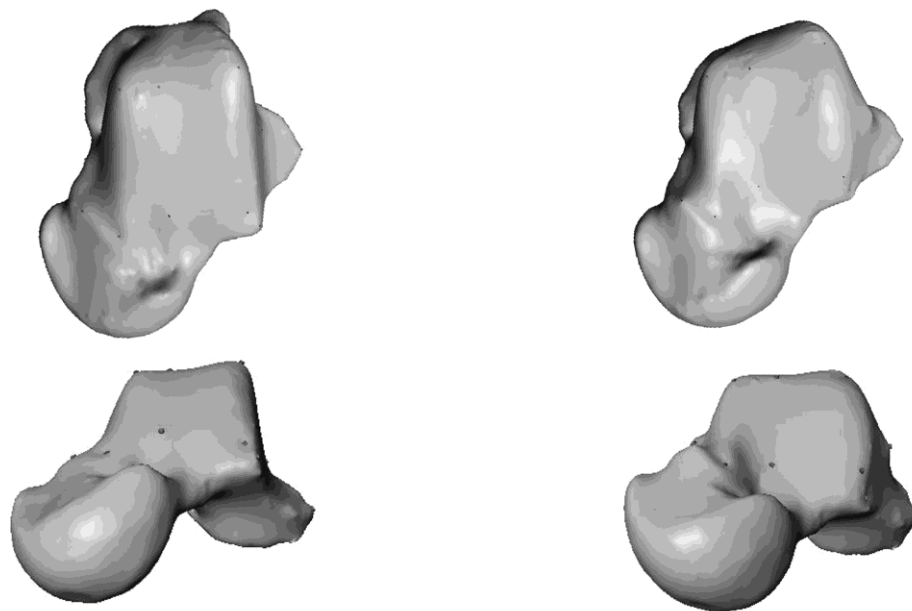
FIGURE 10. Visualizations of the shape change of the Singular Warp of tibia 1 and talus 1 from negative to positive on the X and Y axes, respectively. See methods for details.

component of the primate Bauplan, and conserved and canalized character trait. It is consistent with the designation of a functional unit within the concept of biological role (sensu Bock and von Wahlert, 1965). Further, it has the characteristics of "evolutionary stable units" as proposed by Wagner and Schwenk (2000), character groups which are structural and mechanical, are a composite of morphological components (tibial, talus, and appositional articular shape), and demonstrate internal integration modulating external pressure to change, but providing a mechanism for reorganization of the phenotype in response to such pressures (Schwenk, 2001). During development, it forms the interface of two of the modules of the hindlimb, the zeugopodium proximally, and the autopodium distally (Cachel, 2006). It is the region of greatest developmental modularity evident by the sequencing of ossification centers in the postcranium (Blomquist, 2009). Finally, the appositional articular surface shapes reflect integration, the complex pattern of structural correlation and covariance at the joint interface (Klingenberg, 2008).

This study examined integration of the talo-crural joint by utilizing both singular warp analysis of the matched appositional articular subchondral bone, as well as the more customary relative warps analysis and multivariate regression analysis of each of the matched elements, the distal tibia and proximal talus (Bookstein et al., 2003; Mitteroecker and Gunz, 2009). Using singular warp analysis, we were able to explore information unavailable to prior data analysis (Turley et al., 2011; Turley and Frost, in press). It provided data about the relation of the matched elements, their covariance, allowing inferences as to the relationship of the shapes, and how they work as a coordinated system (Bock and von Wahlert, 1965). The way they are used is influenced

70

by their interrelation, which expresses how the system is integrated; the "intrinsic functional integration" observed by Schwenk (2001) in "evolutionarily stable configurations."

The factors studied functioned as proxy measures to identify signals of the relative importance and interrelationship of the main categories examined: superfamily for phylogeny, mass and size for absolute scale of the studied taxa, and substrate preference for the behavioral interface of the taxa with the environment (Turley et al., 2011; Turley and Frost, in press).

The articular surfaces of the distal tibia and proximal talus were first analyzed separately, since the matched cohort of the current study had additional taxa and a change in sample size from the prior studies (Turley et al., 2011; Turley and Frost, in press). All of the above factors had a significant influence on shape in both the distal tibial and proximal talar subsets ($p < 0.0001$). Substrate preference and superfamily, as in the prior unmatched studies, were major factors, but substrate preference was independent of both proxies for phylogeny and scale (Turley et al., 2011; Turley and Frost, in press). All the great ape taxa were highly canalized, significantly different from each other and all other taxa excepting *Pongo* spp. and Hylobatidae in the distal tibia ($p < 0.001$). *P. hamadryas* likewise was significantly different from most other taxa excepting in the proximal talus of *M. fascicularis* and *M. thibetana.* Hylobatidae were not significantly different from *M. fascicularis* in the proximal talus, but all cercopithecoids excepting *M. mulatta* in the distal tibia. Among the other cercopithecoids, significant differences were observed in shape of *M. thibetana* and both *M. mulatta* and *N. larvatus, M. mulatta* and both

71

colobines, and *M. fascicularis* and *C. guereza* in the proximal talus. These findings were consistent with the highly canalized nature of the two components of the joint complex, but demonstrated the differences evident between superfamilies.

The articular surfaces were then analyzed together using singular warp analysis. The singular warp analysis of the cross-covariance matrix provided important insights into the appositional articular morphology of the studied taxa not evident in the individual analysis. Since the cross-covariance matrix has only the covariances of the matched distal tibial and proximal talar landmark sets without the within-set covariances, morphological integration of the appositional surfaces can be assessed. Figure 7 demonstrates the singular warp summarizing cross-covariation between two sets and integration of the two components of the talo-crural module. The mean values of the studied taxa sorted by the behavioral proxy, substrate preference, rather than phylogeny or scale (Fig. 7) or sex (Fig. 8). Sorting was not evident in the relative warps analysis of the tibial and talar sets. The terrestrial cercopithecoids, *M. thibetana* and *P. hamadryas* sorted with the *H. sapiens*, *Gorilla* spp*., P. troglodytes* and *Pongo* spp*., while large-bodied taxa such as *P. paniscus*, *M. mulatta* and *N. larvatus* sorted with the smaller bodied Hylobatidae, *M. fascicularis* and *C. guereza.*

Several taxa had inconsistencies between substrate preference documented from the literature and the sorting observed (Table 8). The substrate preference of *Pongo* spp*.* is highly arboreal (with females even more so than males); however, its positional behavior (males more so than females) is similar to *Gorilla* spp*.*, and the stresses induced by squatting and arboreal walking suggest the influence of use on the sorting, as well as a

behavioral effect influencing the male cohort greater than the female in Figure 8 (Thorpe and Crompton, 2006; Thorpe et al., 2007). All specimens of *M. mulatta* were from the free-ranging colony at Cayo Santiago, Puerto Rico. Wells and Turnquist (2001) have documented the terrestrial substrate preference (here scored as 6.4) of the adult population, as well as a lesser (4) juvenile preference and the nature of the island habitat. Greater terrestrial use has been suggested in native Asian populations, and the nature of the substrate, both terrestrial and arboreal, in Cayo Santiago versus Asian habitats may influence the findings of the current study (Fleagle, 1999; Goldstein and Richard, 1989; Lindberg, 1980). Finally, the difference observed between *P. paniscus* and *P. troglodytes* is consistent with terrestrial use of only 0.5 in *P. paniscus* observed by White (1992). This may reflect a greater difference in substrate preference than previously documented due to terrestrial provisioning in some prior studies in the *P. paniscus*, and greater terrestrial use (patrolling, etc.) in *P. troglodytes* (Doran, 1992, 1993, 1997).

The singular warp scores also provided potential signals of convergent and divergent evolution. Phylogenetically distant, more terrestrial taxa, such as *H. sapiens*, *M. thibetana*, *Gorilla* spp. and *P. hamadryas*, sorted together, as did both large-bodied arboreal taxa, such as *P. paniscus* and *N. larvatus*, and small-bodied arboreal taxa, such as *M. fascicularis* and Hylobatidae, consistent with homoplasy. Conversely, closely related taxa, such as *P. troglodytes* and *P. paniscus*, as well as *M. thibetana* and *M. fascicularis*, sorted away from each other, suggesting morphological differentiation within these genera.

The etiology of the shape differences observed may be related to both intrinsic and extrinsic influences, the nature of the joint complex itself and its environmental interface. The talo-crural joint is a highly modular and integrated structure consistent with an evolutionary stable configuration—i.e., a functional unit with a biological role (sensu Bock and von Wahlert, 1965; Schwenk, 2001). It is a complex unit consisting of multiple elements, including the synovial fluid and sac, tendons and ligaments, and the cartilaginous surfaces with underlying subchondral bone and appositional articular surfaces (Kelikian, 2011). The interrelation of these elements during development and in the adult organism is reflected in the end point morphology. The development of the joint involves progenitor cells responsible for all its elements (Koyama et al., 2008). The formation of articular cartilage and subchondral bone involves cartilage resorption to a single postnatal articular layer in the former and modeling of the underlying bone by the deep chondrocyte layer (Hunziker et al., 2007; Stempel et al., 2011). Environmental variances have been observed to increase distally in the mammalian limb (Hallgrimsson et al., 2002). Further, the constraints due to covariation have been proposed to be "weak enough" that differences in development of distal components may occur (Young and Hallgrimsson, 2005). Differences in phenotypes reflect genetic variation, and changes in genetic networks are a mechanism proposed for change (Carroll, 2008). Evolutionary developmental theory suggests that these may be due to natural selection for "deep homology," commonality of genetic developmental processes among distantly related organisms (Hall, 2012; Shubin et al., 2009). They also may result from adaptive developmental plasticity manifest by either modification in gene expression or evolving

reactivity to systems responsive to external signals (Beldade et al., 2011; West-Eberhard, 2003, 2005). Conversely, they can result from plasticity, an epigenetic response of bone to strain, producing permanent changes in shape from a behavioral difference altering the mechanical loads experienced (Cobb and O'Higgins, 2004; Singleton, 2012).

This begs the question of whether the phenotypic differences observed among the catarrhine taxa in this study were the result of natural selection or plasticity. Bone morphogenic proteins have been shown to be involved in both joint development and bone remodeling in response to external stimuli (Francis-West et al., 1999; Young and Badyaev, 2007). They are, therefore, likely to be important in both the way natural selection can shape a joint's predisposed developmental pathway and in the way that bone remodels. In terms of remodeling, a chondral response to different loads has also been proposed to shape joints (Frost, 1999). Hydrostatic pressure differences with development and changes in locomotor and postural behavioral activity are a purported mechanism producing a mechanically induced change in shape of the integrated modular structure (Hamrick, 1999a,b). Finally, remodeling of subchondral bone to load and strain has been demonstrated (Hammond et al., 2010).

Thus, the mechanism by which the shape differences observed in the sorting of the singular warps cross-covariance matrices occur remains to be elucidated. However, the developmental timing of the observed differences among the taxa used in this study can provide a lens to separate genetic from epigenetic (Frelat and Mittereocker, 2011). Ontogenetic trajectories can be used to compare taxa as subadults and adults to determine

if sorting by substrate use is consistent throughout (genetic) or changes with behavior during development (epigenetic).

These results demonstrate that Null Hypotheses H-3 and H-4 are rejected since adult appositional shape was significantly affected by the factors studied ($p < 0.0001$) and appositional articular shape was related to substrate (preference) use. The next chapter will explore the ontogeny of appositional articular morphology in subadults, exploring its relation to the finding among adults, and Null Hypotheses H-5 and H-6.

CHAPTER IV

THE ONTOGENY OF TALO-CRURAL JOINT SHAPE

This chapter has been submitted for publication and is co-authored by my advisor Stephen Frost, who provided direction in designing the statistical analysis of the data and the programs used, as well as assistance with the figures. The intellectual content is mine, and I performed all specimen acquisition, processing, and analysis.

The appositional articular morphology, the subchondral surfaces, of the talo-crural joint of adult catarrhine taxa is the interface between organism and substrate, and presents a single articular surface. Differences in shape of this surface allow assessment of this "evolutionary stable configuration," a functional unit with a distinct biological role, and the factors which influence that shape (Schwenk, 2001). The proximal (tibial facets) and distal (talar facets) components have been demonstrated to reflect substrate preference unrelated to phylogeny (Turley et al., 2011; Turley and Frost, in press). Singular Warp analysis of the cross-covariance matrix of these surfaces suggests that this is consistent with differences in substrate use, with evidence of both convergent and divergent evolution of articular shape, among the studied taxa (Turley and Frost, in press).

These shape differences may be explained by either a genetic or epigenetic response to behavior. Deep homology, a genetic response, is characterized by mobilization of traits within the genome due to environmental pressure (Hall, 2003, 2007), while plasticity is an epigenetic response to these same environmental pressures directly and permanently altering shape (True and Haag, 2001; West-Eberhard, 2005). Shape change resulting from the former may be due to selection at the level of the

genome, or cis-regulatory networks (Carroll, 2008; Davidson, 2006), while the latter may result from developmental plasticity, or strain-induced structural remodeling (Frost, 1999; Hamrick, 1999a; Young and Badyaev, 2007). However, as Bookstein et al. (2003) observed, the genetic and epigenetic can be separated by investigating the ontogeny of shape, in this case the development of talo-crural appositional articular morphology.

Dental eruption sequences and, specifically, the timing of molar eruption provide a mechanism by which to compare relative development of diverse taxa (Dean and Wood, 1981; Hillson, 1996; King, 2004; Lukacs, 2009; Schultz, 1935; Schultz, 1960). This method has been used for life history analysis (Dirks and Bowman, 2007; Godfrey et al., 2001; Harvati and Frost, 2007; Kelley and Schwartz, 2010; Lukacs, 2009; Smith, 1994). Using gross categories, such as fully erupted M1, M2 and M3, we can perform a comparison of a sample (e.g., McNulty et al., 2006; Singleton et al., 2010), much as the gross factors of behavior (substrate preference-terrestrial or arboreal), phylogeny (superfamilies), and physical attributes (mass and size) have been used in our prior analysis (Turley et al., 2011).

This study examines a diverse sample of 12 catarrhine taxa. In a previous analysis of adults of the same taxa, evidence of convergent and divergent evolution reflecting substrate use was observed (Turley and Frost, in press). Here we use Singular Warp analysis to examine the appositional articular morphology of the talo-crural joint, using an ontogenetic series, to examine whether a genetic or epigenetic signal is manifest (Bookstein et al., 2003).

Materials and Methods

Sample

Matched distal tibial and proximal talar articular facets from 408 specimens representing 12 catarrhine taxa formed the study sample (Table 14). Ontogenetic stage was assessed by dental development, with specimens divided into groups based on

TABLE 14. Number of Specimens of Different Taxa and Dental Eruption Classification Used in This Analysis with Their Age of Molar Eruption for Male Upper and Lower Dentition (M u/l) and Female Upper and Lower Dentition (F u/l) in the Available Taxa from the Literature Cited

Taxon	M3	M u/l F u/l	M2	M u/l F u/l	M1	M u/l)F(u/l)
Homo sapiens	50	21/20 21/20	8	10.5/12 12/11	16	6.4/6.3 6.4/6.2
Pan troglodytes	54	11/10 11/11	12	6.8/6.5 6.8/6.8	23	3.8/3.3 3.2/3.2
Gorilla sp.	42	11.4/10.4	13	6.8/6.6	13	3.5/3.5
Pongo sp.	10	(~10)	3	(~5)	0	(4.6)
Hylobatidae	12	(4.6)	6	(2.6)	1	(1.2)
Macaca fascicularis	13	5.5/5.5	9	3.5/3.5	5	1.5/1.3
Macaca thibetana	7		0		0	
Papio hamadryas	12	7.1/7.1 7/7	3	4.9/4.9 3.6/3.8	2	1.7/1.7 1.6/1.6
Nasalis larvatus	11		3		5	
Macaca mulatta	12	5.6/5.4 6.4/5.8	9	3.3/3.2 3.4/3.2	11	1.5/1.4 1.4/1.3
Colobus guereza	12		1		4	
Pan paniscus	10	(~11/10)	9	(~6.8/6.5)	7	(~3.8/3.3)

Age of molar eruption obtained from Bolter and Zihlman (2011), Dirks and Bowman (2007), Jogahara and Natori (2012), Kelley and Schwartz (2010), Smith (1994), and Smith et al. (2010).

maxillary and mandibular molar eruption: M1s fully erupted, but not M2s; M2s fully erupted but not M3; or M3s fully erupted. Data were collected and documented by a single observer (KT), and all were without evidence of pathology (Hillson, 1996; Swindler, 2002). Nonhuman specimens had provenience documented, and all were wild-shot or in the case of *Macaca mulatta* a fatality of known age within a free-ranging population. There were 87 M1, 76 M2, and 245 M3 stage specimens (see Acknowledgements for institutional sources) (Table14). Among the M1 subgroup,

M. thibetana and *Pongo* spp. were not represented, with only a single specimen of
Hylobatidae and two specimens of *P. hamadryas*. There were no M2 specimens of
M. thibetana and only one *C. guereza*. There was a minimum of three specimens
represented for analysis for each of the remaining developmental stages of other taxa, and
in most cases significantly more (Table 14).

The taxa were chosen from each of the superfamilies to provide a spectrum of size
and substrate preference, with comparisons possible of both phylogenetically distant and
closely related taxa (Xing et al., 2007). Estimated ages at eruption among the studied taxa
were also obtained from the literature, with the age range of M1 specimens from the age
at M1 eruption to age at M2 eruption, the age range of M2 specimens from the age at M2
eruption to age at M3 eruption, and the age range of M3 specimens, including all those
with M3 erupted (Table 14).

Data Collection

Each specimen was laser surface scanned and digitally reconstructed using either a
Konica Minolta Vivid 910 Noncontact 3-D Digitizer and Geomagic Studio 8 software, or
a NextEngine Desktop 3-D Scanner and ScanStudio HD software. All specimens were
photographed with distal tibial plafond and proximal talar trochlear, medial and lateral
facets documented. A *Gorilla* spp. sample is illustrated in M1, M2, and M3 (Fig.11).

Twenty-seven landmarks were placed: 12 on the distal tibial facets, and 15 on the
proximal talar facets, using Landmark Editor software by a single observer (KT). These
landmarks were illustrated in our prior publication examining the shape of the tibia and
and Figure 2 for the talus (Turley et al., 2011, Fig. 1).

80

M1

M2

M3
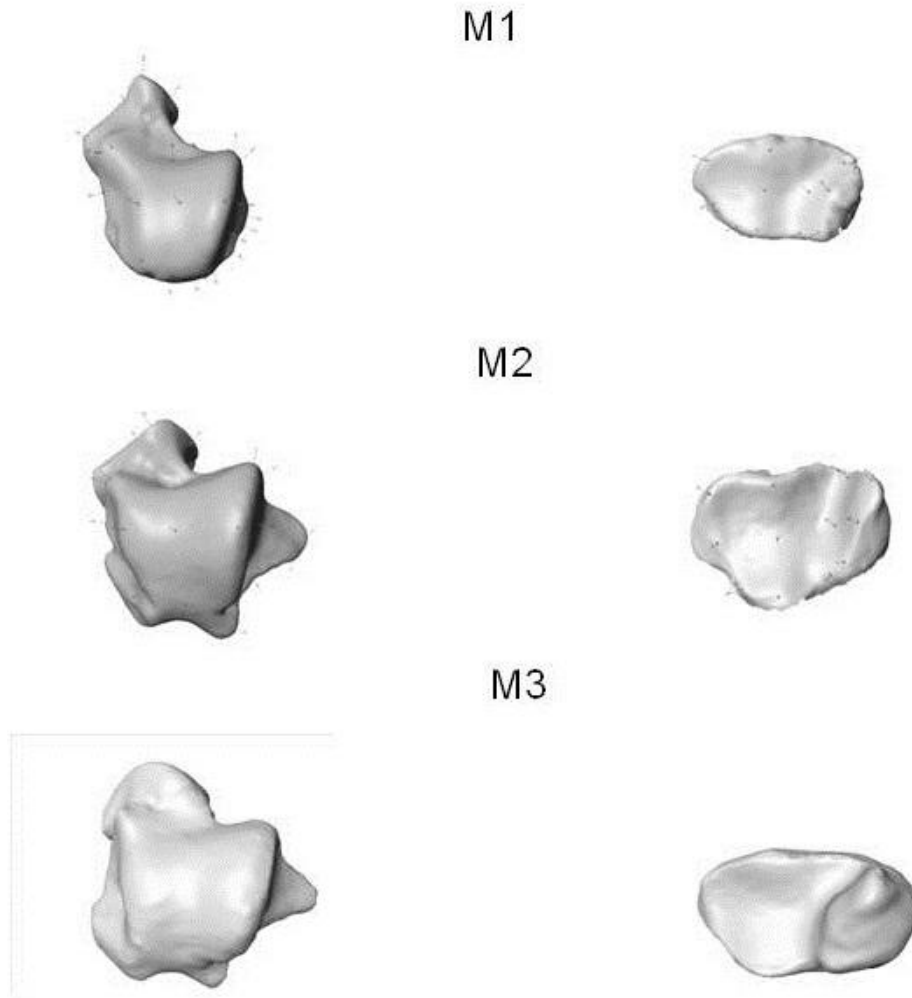
FIGURE 11. Visualization of the appositional articular morphology, the distal tibial and proximal talar surfaces, of *Gorilla* spp., at M1, M2 and M3 dental eruption stages.

Observational error was previously assessed in both the tibial and talar subsets using single specimens of *Homo sapiens* landmarked ten times (Turley et al., 2011; Turley and Frost, in press). Principal component analysis demonstrated tight clustering of the repeated measures compared to variation within and among the taxa studied. This study, like the prior examinations of tibial and talar shape, involves variation above the species level; thus, precision was deemed satisfactory.

Generalized Procrustes Analysis

Generalized Procrustes Analysis (GPA) was performed using Morpheus (Slice, 1998). GPA superimposes landmark configurations and removes variance due to position and rotation, and scales each to unit centroid size (Rohlf and Slice, 1990). Centroid size is the square root of the sum of the squared distances of each landmark to the centroid (Rohlf and Slice, 1990) and is stored as a separate variable during GPA. Centroid size was transformed to its natural logarithm for subsequent analysis. GPA was done with reflection allowed, since our data set included both the right and left specimens. Separate GPAs were performed for the tibial and talar landmark subsets at each developmental stage. All subsequent statistical analyses were performed using SAS 9.1 (SAS, 2006). As GPA-aligned coordinates have a very high correspondence with their Euclidean tangent space projections, unprojected aligned coordinates were used. Shape differences among landmark configurations were measured by Procrustes distance, the Pythagorean distance between the two Procrustes superimposed landmark configurations (Bookstein, 1991; Turley et al., 2011).

Relative Warps Analysis

Relative warps analysis, principal component analysis (PCA) of shape coordinates, was performed separately on each developmental stage (M1, M2, M3) on the covariance matrix of the GPA superimposed landmark coordinates, and used as a data-reduction and exploration technique (Bookstein, 1991; Neff and Marcus, 1980). Here it is used with the components unweighted, although classically it weights the components by bending energy (Bookstein, 1991). Initial visualization of the effect on shape described by

each Principal Component (PC) both within and among superfamilies was performed using Morphologika software (O'Higgins, 2006; O'Higgins and Jones, 1998).

Permutation Test

Differences in shape between individual taxa were assessed using pair-wise permutation tests with 1,000 replicates performed in M1, M2, and M3 cohorts for each landmark subset. Equal random samples were drawn and randomly permuted across the two taxa, and Procrustes distance was calculated between the permuted groups' means. The α was the fraction of permuted values that were greater than the actual Procrustes distance between group means (Good, 2000). Results were reported with a Bonferroni-adjusted significance level for each (Turley et al., 2011).

Singular Warp Analysis

Singular Warp analysis of the cross-covariance matrix of the appositional articular shape was used in this study to explore the relation of the matched surfaces of the distal tibial facets and proximal talar facets in the total set and each subset, M1, M2, and M3. This is the application of Partial Least Squares within morphometrics which computes two unit vectors such that the covariance is a maximum. It describes how two sets of variables covary with each other, as it were a "submatrix" of the covariance matrix (McNulty, 2009). In this case, shape coordinates from the tibia form one matrix and shape coordinates from the talus the other that have the greatest mutual linear predictive power (Bookstein et al., 2003: Frost et al., 2003; Harcourt-Smith et al., 2008; Rohlf and Corti, 2000). A scatter plot of Singular Warp of the cross-covariance matrix of the appositional articular shapes was plotted for the total set M1, M2, and M3, as well as each subset.

83

Likewise, scatter plots of comparative groups, as well as their means, were also plotted. The correlation "r," a measure of integration, was computed for each (Bastir and Rosas, 2005; Bookstein et al., 2003).

Visualization

Visualization of shape differences in the Singular Warp and Relative Warps were accomplished by calculating the landmark configurations in Morpheus and warping an exemplar surface to fit those landmark configurations using Landmark Editor (Turley et al., 2011). The Singular Warp were visualized for the individual subsets.

Results

Relative Warps Analysis

Table 15 provides the Relative Warps analysis of the distal tibial and proximal talar matched subsets. The eigenvalues and cumulative percentage of variance are consistent with analysis of matched M3 and unmatched distal tibial and proximal talus data previously reported, with 66% of the distal tibial and 70% of the proximal talar variance accounted for by PC 1-5 in M1, 59% of the distal tibial and 74% of the proximal talar variance accounted for by PC 1-5 in M2, and 57% of the distal tibial and 58% of the proximal talar variance accounted for by PC 1-5 in M3 (Turley et al., 2011; Turley and Frost, in press). The plots of the PCs of shape differences separated the studied taxa consistent with prior studies (Turley et al., 2011; Turley and Frost, in press)

Permutation Tests

Table 16 demonstrates the highly canalized appositional articular shape observed in the end-point morphology, the adult phenotype (M3), of the talo-crural joint among the

TABLE 15. Eigenvalues of the Covariance Matrices

	#	Eigenvalue	Proportion	Cumulative
Proximal talus M1				
	1	0.00695923	0.2754	0.2754
	2	0.00465039	0.1840	0.4594
	3	0.00231500	0.0916	0.5510
	4	0.00148169	0.0586	0.6097
	5	0.00127649	0.0505	0.6602
Distal tibia M1				
	1	0.00555278	0.2309	0.2309
	2	0.00508707	0.2115	0.4424
	3	0.00296729	0.1234	0.5658
	4	0.00179995	0.0748	0.6407
	5	0.00142449	0.0592	0.6999
Proximal talus M2				
	1	0.00593943	0.2582	0.2582
	2	0.00248037	0.1078	0.3660
	3	0.00224326	0.0975	0.4635
	4	0.00150366	0.0654	0.5289
	5	0.00141811	0.0616	0.5905
Distal tibia M2				
	1	0.01130777	0.3917	0.3917
	2	0.00403331	0.1397	0.5314
	3	0.00243688	0.0844	0.6158
	4	0.00192315	0.0666	0.6824
	5	0.00163059	0.0565	0.7389
Proximal talus M3				
	1	0.00440300	0.1761	0.1761
	2	0.00342392	0.1369	0.3130
	3	0.00237089	0.0948	0.4078
	4	0.00228114	0.0912	0.4991
	5	0.00186439	0.0746	0.5736
Distal talus M3				
	1	0.00394096	0.1798	0.1798
	2	0.00284317	0.1297	0.3095
	3	0.00260989	0.1191	0.4285
	4	0.00161724	0.0738	0.5023
	5	0.00160665	0.0733	0.5756

TABLE 16. Shape Differences Observed Among Taxa (M3)

	Hs	Pt	Pp	Go	Po	Hy	Ph	Mt	Mm	Mf	Nl	Cg
PTAM3												
Hs	x	0.137169	0.167772	0.136219	0.162395	0.176359	0.165887	0.156942	0.19985	0.181042	0.187819	0.184896
Pt	0	x	0.132431	0.08582	0.135616	0.111888	0.103169	0.138457	0.150009	0.121468	0.112119	0.13477
Pp	0	0	x	0.131379	0.174043	0.131496	0.190634	0.205859	0.161659	0.146405	0.120273	0.127912
Go	0	0	0	x	0.146726	0.139816	0.149287	0.162694	0.167246	0.147005	0.142743	0.150476
Po	0	0	0	0	x	0.179089	0.135621	0.178923	0.159916	0.157528	0.172174	0.180283
Hy	0	0	0	0	0	X	0.13518	0.144598	0.107109	0.084933	0.104387	0.112304
Ph	0	0	0	0	0	0	x	0.11096	0.130911	0.101148	0.140774	0.156833
Mt	0	0	0	0	0	0	0.003	x	0.172245	0.133692	0.172787	0.182571
Mm	0	0	0	0	0	0	0	0	x	0.076496	0.123089	0.129038
Mf	0	0	0	0	0	0.022	0.009	0.003	0.031	x	0.095597	0.11087
Nl	0	0	0	0	0	0	0	0	0	0.008	x	0.070306
Cg	0	0	0	0	0	0	0	0.001	0	0	0.004	X
DTIM3												
Hs	x	0.112804	0.216696	0.118074	0.154055	0.132218	0.124443	0.105229	0.14531	0.116794	0.146904	0.119843
Pt	0	x	0.175353	0.08864	0.128465	0.089939	0.120938	0.120938	0.14174	0.116047	0.113637	0.121467
Pp	0	0	x	0.195862	0.185001	0.152872	0.25908	0.208287	0.212776	0.205784	0.209981	0.215299
Go	0	0	0	x	0.144878	0.103357	0.110994	0.14676	0.140298	0.131241	0.132223	0.138707
Po	0	0	0	0	x	0.10154	0.18938	0.147133	0.174123	0.136902	0.135596	0.126558
Hy	0	0	0	0	0.001	x	0.147402	0.12571	0.109584	0.087515	0.085828	0.094012
Ph	0	0	0	0	0	0	x	0.138875	0.126414	0.120481	0.131353	0.137048
Mt	0	0	0	0	0	0.003	0	x	0.135698	0.102789	0.139942	0.112904
Mm	0	0	0	0	0	0	0	0	x	0.112904	0.098634	0.105909
Mf	0	0	0	0	0	0.019	0	0.015	0.05	x	0.083964	0.069489
Nl	0	0	0	0	0	0.033	0	0	0	0.044	x	0.07666
Cg	0	0	0	0	0	0.007	0	0.002	0	0.133	0.089	x

Procrustes distance between taxon means are shown above the diagonal and P values below the diagonal (1,000 permutations). Legend: *Hs = Homo sapiens*; *Pt = Pan troglodytes*; *Pp = Pan paniscus*; *Go = Gorilla spp.*; *Po = Pongo spp.*; Hy = Hylobatidea; *Ph = Papio hamadryas*; *Mt = Macaca thibetana*; *Mm = Macaca mulatta*; *Mf = Macaca fascicularis*; *Nl = Nasalis larvatus*; *Cg = Colobus guereza.*

catarrhine taxa examined. The humans and all great apes were significantly different from all other taxa with the exception of *Pongo* spp. and Hylobatidae (tibial plafond) with a Bonferroni-adjusted significance level of $p < 0.00008$. Hylobatidae were significantly different from all cercopithecoids excepting *M. fascicularis* in the proximal talus, but only *P. hamadryas* and *M. mulatta* in the tibial plafond. Among the cercopithecoids, *P. hamadryas* differed from all excepting *M. thibetana* and *M. fascicularis* in the proximal talus, *M. thibetana* differed from *M. mulatta* and *N. larvatus* in both subsets, *M. mulatta* from the colobines, and *M. fascicularis* from *C. guereza* in the proximal talus.

The subadult shape comparisons do not demonstrate this degree of shape difference, reflecting both immaturity of subchondral bone development (most marked in the human and great ape samples, i.e., ossification of the medial malleolus in *H. sapiens* age 8 years) and small sample size among specific taxa (*C. guereza*, *N. larvatus*, *P. hamadryas*, *M. fascicularis* [M1], *Pongo* spp. and Hylobatidae) in both M1 (Table 17) and M2 (Table 18). Significant differences were observed in the M1-aged proximal talus subset between all taxa with samples ($N > 4$) excepting *P. troglodytes* and *P. paniscus*, and in the tibial plafond subset excepting *H. sapiens* and *M. fascicularis*, *P. troglodytes* and *Gorilla* spp. and *P. paniscus*, and *M. fascicularis* and *M. mulatta* with a Bonferroni-adjusted significance level of $p < 0.003$ (Table 17). Among taxa with samples ($N > 4$) of M2 specimens, significant differences were observed in the proximal talus subset between all taxa excepting *P. troglodytes* and P. *paniscus*, and *M. fascicularis* and *M. mulatta*, and in the tibial plafond subset excepting *P. paniscus* and *Gorilla* spp., *P.*

troglodytes and *M. fascicularis*, and *M. fascicularis* and *M. mulatta* with a Bonferroni-

adjusted significance level of $p < 0.003$ (Table 18).

TABLE 17. Shape Differences Observed Among Taxa (M2)

	Hs	*Pt*	*Pp*	*Go*	*Mm*	*Mf*
PTAM2						
Hs	x	0.114496	0.135425	0.135425	0.204151	0.194288
Pt	0	x	0.071753	0.107179	0.178005	0.154212
Pp	0	0.047	X	0.112579	0.153079	0.143593
Go	0	0	0	x	0.167415	0.173576
Mm	0	0	0	0	X	0.084117
Mf	0	0	0	0	0	x
DTIM2						
Hs	x	0.116979	0.101681	0.129911	0.10802	0.117738
Pt	0.001	x	0.073884	0.081653	0.124036	0.158323
Pp	0	0.022	X	0.111891	0.140551	0.152103
Go	0	0.011	0	x	0.13888	0.184899
Mm	0	0	0	0	X	0.135774
Mf	0.36	0	0	0	0.005	x

Procrustes distance between taxon means are shown above the diagonal and P values below the diagonal (1,000 permutations). Legend: *Hs = Homo sapiens*; *Pt = Pan troglodytes*; *Pp = Pan paniscus*; *Go = Gorilla spp.*; *Mm = Macaca mulatta*; *Mf = Macaca fascicularis.*

TABLE 18. Shape Differences Observed Among Taxa (M1)

	Hs	*Pt*	*Pp*	*Go*	*Mm*	*Mf*
PTAM1						
Hs	x	0.145704	0.207202	0.145352	0.176798	0.198720
Pt	0	x	0.090229	0.108895	0.138422	0.160323
Pp	0	0.01	x	0.150524	0.161298	0.169686
Go	0	0	0	x	0.173542	0.204727
Mm	0	0	0	0	x	0.092893
Mf	0	0	0.002	0	0.005	x
DTIM1						
Hs	x	0.133459	0.118959	0.189351	0.129948	0.183420
Pt	0	x	0.052803	0.109481	0.106568	0.146983
Pp	0	0.52	x	0.098545	0.103145	0.150278
Go	0	0.001	0.038	x	0.160566	0.179303
Mm	0	0	0	0	x	0.113984
Mf	0	0.001	0.012	0.002	0.107	x

Procrustes distance between taxon means are shown above the diagonal and P values below the diagonal (1,000 permutations). Legend: *Hs = Homo sapiens*; *Pt = Pan troglodytes*; *Pp = Pan paniscus*; *Go = Gorilla spp.*; *Mm = Macaca mulatta*; *Mf = Macaca fascicularis.*

Singular Warp Analysis

Figure 12 plots the scores of the 408 specimens from all three age cohorts examined for the first Singular Warp (tal1-tib1) of the cross-covariance matrix ($p < 0.0001$; $r = 0.66$) with the mean values for each taxon recorded ($p < 0.0001$; $r = 0.79$). Sorting of the taxa by substrate use in the M3 cohort was observed with the arboreal *N. larvatus*, *M. mulatta*, *M. fascicularis*, *C. guereza*, *P. paniscus* and Hylobatidae separating from *H. sapiens*, *M. thibetana*, *P. hamadryas*, *Gorilla* spp., *P. troglodytes* and *Pongo* spp. (Turley and Frost, in press). The shape differences are presented in Figure 13.

Figure 14 is a scatter plot ($p < 0.0001$; $r = 0.8$) of the means ($p < 0.0001$; $r = 0.91$) of the second Singular Warp (tal2-tib2) with sorting of the African hominoids from cercopithecoids, except *H. sapiens*, which sorted with the cercopithecoids. *Pongo* spp. and Hylobatidae were on the fringe of the latter cluster. Of note, PC-2 of both the talus and tibia in prior studies was associated with the shape of the apposing trochlea facets, in particular, the anterior margin, and the shape of the medial talar crest and the curvilinear shape of the medial malleolar-trochlear groove critical in stabilizing the joint in vertical climbing. The sorting of the second Singular Warp was again consistent with substrate use. A visualization of the shape differences represented by the second Singular Warp is shown in Figure 15, as well as a visualization of warped composite African apes surfaces from the Relative Warps data, and a picture of a representative *Gorilla* spp. scanned surfaces. The similarity of the latter with the warped visualization of the negative pole of the distribution of the second Singular Warp scores is observed.
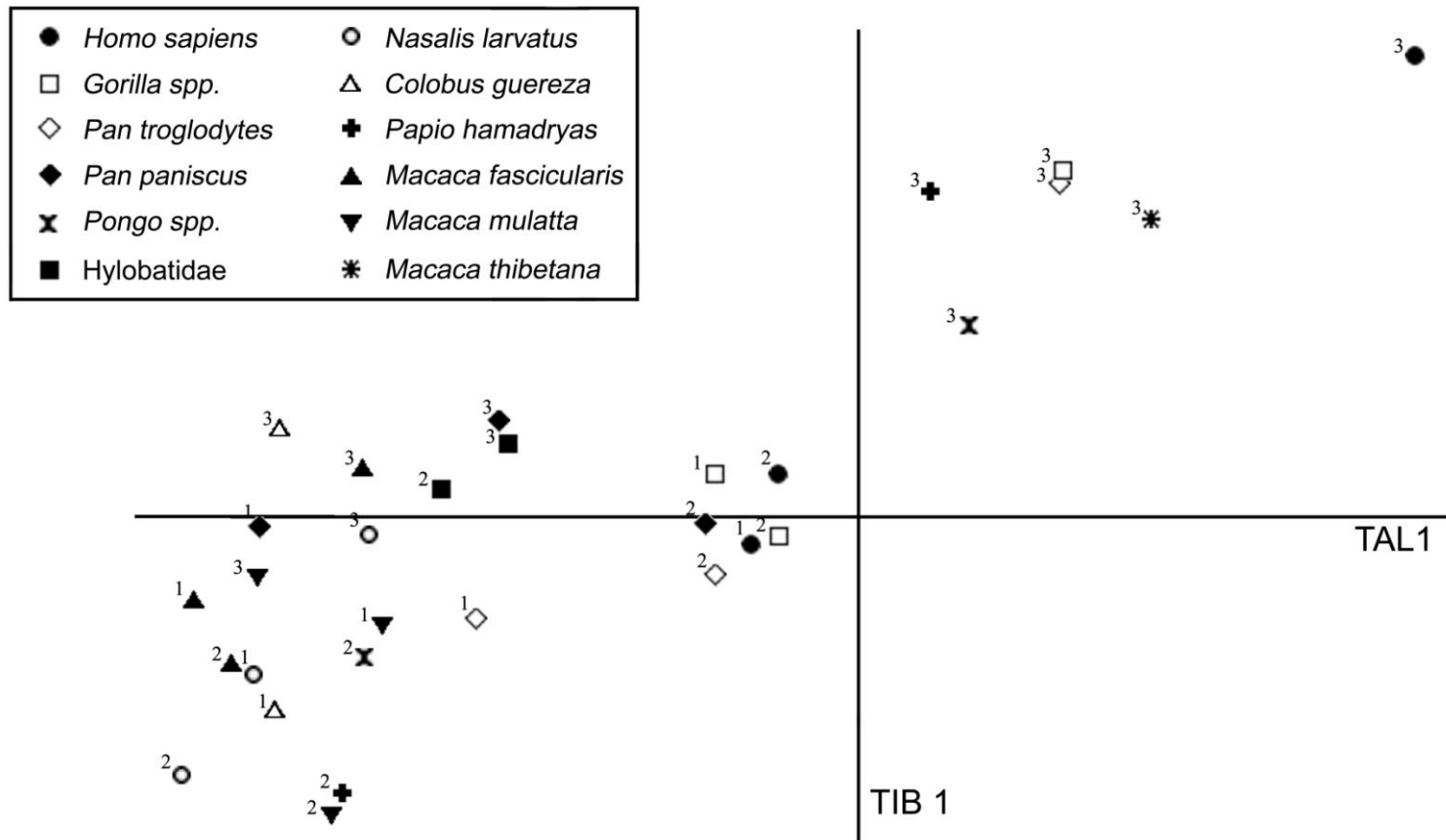
FIGURE 12. Scatter plot demonstrating the first Singular Warp mean scores for the 408 individual talo-crural joints based on the Singular Warp of Procrustes aligned coordinates. Tibia 1 (TIB 1) is on the X-axis and talus 1 (TAL 1) on the Y-axis. M1 (1), M2 (2), and M3 (3) mean values for each taxa: *H. sapiens*, *Gorilla* spp., *P. troglodytes*, *P. paniscus*, *Pongo* spp., Hylobatidae, *P. hamadryas*, *M. thibetana*, *M. mulatta*, *M. fascicularis*, *N. larvatus*, and *C. guereza* are recorded.
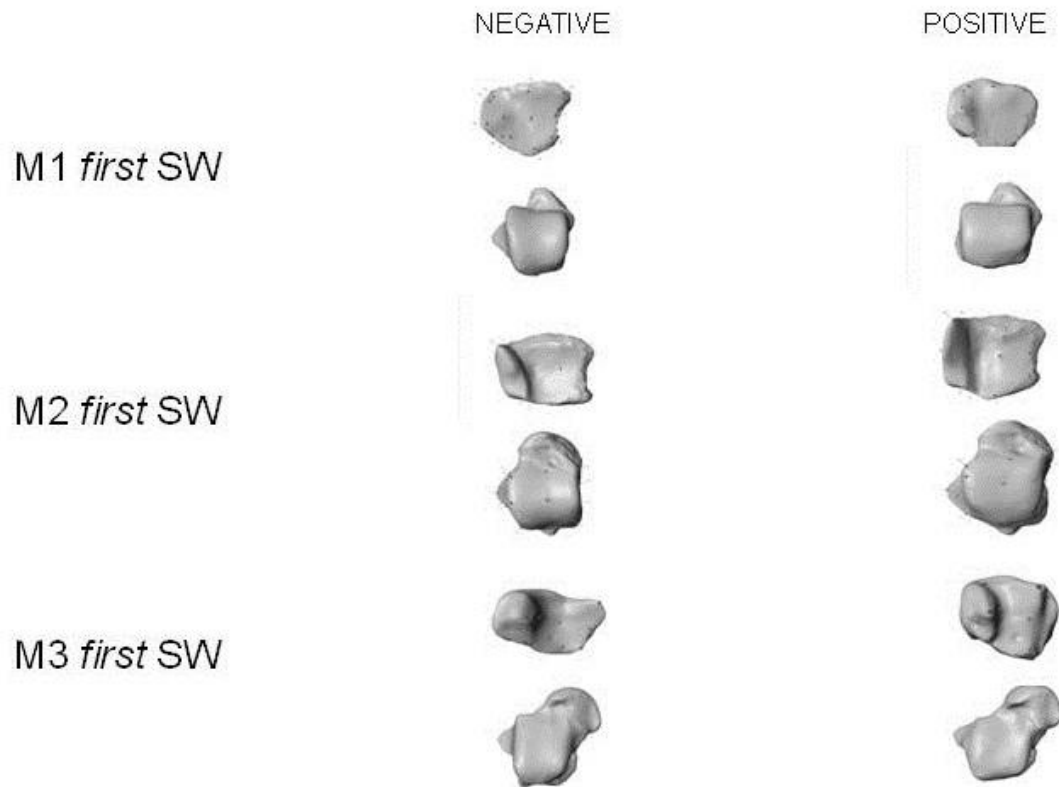
FIGURE 13. Visualizations of the shape change of the first Singular Warp (SW) of the M1, M2, and M3 subsets from negative to positive on the X and Y axes, respectively. See methods for details.

A scatter plot of the M1 scores in taxa with three or more specimens from the Singular Warp analysis of the cross-covariance matrix was highly significant ($p < 0.0001$; $r = 0.81$), as were the mean scores for the taxa ($p < 0.0001$; $r = 0.87$). Sorting into three clusters, *H. sapiens* and *Gorilla* spp., both species of *Pan* and *N. larvatus*, and *M. mulatta*, *M. fascicularis*, and *C. guereza*, was observed in the scatter plot of M1 (Fig. 16). The shape differences of the first singular warps are presented in Figure 13. The second singular warp demonstrated no sorting ($p < 0.04$; $r = 0.66$).
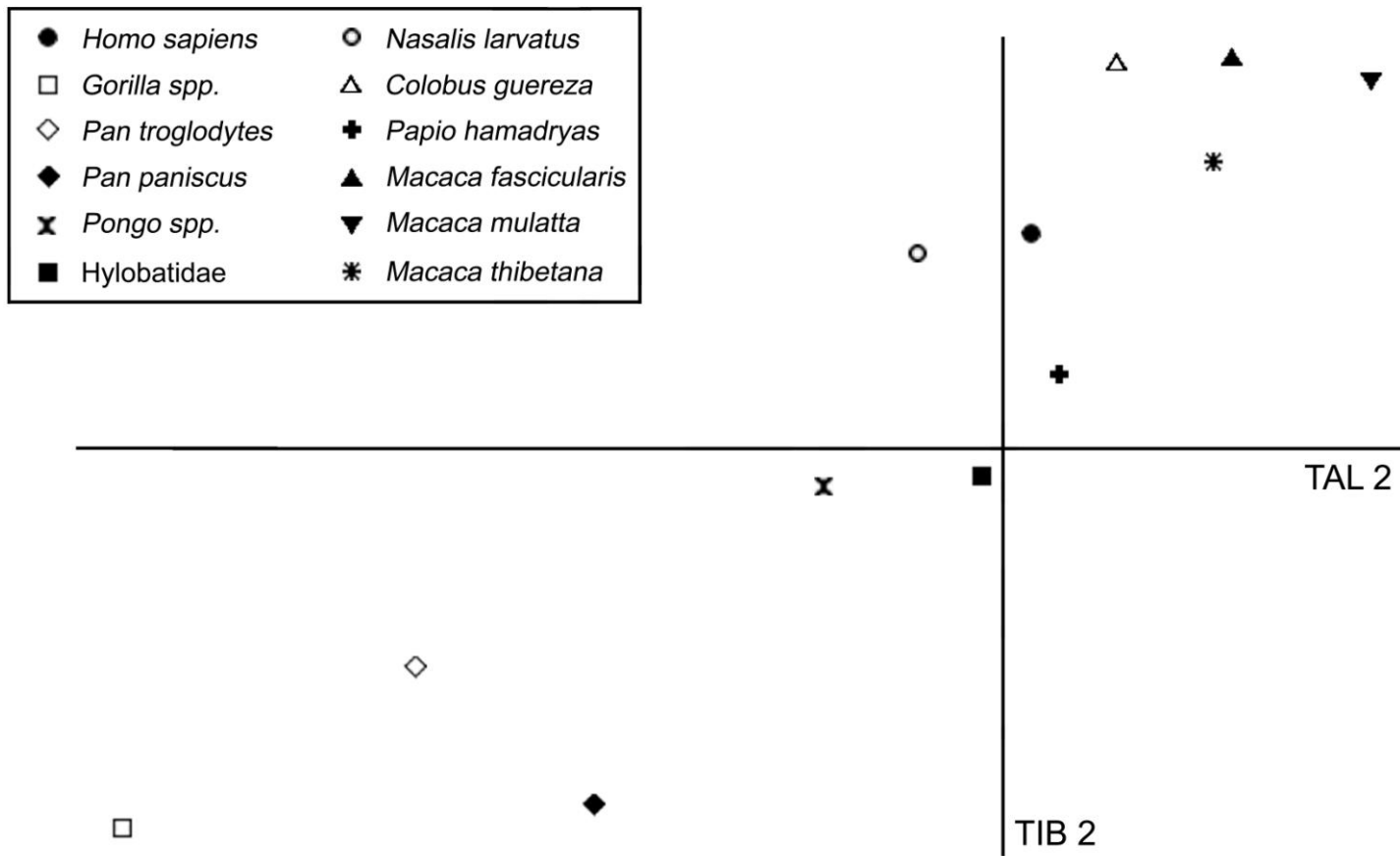
FIGURE 14. Scatter plot of the second Singular Warp scores of the M3 mean values of the studied taxa, Tibia 2 and Talus 2.
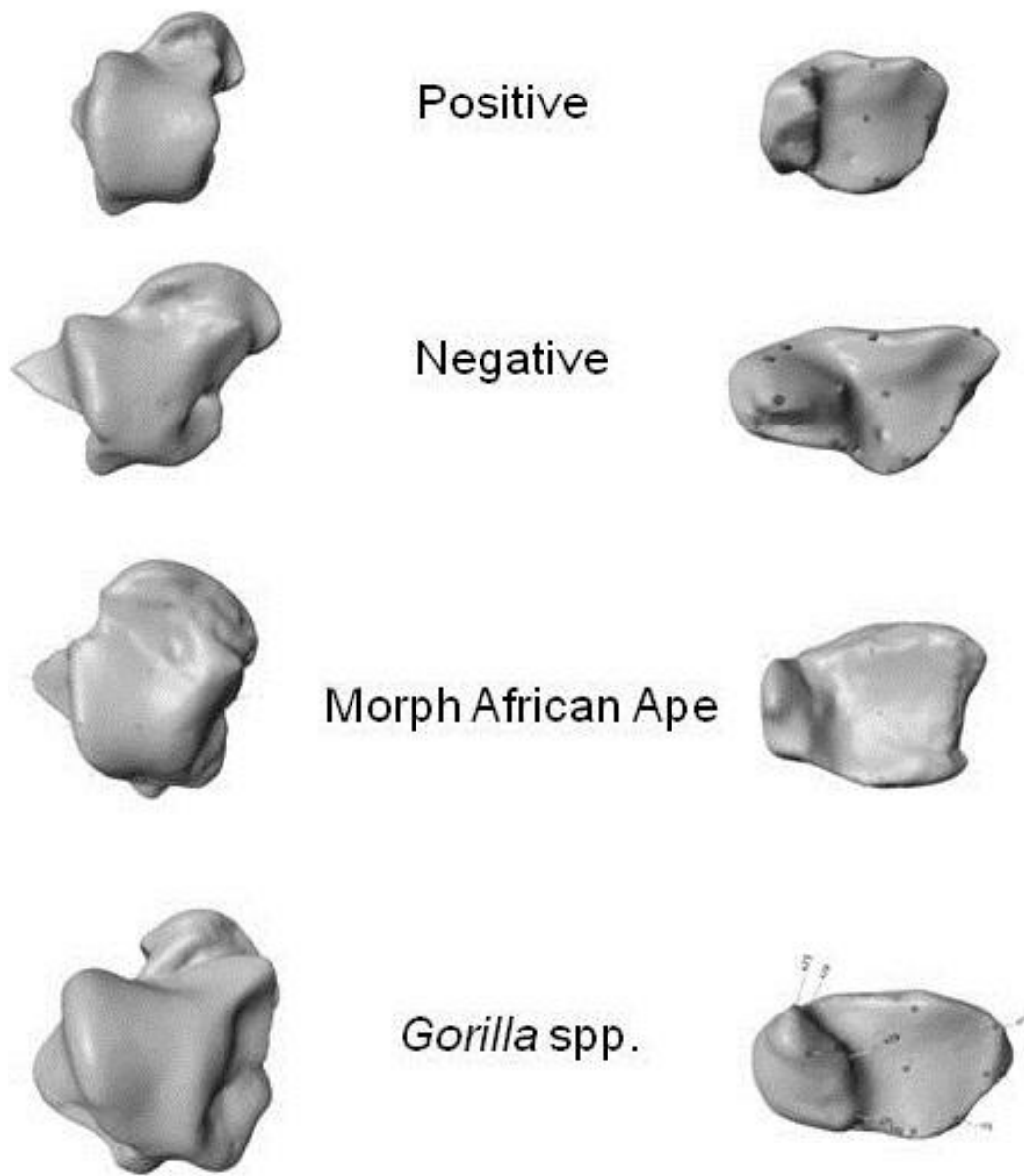
FIGURE 15. Visualizations of the shape change of the second Singular Warp of the M3 sample from negative to positive on the X and Y axes, respectively. See methods for details. Visualizations of the Relative Warps of the African apes (*Gorilla* spp., and *Pan* spp.) appositional articular morphology morphed to an exemplar surface. See methods for details. Visualization of a representative M3 *Gorilla* spp. laser scan digital reconstruction.

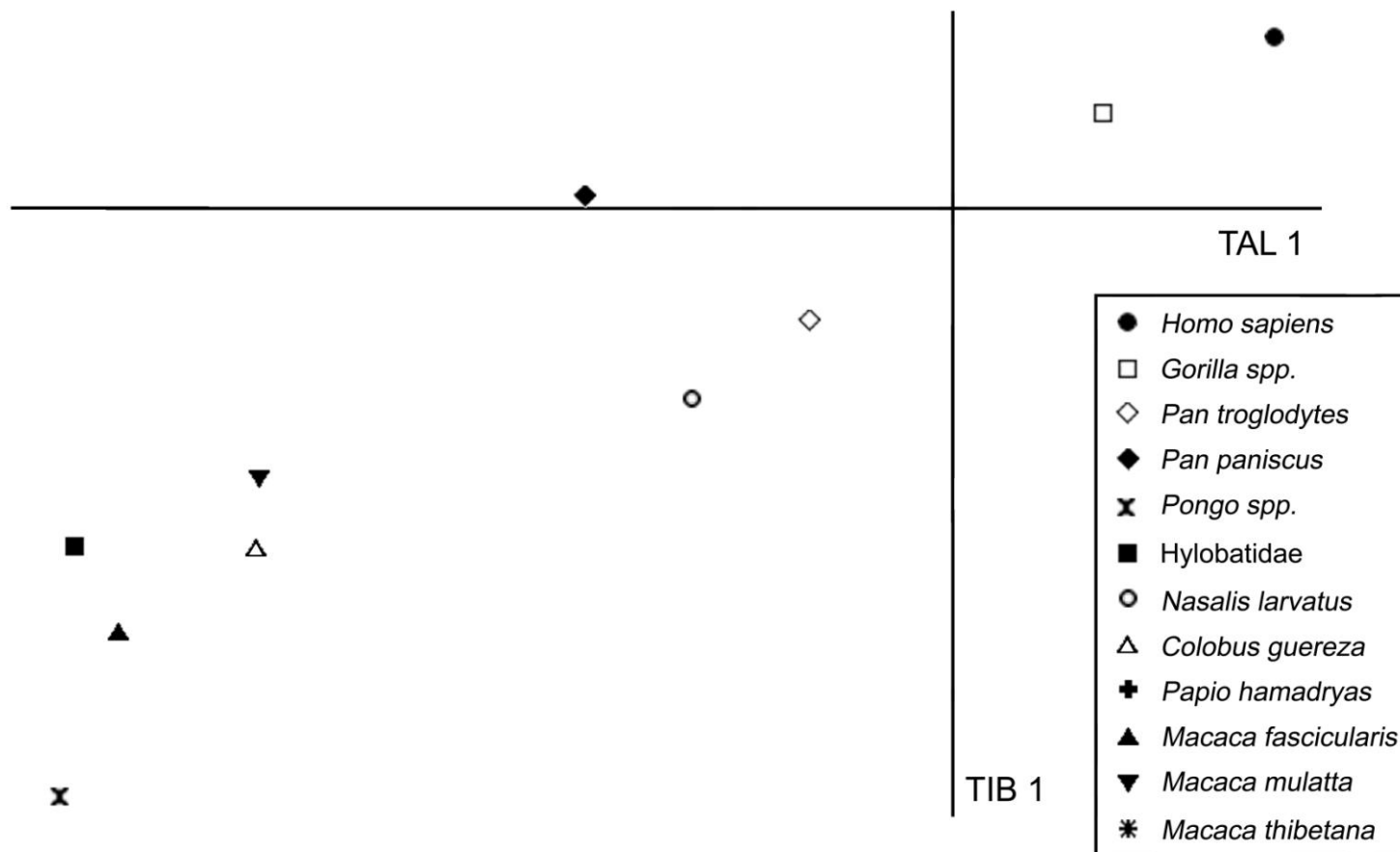FIGURE 16. Scatter plot of the first Singular Warp scores of the M1 sample mean values.

The scatter plot of scores from the M2 cohort was again highly significant ($p < 0.0001$; $r = 0.72$). Taxon means scores ($p < 0.001$; $r = 0.87$) revealed separation of Hylobatidae, *Pongo* spp., *P. hamadryas*, *M. mulatta*, *M. fascicularis*, and *N. larvatus* from the cluster of *H. sapiens*, *Gorilla* spp., and both species of *Pan* as observed in the combined scatter plot of M1, M2 and M3, in which the clustering of the latter four with M1 *H. sapiens* and *Gorilla* spp. was evident (Fig. 12, Fig. 17). Shape differences are shown in Figure 13. The second singular warp demonstrates no sorting ($p < 0.007$; $r = 0.75$).

Figures 18 and 19 are scatter plots of the mean scores of the Singular Warp analyses of the cross-covariance matrix for all three cohorts (M1-3) of the hominoid and cercopithecoid subsets, respectively. The hominoid regression was highly significant ($p < 0.0001$; $r = 0.83$) and demonstrated sorting of M3 specimens of *Pongo* spp., *H. sapiens*, *Gorilla* spp., and *P. troglodytes* by terrestrial use, and Hylobatidae and *P. paniscus* by arboreal use, with the latter moving from a cluster in M2 of other African hominoids. The cercopithecoid regression was, likewise, highly significant ($p < 0.0006$; $r = 0.8$), and with clustering of all the subadults and the arboreal adults. One African terrestrial taxa, *P. hamadryas*, and one Asian terrestrial taxa, *M. thibetana*, sorted with the hominoid terrestrial taxa.

Discussion

The appositional articular morphology, or the shape of the subchondral surfaces of the talo-crural joint, has been previously demonstrated to reflect substrate use (Turley and
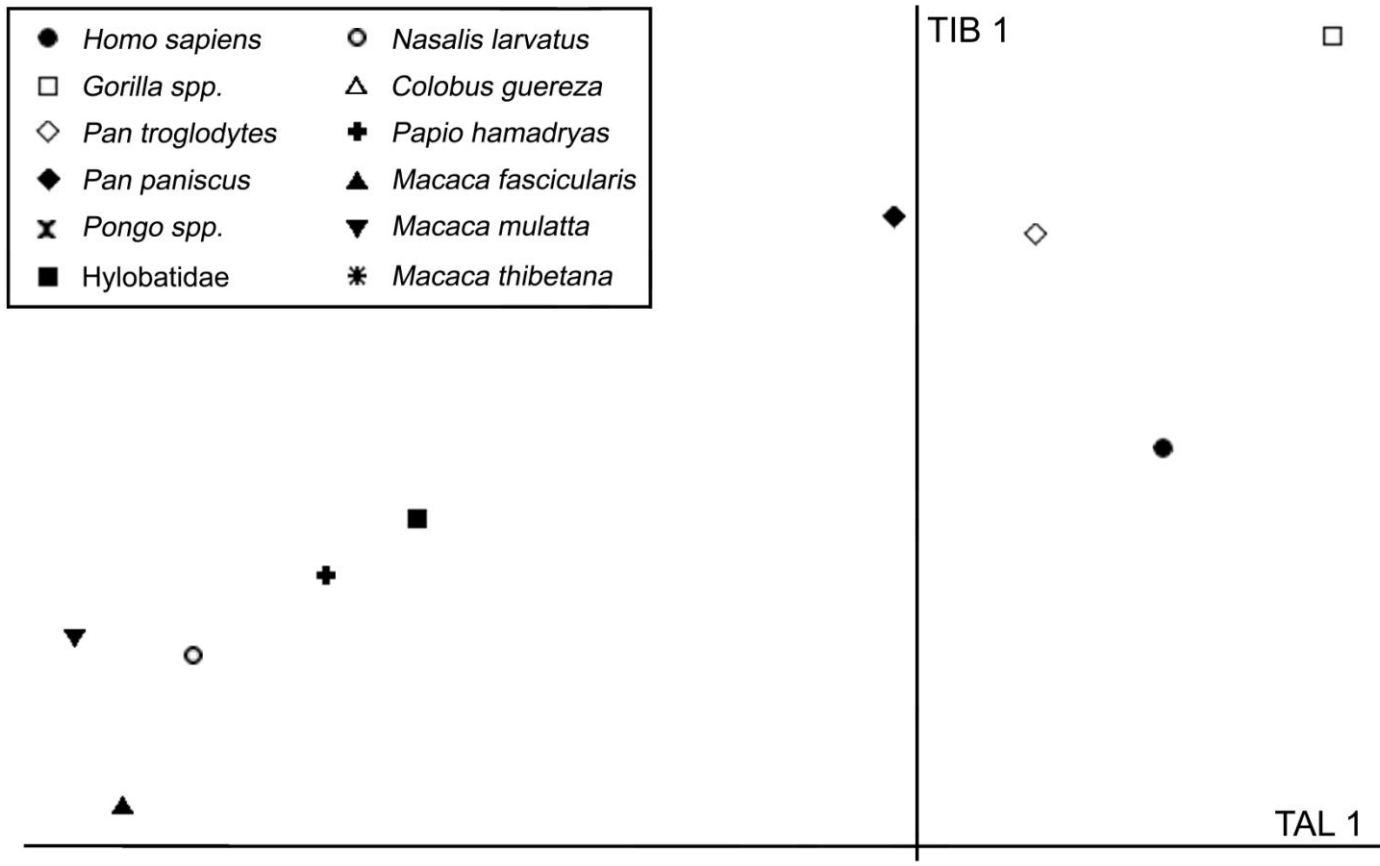
FIGURE 17. Scatter plot of the first Singular Warp scores of the M2 sample mean values.
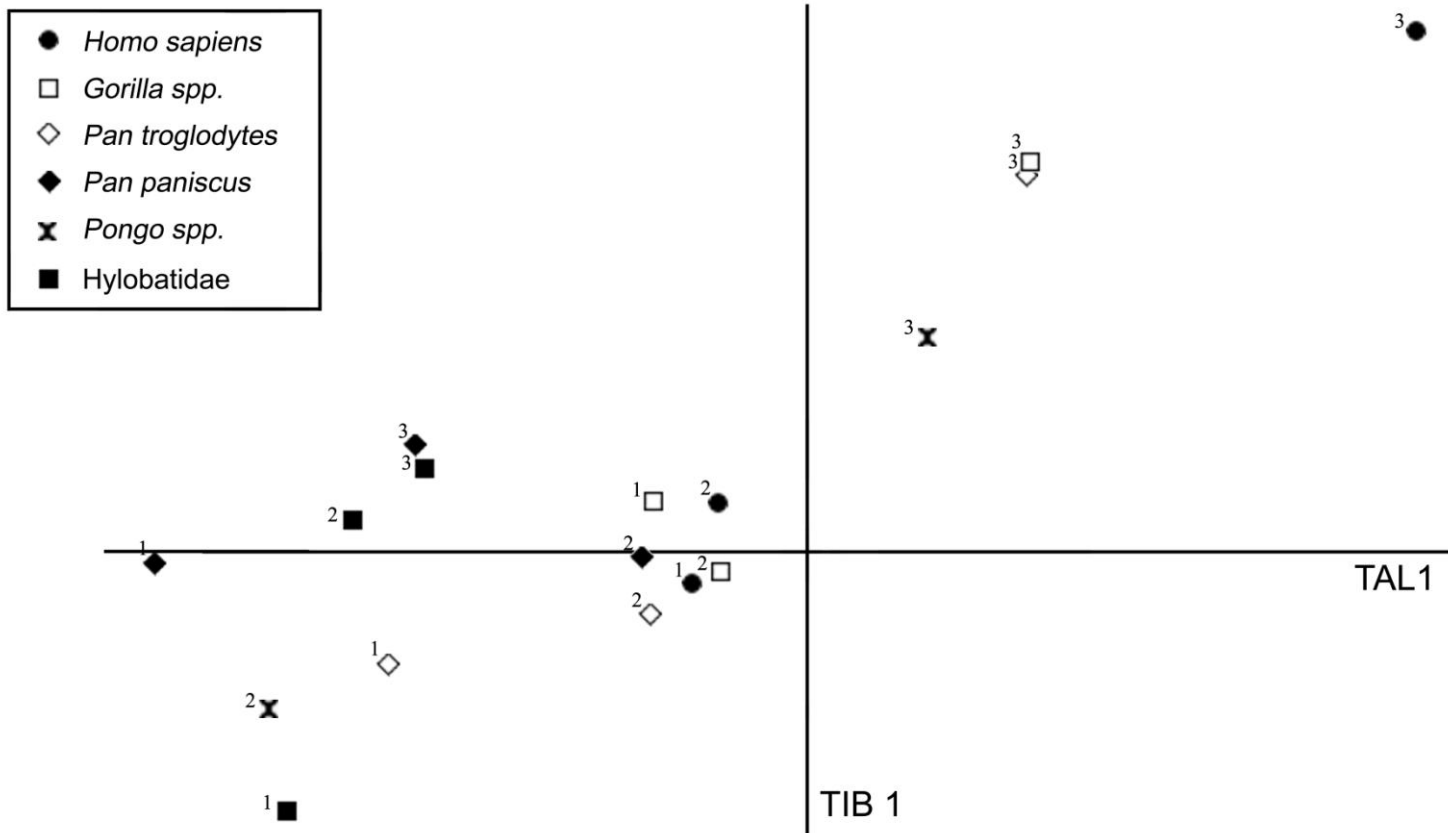
FIGURE 18. Scatter plot of the first Singular Warp scores of the M1, M2 and M3 hominoid taxa mean values.
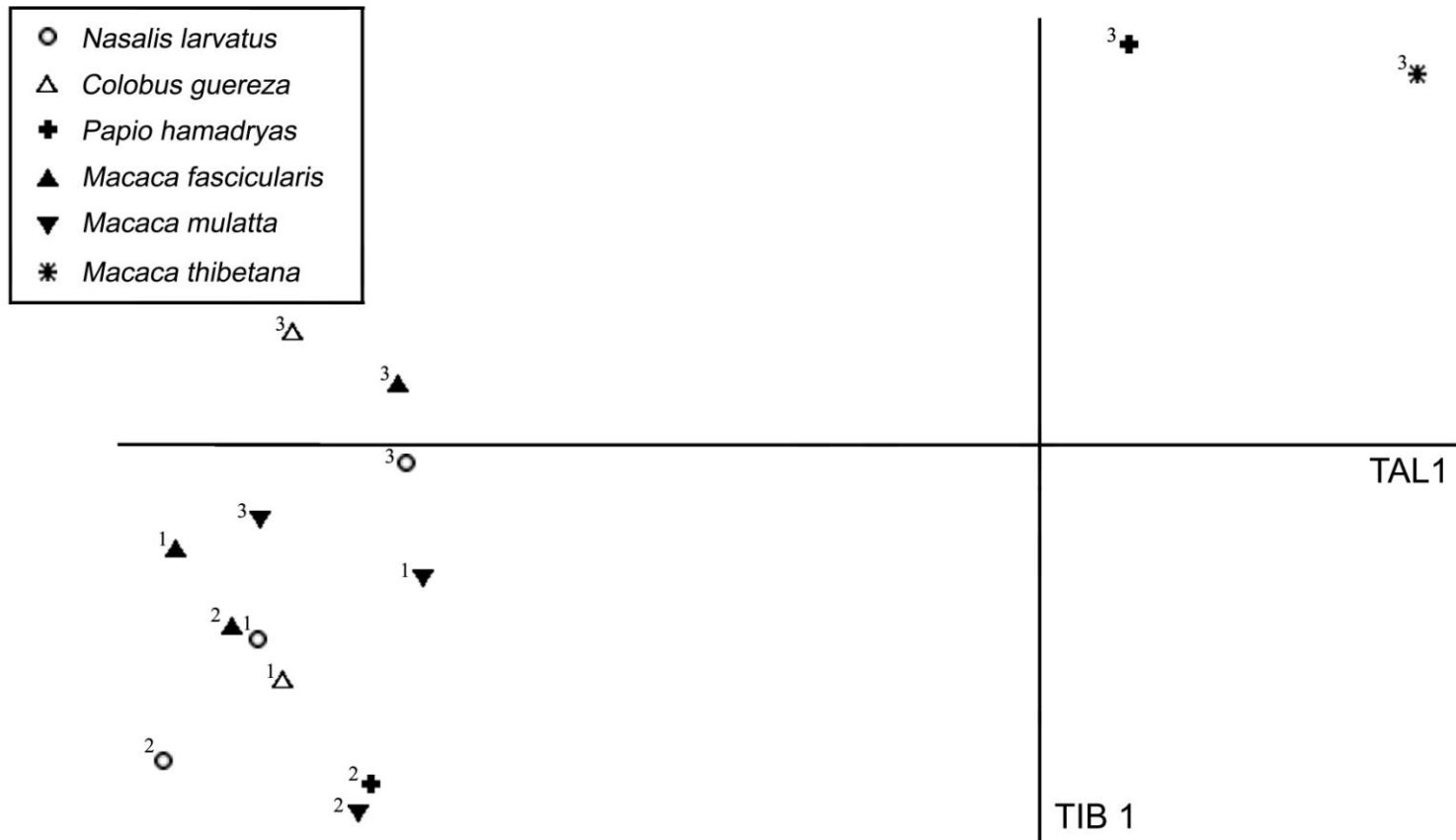
FIGURE 19. Scatter plot of the first Singular Warp scores of the M1, M2 and M3 cercopithecoid taxa mean values.

Frost, in press). In that study, signals of both convergent evolution in joint shape between superfamilies, and divergent evolution of joint shape between closely related species, was observed. In order to explore whether these findings represent a genetic or epigenetic effect, Singular Warp analysis, as employed by Bookstein et al. (2003), to examine the ontogeny of shape, was used to compare subadult and adult specimens and determine if shape was consistent across ontogeny (a genetic signal) or change in shape (epigenetic signal) was observed (Bookstein et al., 2003, Frelat and Mittereocker, 2011).

The study design employed the timing of molar eruption to compare relative development of a diverse taxonomic sample (Dean and Wood, 1981; Hillson, 1996; King, 2004; Lukacs, 2009; Schultz, 1935; Schultz, 1960; Winkler, 1996). Prior use of categories based on molar eruption have validated its use in hominoid taxa; however, the methodology was extended, as proposed by King (2004), to Cercopithecoidea and Hylobatidae (Dean and Wood, 1981; Jogahara and Natori, 2012; Lukacs, 2009; Winkler, 1996). The reported ages of molar eruption among sample taxa are cited from the literature in Table 14. Consistent with "Schultz's rule," as articulated by Smith (2000), the molars, which Schultz characterizes as "additions" to the deciduous teeth, as opposed to permanent "replacement" teeth, develop later in longer lived, larger, and slower developing species, and conversely, the "replacement" teeth erupt earlier. When the sample used in the current study was examined, the Hylobatidae and Cercopithecoidae molar eruption timing was earlier, and *Papio hamadryas*, the largest of the latter superfamily, was the longest of that superfamily documented in the literature. However, the differences between superfamilies and size appear to have been manifest in the

resolution that prolonged development provides to the examination of shape change. In all taxa, landmarks were evident, but in the longest living and slowest maturing hominoids, as exemplified by *Homo sapiens*, the greatest immaturity of subchondral bone was observed. Joint development involves the complex interaction of subchondral bone formation with the articular cartilage functioning as a "surface growth plate" for the underlying bone (Hunziker et al., 2007). In *Homo sapiens*, the medial malleolus begins ossification at 3-5 years with completion at 8 years of age, the distal tibial epiphysis fuses at 14-18 years, and talar articular facets are not clearly delineated until 6 years of age (Scheuer and Black, 2000). Further, ossification of the ankle and dental development do not appear to be closely related across catarrhines (Winkler, 1996). Yet, in the Singular Warp analysis of the M1 cohort the shape change of *Gorilla* spp. and *Homo sapiens* were comparable to M2, and clustering of both species of *Pan* with them by M2 was noted, consistent with a possible genetic signal among these taxa. In the remaining taxa, all clustered together consistent with a genetic signal among subadult terrestrial, and both subadult and adult arboreal cercopithecoids and hylobatids.

Life history parameters among catarrhines include dental eruption, lifespan, brain size, age of weaning, diet, menarche, and age of first reproduction (Godfrey et al., 2001). In humans, developmental milestones encompass both the physical, such as height, weight, and head circumference, and the behavioral, such as crawling, standing, and walking (modes of locomotion, and substrate use) at specific points (ages) in ontogeny (Kliegman et al., 2007). Such milestones may apply to the physical development and behavioral change observed within the context of catarrhine life history (Inouye, 1994;

Leigh and Shea, 1995; Reichard and Barelli, 2008; Robbins et al., 2004; Ross, 1998;

Wells and Turnquist, 2001). Each taxon presents a specific developmental profile of their

interaction with the physical world. These include parental care, early activity,

interactions with peers, change in body size and musculature, and maturity among many,

and the timing and duration of activities within multiple age groups. These have been

studied in humans across numerous cultures, as well as in *Gorilla* spp., *Pan troglodytes*,

Pan paniscus, Hylobatidae, *Macaca mulatta*, and *Papio hamadryas* and potentially

impact joint shape (Breuer et al., 2009; Dirks and Bowman, 2007; Doran, 1992, 1993,

1997a,b; Goldstein and Richard, 1989; Hutchinson and Fletcher, 2010; Lindberg, 1980;

Reichard and Barelli, 2008; Remis, 1995; Sarrafian and Kelikian, 2011; Thorpe and

Crompton, 2006; Wells and Turnquist, 2001). Unfortunately, it was beyond the scope and

resolution of this study to correlate such profiles with the ontogeny of ankle shape;

however, the onset of specific modes of locomotion (i.e., human bipedalism at

approximately 1 year of age (Kliegman et al., 2007), or dramatic changes in body mass

(i.e., *Gorilla* spp. [50 kg.]) at approximately 3 years of age (Leigh and Shea, 1995) may

have resulted in M1 clustering, and the later M2 clustering of *Pan* spp. (30-40 kg. at 10

years) due to such epigenetic stimuli (Leigh and Shea, 1995).

The mechanism of epigenetic effects manifest in bone and joint shape is suggested

by the theories and experimental results in the field of "mechanobiology" (Hammond et

al., 2010). In bone, osteocytes and osteoblasts are the mechano-responsive elements, and

in cartilage chondrocytes, these respond to strain and hydrostatic pressure through the

mediation of signaling molecules (Ehrlich and Lanyon, 2002; Frost, 1999; Hammond et

101

al., 2010; Hamrick, 1996, 1999b; Ravosa et al., 2007; Wu and Chen, 2000). Bone morphogenetic proteins represent a potential mechanism at the cellular and subcellular level for a postnatal response of cartilage and subchondral bone to environmental stimuli and Young and Badyaev have proposed that such BMP-mediated skeletal adaptations may reflect the evolution of reactivity of BMPs to external signals (Young and Badyaev, 2007).

In the current study, talo-crural shape differences in subchondral bone were observed among closely related taxa and similarities among distantly related taxa, most notably in the adult (M3) subset (Turley and Frost, in press). Sorting of taxa by substrate use in the first and second singular warp strongly suggests an epigenetic signal in the adults (M3). A behavioral effect was identified, with changes in subchondral bone shape observed during ontogeny. These changes reflect changes in the interaction of taxa with the environment altering phenotypic expression. The sorting by substrate use also suggests the potential for expression of adaptive developmental plasticity producing the dramatic differences in talo-crural joint in closely related taxa (Beldade et al., 2011; West-Eberhard, 2003).

This study could be improved by expanding the sample sizes and the diversity of the entire cohort, but, in specific, the subadult specimens, increasing the power for the pair-wise comparisons, and providing further insights into the ontogenetic changes observed. Likewise, the implications of these results on studies of the fossil assemblage and its phylogenetics need to be examined.

In conclusion, Singular Warp analysis examining the integration of an "evolutionary stable configuration," the talo-crural joint, demonstrated the influence of substrate use on appositional articular shape in the study taxa (Bookstein et al., 2003). A genetic signal was observed in the subadult subsets, while an epigenetic, behavioral signal was manifest in the adult (M3) subset, reflecting how loads were applied to the joint complex rather than the nature of the habitat. The sorting of joint shape and change with ontogeny suggests evidence consistent with the concept of adaptive developmental plasticity.

These results demonstrate that Null Hypotheses H-5 and H-6 are rejected since subadult appositional shape was different from adult appositional articular shape, most markedly in the terrestrial taxa, and it was related to substrate (preference) use. The final chapter will discuss the results of these studies in light of the history of the study of the talo-crural joint, its embryology, the relation to life history parameters in the taxa studied and possible mechanisms for the findings observed, as well as their implications within the context of evolutionary-developmental theory and the significance of genetic and epigenetic signals in both extant and fossil assemblages.

CHAPTER V

DISCUSSION AND CONCLUSIONS

The construction of theoretical frameworks in evolutionary biology finds its origin

in the work of Jean-Baptiste Lamarck. Gould has characterized him as the "primary

evolutionary theorist" since his theoretical context and development has influenced

subsequent evolutionary theory (Gould, 2002). *Philosophie Zoologique* was published in

1809, the year of Darwin's birth. In this systematic theoretical framework for

understanding evolution, Lamarck envisioned two processes. The first was the

development of more and more complex forms; and the second, adaptation through use

and disuse of a character as a result of interaction with the organism's environment

(Gould, 2002). It is this second process and its association with soft inheritance (traits

acquired during one's lifetime due to interaction with the environment and passed on to

future generations) which has been most identified with him. Georges Cuvier, a

vertebrate paleontologist, and an opponent of evolutionary theory, introduced the concept

of extinction, and more important for this dissertation, the Bauplan or form of the

organism (Delson et al., 2000b).

Fifty years later, Darwin and Wallace proposed the theory of evolution due to

natural selection (Watson, 2005). Within this context, environment functioned to

determine if a trait was beneficial, with the outcome of extinction or reproductive

success. The anatomist Richard Owen, an opponent of evolution, provided the term

homology to its lexicon (Watson, 2005). "Homoplasy" (similarity resulting from

independent evolution) was added by Lankester and phylogeny (pattern and history of

decent of organisms) by Haeckel (Mayr, 2001). Finally, the germ plasm theory of Weisman in 1896 separated the germ line (evolution) from the soma (development) (Hall, 2012).

The subsequent fifty years were marked by the development of the field of embryology, and the rediscovery of Gregor Mendel's 1865 manuscript on genetics by deVries Correns and Tschermak in 1900 with development of that field (Watson, 2005). However, evolutionary theory, genetic and natural history studies followed separate courses until the 1940s. Then in rapid succession through the work of Mayr, Simpson and Huxley, a "modern synthesis" was proposed, combining evolutionary theory and genetics, to be followed in the postwar era with the synthesis and description of DNA function (Mayr, 2001; Watson, 2005). An important contribution germane to this dissertation, which first appeared in 1917, and then, as a second edition in 1942 at the time of this synthesis, was D'Arcy Thompson's *On Growth and Form* (Thompson, 1917, 1942). Gould observes that Thompson relates change in shape with growth to the physical forces encountered (Gould, 2002). These changes alter the Bauplan in response to interaction with the physical world, producing changes in its geometry. Thompson constructed "transformation coordinates" to illustrate these, much like the "thin plate splines" of Bookstein, and the visualizations employed in this dissertation (Bookstein et al., 2003).

The last fifty years have seen the development of the field of molecular genetics with increasing understanding of the workings of its mechanisms. However, parallel to this development has been the recognition of epigenetics (environment and developmental influences on the genomic development of the phenotype). The epigenetic

105

landscape was Waddington's metaphor for the influence of the environment on development. He termed this effect on the phenotype "genetic assimilation" (Hall, 2012). The theme has expanded and forms the basis for evolutionary developmental biology and many of the concepts proposed in the current dissertation, in specific, the influence of deep homology, as in the morphogenetic protein system, genetic regulatory networks, as in chondral development, epigenetic inheritance systems and developmental plasticity (Cole, 2011; Gissis and Jablonka, 2011; Hallgrimsson and Hall, 2015; Jablonka and Lamb, 1995; West-Eberhard, 2003). Hall observes that understanding these "Lamarckian" topics, such as soft inheritance, within the context of ecology and behavior links form and function with the individual's environment (Hall, 2012).

The turn of the twentieth century saw a burgeoning of interest in evolutionary biology (comparative anatomy), genetics and embryology (Jablonka and Lamb, 1995). The ankle joint was addressed in the early literature in comparative anatomy, with interest in the origins of bipedalism in humans. Gregory, Keith and Morton all agreed on a hylobatid ancestor, but differed in whether it developed into a more *Pan*-like precursor (in the former two) or something more *Gorilla*-like (in the latter) (Gregory, 1916; Keith, 1923; Morton, 1924, 1935). Wood-Jones proposed a "tarsoid-like ancestor" while Schultz a more "generalized ape" (Harcourt-Smith and Aiello, 2004; Langdon, 1985; Wood-Jones, 1929; Schultz, 1930).

Comparative studies by Morton, in multiple primate taxa *Pan* and *Gorilla*, and by Elftman and Manter in *Pan* demonstrated differences in their respective taxa in talar shape and angulation (Elftman and Manter, 1935; Morton, 1935). Studies were extended

to the fossil assemblage and multivariate analysis applied to both extant primate tali and

fossil specimens (Kidd et al., 1996; Lisowski, 1967; Lisowski et al., 1974; Lisowski et

al., 1976; Oxnard, 1972). Concurrently, Lewis expanded the understanding of the

function and phylogenetic history of the ankle joint, (Lewis, 1980, 1989). Ankle anatomy

in both semiplantigrade, plantigrade and bipedal ankle articular surfaces among extant

and fossil taxa has been explored by Gebo (1992), Gebo and Sargis (1994), and Latimer

et al. (1987), with all using standard measurements and angles. Finally, Harcourt-Smith

(2002) introduced the use of geometric morphometrics for examination of talus, and

Turley et al. (2011) for examination of the tibia. This methodology was used in the

current study to avoid the problems, detailed by both authors, associated with scaling and

multiple angular measurements (Harcourt-Smith, 2002; Turley et al., 2011).

The embryology of the talo-crural joint involves the interplay of structural,

cellular and subcellular elements in the developmental process. The first of these, the

gross embryology of the foot and leg, was examined by Bardeen (1905) at the turn of the

20th century. Using Streeter's subsequent division of the embryonic period into 23 stages

or horizons, Sarrafian and Kelikian observe that Bardeen found that the mesenchymal

stage of the foot and ankle developed in horizon 18, the primitive cartilaginous stage in

horizon 19, and a well-developed cartilaginous stage in horizon 23 between 6 and 9

weeks of age (Bardeen, 1905; Streeter, 1942; Sarrafian and Kelikian, 2011).

The limbs develop from buds on which a ridge of ectoderm forms at the apex

covering mesenchymal cells (Scheuer and Black, 2000). This apical ectodermal ridge

(AER) forms a "progress zone" at the tip which is active until the most distal structures

(digits) are formed (Johnson and Tabin, 1997). Three axes, the proximodistal, craniocaudal, and dorsoventral, are determined by signaling from the progress zone to the underlying mesenchymal elements, which in turn affect the ectodermal structure. Chondrification of the ankle begins at horizon 18, the earliest in the sequence of the foot (Sarrafian and Kelikian, 2011). The ankle is the juncture of two modules, the zeugopodium and autopodium, with overlap of these two modules in this region. Differences between the forelimb and hind limb are produced by differential expression of *Hox Homeobox* genes with the existence of two separate modules producing major variations in the hind limb structure, both in extant and fossil taxa, and explaining "the mosaic nature of traits" in hind limb evolution (Cachel, 2006).

Once pattern formation occurs in the embryo, "semi autonomous regions" form, and for the hind limb, a limb field is established. Signals from defined centers pattern the field with specific chain expression results in positional information. There is then "regulated differentiation of the limb structures" based on this positional information (Johnson and Tabin, 1997). In the ankle, chondrogenesis proceeds from a cartilage analog to proto cartilage to cartilage condensation based on differences in gene regulatory networks (Cole, 2011).

The synovial joint and articular cartilage formation is the result of "a distinct cohort of progenitor cells", and Koyama et al. (2008) observe that "these cells appear to pattern along specific limb symmetry axes and rely on local signaling tools" in joint formation (p. 62). They observe that "articular cartilage and other joint tissue are structurally and functionally different from shaft and growth-plate cartilage" (Koyama

108

et al., 2008, p. 70). Unlike shaft and growth-plate cartilage, which is eventually replaced, articular cartilage is composed of "phenotypical stable cells" that function throughout life (Koyama et al., 2008). However, they are "phenotypically malleable" both in their formation and long-term maintenance signaling pathways (Koyama et al., 2008). Unlike the epiphyseal growth plate of long bones, articular cartilage acts as a "surface growth plate" for underlying subchondral bone and is responsive to reorganization by "resorption and neoformation," which are critical to "functional engineering and repair of articular cartilage tissue" (Hunziker et al., 2007). Hunziker et al. observed that, during postnatal development, the articular "growth plate" provides lateral growth through horizontal replication of stem cells and cartilage tissue resorption and replacement by bone through vertical delivery of donator cells. Resorption of immature cartilage is complete in all zones except the superficial "stem cell" layer on the appositional surface (Hunziker et al., 2007).

The signaling observed in limb development involves *Hox, Ihh, Shh, Sox*, and microRNAs (mmiRNAs), with signaling influencing both cartilage and bone development (Boyle et al., 2003; Hornstein et al., 2005; Kmita et al., 2002; Koyama et al., 2007; Kronenberg, 2003; Nagy et al., 2011; Stefan and Slack, 2008). In the ankle joint, *Hox 11* genes have been shown to regulate articular surface organization, and TRAP (tartrate-resistant acid phosphatase) cells, vascular endothelial growth factor, and endostatin regulate articular cartilage and subchondral bone, while synovia joint formation is regulated by Indian Hedgehog (Ihh) (Koyama et al., 2007; Koyama et al., 2010; Stempel, 2011). The role of bone morphogenetic proteins (BMPs) has increasingly

become evident in signaling interaction during embryonic development, synovial joint development, cartilage development, bone phenotypic expression, and bone repair (Francis-West et al., 1999; Grgurevic et al., 2011; Guo and Wang, 2009; Kobayashi, et al., 2005; Kronenberg, 2003; Li et al., 2008; Paulson et al., 2011; Zhao, et al., 2002; Zoricic, et al., 2003). BMP signaling has also been identified in adult remodeling, regeneration and pathology (osteophyte formation), suggesting a potential mechanism at the cellular and subcellular level for the postnatal response of cartilage and subchondral bone to environmental stimuli (strain/hydrostatic pressure). The data on osteophyte formation in particular shows that BMP-7 was present in hypertrophic chondrocytes, osteoblasts and young osteocytes in bone-formation sites, BMP-3 in osteoblasts, BMP-6 in young osteophytes and bone matrix, and both BMP-3 and BMP-6 in the osteoclasts of bone-resorption sites (Zoricic et al., 2003). This is consistent with the hypothesis of Young and Badyaev (2007) that BMP-mediated skeletal adaptation may produce phenotypic plasticity in skeletal development.

Examination of the evolutionarily stable configuration, the talo-crural joint, has demonstrated an epigenetic signal of behavior in the form of individual taxa substrate use. This signal was first manifest in studies of the tibia in which the percent variance attributable to the factors studied revealed that robusticity (51.5%), mass (30.3%) and superfamily (18.2%) predominated, with substrate preference accounting for only 10.6% (Turley et al., 2011). However, angular differences between the vectors showed that robusticity, mass and superfamily were strongly related while substrate preference was extremely weakly correlated with the others: robusticity 74.2°, mass 80.2°, and

superfamily 79.8°, respectively. When the distal tibial subsets were examined they showed an increase in percent variance associated with substrate preference over the other factors, but continued to demonstrate an extremely weak correlation between substrate preference and all three of the other factors studied, most notably, superfamily at 88° in the distal tibia. These findings suggested that a relationship of shape to substrate preference in the talo-crural joint might be observed.

In this dissertation the talar structure (Chapter II), appositional articular morphology of the tibial and talar joint surfaces in the adult (Chapter III), and the ontogeny of that appositional articular morphology were explored (Chapter IV). In Chapter II the whole talar subset revealed an influence of both superfamily and substrate preference; however, the proximal facets showed the influence of substrate preference only weakly related to the other factors studied. Examination of the appositional articular morphology of the adult showed that differences in articular shape reflected substrate use, both in the first and second Singular Warp, the former terrestrial or terrestrial-type activity, and the later vertical climbing in *Gorilla* and the *Pan* species. In the ontogenetic series at M3 a signal of divergent and convergent evolution was identified in the Singular Warp analysis. *Pan paniscus* and *Pan troglodytes* appear to have diverged in talo-crural morphology, with the former demonstrating morphology more consistent with arboreality and the latter terrestriality. A similar divergence in talo-crural morphology can be observed in the genus *Macaca* with *Macaca thibetana*, a terrestrial taxon quite divergent from the more arboreal *Macaca mulatta* and *Macaca fascicularis*. Evidence for convergent evolution was found between the terrestrial cercopithecoid taxa *Papio*

111

hamadryas and *Macaca thibetana* and the hominoids *Homo*, *Gorilla* spp., *Pongo* spp., and *Pan troglodytes.* These terrestrial cercopithecoids differed in the total and subset analysis from the remaining cercopithecoids, Hylobatidae, and *Pan paniscus*.

The study of appositional articular morphology in the ontogenetic series, which used molar eruption to compare taxa-relative development, demonstrated an epigenetic signal in the adults reflecting substrate use. In subadults, changes in African hominoid articular shapes from M1 to M2 suggested a possible genetic signal, but further study will be necessary to separate it from a signal of developmental plasticity. The morphology of M1 and M2 stage means in the other taxa suggests a common genetic developmental signal with evidence of immaturity of bone shape in the younger specimens. Finally, the implications of the epigenetic signal in the adult cohort have an impact on the interpretation of articular shape in the evaluation of the fossil record and its usefulness in phylogenetics. In this dissertation, substrate use altered talo-crural joint shape in the adult, reflecting both behavior and joint dynamics. Since, due to taphonomy, most known catarrhine fossils are from M3 aged individuals, these factors alter the interpretation of the shapes observed. Conclusions drawn from the shape differences among adult taxa appear from the data to reflect substrate use, as well as phylogeny and the physical attributes to which they are commonly attributed, with substrate use a function of behavior.

Some of the questions that have arisen in these studies may be clarified by enlarging the sample, both in the number of specimens and taxa and the adult and subadult subsets. Subadult *Papio hamadryas*, *Macaca thibetana* and *Pongo* spp., in

112

specific, will clarify their appositional articular shape at M1 and M2. An expansion of the diversity of the sample taxa to include small terrestrial and arboreal monkeys and the inclusion of large-bodied taxa, such as *Semnopithecus entellus, Lophocebus albinega* and *Theropithecus gelada*, would increase the scope of the study. Information would be garnered by the addition of wild *Macaca mulatta* from Asia, comparative captive and wild specimens of multiple species, and specimens of *Macaca fuscata* both wild, free-walking prior to training, during trained ambulation, and in retirement. These would present insights into the effects of changes in the nature of the habitat in the former two, and the potential for reversibility of the changes observed in the latter. Finally, magnetic resonance imaging of ankle joints would provide information concerning cartilage shape at M1, M2, and M3 in representative taxa. The problem of comparison of cercopithecoids and hominoids due to heterochrony may be addressed by separating these two groups and examining the relative MRI data. Likewise, improved life history data concerning dental eruption timing, joint calcification and substrate use, including the implementation of "developmental milestones" among studied taxa, as have been described elegantly in multiple studies but not codified in the primatology literature, would greatly improve the study (Breuer et al., 2009; Hutchinson and Fletcher, 2010; Inouye, 1994; Leigh and Shea, 1995; Remis, 1995; Robbins et al., 2004; Ross, 1998; Wells and Turnquist, 2001).

Within the theoretical framework of evolutionary developmental theory the talo-crural joint has been demonstrated to be a highly canalized, integrated, modulated, evolutionarily stable configuration responsive to epigenetic signals. The findings of this dissertation may be due to responsive systems present in deep homology, such as bone

morphogenetic proteins, and may, through cis-regulatory elements during development,

predispose to a greater response to epigenetic influences seen in developmental plasticity

(Beldade et al., 2011; Prud'homme et al., 2007; Shubin et al., 2009). The study suggests

the theoretical potential for change in character traits and the possible origin of

homoplasy and rapid divergence in the context of an altered relation to the environment.

REFERENCES CITED

Aiello L, Dean C. 2002. An Introduction to Human Evolutionary Anatomy. New York: Elsevier Academic Press.

Anapol F, German RZ, Jablonski NG. 2004. Shaping Primate Evolution. Cambridge: Cambridge University Press.

Auger F, Jamison PL, Balslev-Jorgensen J, Lewin T, De Pena JF, Skrobak-Kaczynski J. 1980. Anthropometry of Circumpolar Populations. In: Milan FA, editor. The Human Biology of Circumpolar Populations. Cambridge: Cambridge University Press. p 213-255.

Baab KL, McNulty KP, Rohlf J. 2012. The shape of human evolution: a geometric morphometrics perspective. Evol Anth 21:151-165.

Baker BJ. 2005. The Osteology of Infants and Children. College Station: Texas A&M Press.

Bardeen CR. 1905. Studies of the development of the human skeleton. Am J Anat 4:265.

Bastir M, Rosas A. 2005. Hierarchical nature of morphological integration and modularity in the human posterior face. Amer J Phys Anth 128:26-34.

Begun DR. 2007. How to identify (as opposed to define) a homoplasty: examples from fossil and living great apes. J Hum Evol 52:559-572.

Beldade P, Mateus ARA, Keller RA. 2011. Evolution and molecular mechanisms of adaptive developmental plasticity. Mol Ecol 20:1347-1363.

Blomquist GE. 2009. Brief communication: methods of sequence heterochrony for describing modular developmental changes in human evolution. Am J Phys Anthropol 138:231-238.

Bock WJ, von Wahlert G. 1965. Adaptation and the Form-Function Complex. Evolution 19:269-299.

Bolter DR, Zihlman AL. 2011. Brief communication: dental development timing in captive Pan paniscus with comparisons to Pan troglodytes. Amer J Phys Anth 145:647-652.

Bookstein FL. 1991. Morphometric Tools for Landmark Data. Cambridge: Cambridge University Press.

Bookstein FL. 1996a. Landmark methods for forms without landmarks: morphometrics of group differences in outline shape. Med Image Anal 1(3):225-243.

Bookstein FL. 1996b. Standard formula for the uniform shape component in landmark data. In: Marcus LF, Corti M, Loy A, Naylor GJP, Slice DE, editors. Advances in Morphometrics. New York: Plenum Press. p 153-169.

Bookstein FL, Gunz P, Mitteroecker P, Prossinger H, Schaefer K, Horst S. 2003. Cranial integration in Homo: singular warps analysis of the midsagittal plane in ontogeny and evolution. J Hum Evol 44:167-187.

Bookstein FL, Slice DE, Gunz P, Mitteroecker P. 2004. Anthropology takes control of morphometrics. Coll Anthropol 28 (Supplement) 2:121-132.

Boyle WJ, Simonet WS, Lacey DL. 2003. Osteoclast differentiation and activation. Nature 423:337-342.

Breuer T, Hockemba MB, Olejniczak C, Parnell RJ, Stokes EJ. 2009. Physical maturation, life history classes and age estimates of free-ranging Western gorillas—insights from Mbeli Bai, Republic of Congo. Amer J Primatol 71:106-119.

Cachel S. 2006. Primate and Human Evolution. Cambridge: Cambridge University Press.

Callebaut W, Rasskin-Gutman D. 2005. Modularity. Boston: MIT Press.

Campbell CJ. 2007. Primates in Perspective. Oxford: Oxford University Press.

Carroll SB. 2008. Evo-devo and the expanding evolutionary synthesis: a genetic theory of morphological evolution. CELL 134(1):25-36.

Chiang C, Litingtung Y, Harris MP, Simandl BK, Li Y, Beachy PA, Fallon JF. 2001. Limb manifestation of limb prepattern: limb development in the absence of sonic hedgehog function. Dev Biol 236:421-435.

Chiu C, Hamrick MW. 2002. Evolution and development of the primate limb skeleton. Evol Anthropol 11:94-107.

Clarke RJ, Tobias PV. 1995. Sterkfontein Member 2 foot bones of the oldest South African hominid. Science 269:521-524.

Cobb SN, O'Higgins P. 2004. Hominins do not share a common postnatal facial ontogenetic shape trajectory. J Exp Zool B Mol Dev Evol 302B:302-321.

Cole AG. 2011. A review of diversity in the evolution and development of cartilage: the search for the origin of the chondrocyte. Euro Cell Mat 21:122-129.

Conroy GC. 2005. Reconstructing Human Origins, 2nd ed. New York: W. W. Norton.

Davidson EH. 2005. The Regulatory Genome: Gene Regulatory Networks in Developmental and Evolution. Oxford: Academic Press.

Davidson EH. 2006. The Regulatory Genome. Oxford: Academic Press.

Davies AG, Oates JF. 1994. Colobine Monkeys. Cambridge: Cambridge University Press.

Day, MH, Wood, JR. 1968. Functional affinities of the Olduvai hominid 8 talus. Man 3:440-455.

Dean MC, Wood BA. 1981. Developing pongid dentition and its use for aging individual crania in comparative cross-sectional growth series. Folia Primatol 36:111-127.

Delson E, Terranova CJ, Jungers WL, Sargis EJ, Jablonski NG, Dechow PC. 2000a. Body mass in Cercopithecidae (primates, mammalia): estimation and scaling in extinct and extant taxa. Anthropol Pap Am Mus Nat Hist 83:1-159.

Delson E, Tattersall I, Van Couvering JA, Brooks AS. 2000b. Encyclopedia of Human Evolution and Prehistory. New York: Garland.

DeSilva JM. 2009. Functional morphology of the ankle and the likelihood of climbing in early hominins. Proc Nat Acad Sci 106: 6567-6572.

Dirks W, Bowman JE. 2007. Life history theory and dental development in four species of catarrhine primates. J Hum Evol 53:309-320.

Dobbs MB, Gurnett CA, Pierce B, Exner GU, Robarge J, Morcuede JA, Cole WG, Templeton PA, Foster B, Bowcock AM. 2006. HOXD10 M319K mutation in a family with isolated congenital vertical Talus. J Orthoped Res 24(3):448-453.

Doran DM. 1992. The ontogeny of chimpanzee and pygmy chimpanzee locomotor behavior: a case study of paedomorphism and its behavioral correlates. J Hum Evol 23:139-157.

Doran DM. 1993. Comparative locomotor behavior of chimpanzees and bonobos: the influence of morphology on locomotion. Amer J Phys Anth 91:83-98.

Doran DM. 1997a. Influence of seasonality on activity patterns, feeding behavior, ranging, and group patterns in Tai chimpanzees. Int J Prim 18:183-206.

Doran DM. 1997b. Ontogeny of locomotion in mountain gorillas and chimpanzees. J Hum Evol 32:323-344.

Dryden IL, Mardia KV. 1998. Statistical Shape Analysis. New York: John Wiley.

Ehrlich PJ, Lanyon LE. 2002. Mechanical strain and bone cell function: a review. Osteopros Int 13:688-700.

Elftman HO, Manter JT. 1935. The evolution of the human foot with special reference to the joints. J Anat 70:50-67.

Fleagle JG. 1999. Primate Adaptation and Evolution. San Diego: Academic Press.

Francis-West PH, Parish J, Lee K, Archer CW. 1999. BMP/GDF-signalling interactions during synovial joint development. Cell Tissue Res 296:111-119.

Frelat MA, Mitteroecker P. 2011. Postnatal ontogeny of tibia and femur form in two human populations: a multivariate morphometric analysis. Amer J Hum Biol 23:796-804.

Frost HM. 1999. Joint anatomy, design, and arthroses: insights of the Utah paradigm. Anat Rec 255:162-174.

Frost SR, Marcus LF, Bookstein FL, Reddy DP, Delson E. 2003. Cranial allometry, phylogeography, and systematics of large-bodied papionins (primates: Cercopithecinae) inferred from morphometric analysis of landmark data. Anat Rec Part A 275A:1048-1072.

Gebo DL. 1992. Plantigrady and foot adaptation in African apes: implications for hominid origins. Am J Phys Anthropol 89:29-58.

Gebo DL, Sargis EJ. 1994. Terrestrial adaptations in the postcranial skeletons of guenons. Am J Phys Anthropol 93:341-371.

Gebo DL, Schwartz GT. 2006. Foot bones from Omo: implications for hominid evolution. Am J Phys Anthropol 129:499-511.

Gilbert SF. 2000. Developmental Biology. Sunderland, MA: Sinauer Associates.

Gissis SB, Jablonka E. 2011. Transformations of Lamarckism: From Subtle Fluids to Molecular Biology. Cambridge: MIT Press.

Godfrey LR, Samonds KE, Jungers WL, Sutherland MR. 2001. Teeth, brains, and primate life histories. Amer J Phys Anth 114:192-214.

Goldstein SJ, Richard AF. 1989. Ecology of the rhesus macaques (Macaca mulatta) in northeast Pakistan. Int J Prim 10:531-567.

Good P. 2000. Permutation Tests: A Practical Guide to Resampling Methods for Testing Hypothesis. New York: Springer.

Gould SJ. 2002. The Structure of Evolutionary Theory. Cambridge: The Belnap Press of Harvard University Press.

Gregory WK. 1916. Studies on the evolution of primates. Bull Am Mus Nat Hist 35:239-355.

Grgurevic L, Macek B, Mercep M, Jelic M, Smoljanovic T, Erjavec I, Dumic-Cule I, Promet S, Durdevic D, Vunk D, Lipar M, Stejskal M, Kufner V, Brkljacic J, Maticic D, Vukicevic S. 2011. Bone morphogenetic protein (BMP) 1-3 enhanced bone repair. Biochem Biophys Res Com 408:25-31.

Guo X, Wang X. 2009. Signaling cross-talk between TGF-β/BMP and other pathways. Cell Res 19:71-88.

Guy F, Brunet M, Schmittbuhl M, Viriot L. 2003. New approaches in hominoid taxonomy: morphometrics. Am J Phys Anthropol 121:198-218.

Hall BK. 1998. Evolutionary Developmental Biology. London, New York: Chapman & Hall.

Hall BK. 2003. Descent with modification: the unity underlying homology and homoplasy as seen through an analysis of development and evolution. Biol Rev 78:409-433.

Hall BK. 2005. Bones and Cartilage. New York: Elsevier Academic Press.

Hall BK. 2007. Homoplasy and homology: dichotomy or continuum? J Hum Evol 52:473-479.

Hall BK. 2012. Parallelism, deep homology, and evo-devo. Evol Dev 14:29-33.

Hall BK, Pearson RD, Müller GB. 2004. Environment, Development, and Evolution. Boston: MIT Press.

Hallgrimsson B, Hall BK. 2005. Variation. New York: Elsevier Academic Press.

Hallgrimsson B, Willmore K, Hall BK. 2002. Canalization, developmental stability and morphological integration in primate limbs. Yearb Phys Anthropol 45:131-158.

Hammond AS, Ning J, Ward CV, Ravosa MJ. 2010. Mammalian limb loading and chondral modeling during ontogeny. Anat Rec 293:658-670.

Hamrick, MW. 1996. Articular size and curvature as determinants of carpal joint mobility and stability in strepsirhine primates. J Morphol 230:113-127.

Hamrick MW. 1999a. A chondral modeling theory revisited. J Theo Biol 201:201-208.

Hamrick MW. 1999b. Development of epiphyseal structure and function in Dipelphis virginiana (Marsupiala, Dipelphidae). J Morph 239:283-296.

Harcourt-Smith WEH. 2002. Form and function in the hominoid tarsal skeletal structure. Ph.D. thesis, University College London, London.

Harcourt-Smith WEH, Aiello LC. 2004. Fossils, feet and the evolution of human bipedal locomotion. J Anat 204:403-416.

Harcourt-Smith WEH, Tallman M, Frost SR, Wiley DF, Roklf FJ, Delson E. 2008. Analysis of selected hominoid joint surfaces using laser scanning and geometric morphometrics: a preliminary report. In: Sargis EJ, Dagosto M, editors. Mammalian Evolutionary Morphology: A Tribute to Fredrick S. Szalay. Dordrecht: Springer. p 373-383.

Hartwig WC. 2002. The Primate Fossil Record. Cambridge: Cambridge University Press.

Harvati K, Frost SR. 2007. Dental eruption in fossil colobines and the evolution of primate life histories. Int J Primatol 28:705-728.

Hillson S. 1996. Dental Anthropology. Cambridge: Cambridge University Press.

Hornstein E, Mansfield JH, Yekta S, Hu JK, Harfe BD, McManus MT, Baskerville S, Bartel DP, Tabin CJ. 2005. The microRNA miR-196 acts upstream of Hoxb8 and Shh in limb development. Nature 7068:671-674.

Hunziker EB, Kapfinger E, Geiss J. 2007. The structural architecture of adult mammalian articular cartilage evolves by a synchronized process of tissue resorption and neoformation during postnatal development. Osteoarthritis Cartilage 15:403-413.

Hutchinson JE, Fletcher AW. 2010. Using behavior to determine immature life-stages in captive Western gorillas. Amer J Primatol 72:492-501.

Inouye SE. 1994. Ontogeny of knuckle-walking in African apes. J Hum Evol 26:459-485.

Jablonka E, Lamb MJ. 1995. Epigenetic Inheritance and Evolution. New York: Oxford University Press.

Jogahara YO, Natori M. 2012. Dental eruption sequence and eruption times in Erythrocebus patas. Primates 53:193-204.

Johnson RL, Tabin CJ. 1997. Molecular models for vertebrate limb development. Cell 90:979-990.

Jonsson K, Fredin HO, Cederlund CG. 1984. Width of the normal ankle joint. Acta Radiologica Diag 25:147-149.

Jungers WL. 1988. Relative joint size and hominoid locomotor adaptations with implications for the evolution of hominid bipedalism. J Hum Evol 17:247-265.

Kanamoto S, Ogihara N, Nakatsukasa M. 2011. Three-dimensional orientations of talar articular surfaces in humans and great apes. Primates 52:61-68.

Katzmarzyk PT, Leonard WR. 1998. Climatic Influences on human body size and proportions: ecological adaptations and secular trends. Am J Phys Anthropol 106:483-503.

Keith A. 1923. Man's posture: it's evolution and disorders. Brit Med J 1:451-454, 499-502, 545-548, 587-590, 624-626, 669-672.

Kelikian AS. 2011. Sarrafian's Anatomy of the Foot and Ankle. Philadelphia: Wolters Kluwer.

Kelley J, Schwartz GT. 2010. Dental development and life history in living African and Asian apes. PNAS 107(3):1035-1040.

Kendall DG. 1984. Shape manifolds, procrustean metrics and complex projective spaces. Bull Lond Math Soc 16:81-121.

Kidd RS, O'Higgins P, Oxnard CE. 1996. The OH-8 foot: a reappraisal of the functional morphology of the hindfoot utilizing a multivariate analysis. J Hum Evol 31:269-291.

King SL. 2004. Relative timing of ontogenetic events in primates. J Zool Lond 264:267-280.

Kliegman RM, Behrman RE, Jenson HB, Stanton BF. 2007. Nelson Textbook of Pediatrics, 18th ed. Philadelphia: Saunders Elsevier.

Klingenberg CP. 2008. Morphological integration and developmental modularity. Ann Rev Ecol Evol Syst 39:115-132.

Kmita M, Fraudeau N, Herault Y, Duboule D. 2002. Serial deletions and duplications suggest a mechanism for collinearity in Hoxd genes in limbs. Nature 420:145-150.

Kobayashi T, Lyons KM, McMahon AP, Kronenberg HM. 2005. BMP signaling stimulates cellular differentiation at multiple steps during cartilage development. PNAS 102(50):18023-18027.

Koyama E, Ochiai T, Roundtree RB, Kingsley DM, Enomoto-Iwamoto M, Iwamoto M, Pacifici M. 2007. Synovial joint formation during mouse limb skeletogenesis: roles of Indian hedgehog signaling. Ann NY Acad Sci 1116:100-112.

Koyama E, Shibukawa Y, Nagayama M, Sugito H, Young B, Yuasa T, Okabe T, Ochiai T, Kamiya N, Rountree RB, Kingsley DM, Iwamoto M, Enomoto-Iwamoto M, Pacifici M. 2008. A distinct cohort of progenitor cells participates in synovial joint and articular cartilage formation during mouse limb skeletogenesis. Dev Biol 316:62-73.

Koyama E, Yasuda T, Wellik DM, Pacifici M. 2010. Hox11 paralogous genes are required for formation of wrist and ankle joints and articular surface organization. Ann NY Acad Sci 1192:307-316.

Kraus B. 1961. The western Apache: some anthropometric observations. Amer J Phys Anthropol 19:227-236.

Kronenberg HM. 2003. Developmental regulation of the growth plate. Nature 423:332-336.

Langdon JH. 1985. Fossils and the origin of bipedalism. J Hum Evol 14:615-635.

Langdon JH. 1986. Functional Morphology of the Miocene Hominoid Foot. Basel; New York: Karger.

Latimer B, Ohman JC, Lovejoy CD. 1987. Talocrural joint in African hominoids: implications for Australopithecus afarensis. Am J Phys Anthropol 74:155-175.

Leigh SR, Shea BT. 1995. Ontogeny of the evolution of adult body size dimorphism in apes. Amer J Primato 36:37-60.

Lewis OJ. 1980. The joints of the evolving foot: part I, the ankle joint. J Anat 130:527-543.

Lewis OJ. 1983. The evolutionary emergence and refinement of the mammalian foot pattern of foot architecture. J Anat 137(1):21-45.

Lewis OJ. 1989. Functional Morphology of the Evolving Hand and Foot. New York: Oxford University Press.

Li Z, Hassan MQ, Volinia S, van Wijnen AJ, Stein JL, Croce CM, Lian JB, Stein GS. 2008. A microRNAs signature for a BMP2-induced osteoblasts lineage commitment program. PNAS 105:13906-13911.

Lieberman DE, Delvin MJ, Pearson OM. 2001. Articular area response to mechanical loading: effects of exercise, age, and skeletal location. Am J Phys Anthropol 116:266-277.

Lindberg DG. 1980. The Macaques. New York: Van Nostrand-Reinhold.

Lisowski FP. 1967. Angular growth changes and comparisons in the primate talus. Folia Prim 7:81-97.

Lisowski FP, Albrecht GH, Oxnard CE. 1974. The form of the talus in some higher primates: a multivariate study. Amer J Phys Anth 41:191-216.

Lisowski FP, Albrecht GH, Oxnard CE. 1976. African fossil tali: further multivariate morphometric studies. Amer J Phys Anth 45:5-18.

Logan BM. 2004. McMinn's Color Atlas of Foot and Ankle Anatomy. New York: Wiley.

Lovejoy CO, Cohen MJ, White TD. 2000. The evolution of mammalian morphology: a developmental perspective. In: O'Higgins PO, Cohn ML, editors. Development, Growth and Evolution. San Diego: Academic Press. p 41-55.

Lovejoy CO, Latimer B, Ashaw B, White TD. 2009. Combining prehension and propulsion: the foot of Ardipithecus ramidus. Science 326;72e1-72e8.

Lukacs JR. 2009. Markers of physiological stress in juvenile bonobos (Pan paniscus): are enamel hypoplasia, skeletal development and tooth size interrelated? Amer J Phys Anth 139:339-352.

Marcus LF. 1996. Advances in Morphometrics. New York: Plenum Press.

Mayr E. 2001. What Evolution Is. New York: Basic Books.

McGraw WS. 2007. Monkeys of the Tai Forest: An African Primate Community. Cambridge: Cambridge University Press.

McNulty KP. 2009. Computing singular warps from Procrustes aligned coordinates. J Hum Evol 57:191-194.

McNulty KP, Frost SR, Strait DS. 2006. Examining affinities of the Taung child by developmental simulation. J Hum Evol 51:274-296.

Mitteroecker P. 2009. The developmental basis of variational modularity: insights from quantitative genetics, morphometrics, and developmental biology. Evol Biol 36:377-385.

Mitteroecker P, Bookstein FL. 2007. The conceptual and statistical relationship between modularity and morphometric integration. Syst Biol 56(5):818-836.

Mitteroecker P, Bookstein FL. 2008. The evolutionary role of modularity and integration in the hominoid cranium. Evolution 62(4):943-958.

Mitteroecker P, Bookstein FL. 2009. The ontogenetic trajectory of the phenotypic covariance matrix, with examples from craniofacial shape in rats and humans. Evolution 63(3):727-737.

Mitteroecker P, Gunz P. 2009. Advances in geometric morphometrics. Evol Biol 36:235-247.

Mitteroecker P, Gunz P, Bernard M, Schaefer K, Bookstein FL. 2004. Comparison of cranial ontogenic trajectories among great apes and humans. J Hum Evol 46:679-698.

Morton DJ. 1922. Evolution of the Human Foot I. Amer J Phys Anth 5(4):305-336.

Morton DJ. 1924. Evolution of the Human Foot II. Amer J Phys Anth 7(1):1-52.

Morton DJ. 1935. The Human Foot. New York: Columbia University press.

Müller, GB. 2005. Evolutionary developmental biology. In: Wuketitis FW, Ayala FJ, editors. Handbook of Evolution. New York: Wiley-VCH. p 87-115.

Nagy A, Kenesi E, Rentsendorj O, Molnar A, Szenasi T, Sinko I, Zvara A, Oommen ST, Barta E, Puskas LG, Lefebvre V, Kiss I. 2011. Evolutionarily conserved, growth plate zone-specific regulation of the matrilin-1 promoter: L-Sox5/Sox6 and Nfi factors bound near TATA finely tune activation by Sox9. Mol Cell Biol 31:686-699.

Neff, NA, Marcus, LF. 1980. A Survey of Multivariate Methods for Systematics. New York: American Museum of Natural History.

O'Higgins P. 2000. The study of morphologic variation in the hominid fossil record: biology, landmarks and geometry. J Anat 197:103-120.

O'Higgins P. 2006. Morphologika. PaulO'higgins@hyms.ac.uk

O'Higgins P, Cohn MJ. 2000. Development, Growth and Evolution. New York: Academic Press.

O'Higgins P, Jones N. 1998. Facial growth in Cercocebus torquatus: an application of three-dimensional geometric morphometric techniques to the study of morphologic variation. J Anat 193:251-272.

O'Higgins P, Chadfield P, Jones N. 2001. Facial growth and the ontogeny of morphologic variation within and between the primates Cebus apella and Cerocebus torquatus. J Zool 254:337-357.

Oxnard CE. 1972. Some African fossil foot bones: a note on the interpolation of fossils into the matrix of extant species. Amer J Phys Anth 37:3-12.

Parr CH, Chatterjee HJ, Soligo C. 2011. Inter- and intra-specific scaling of articular surface areas in the hominoid talus. J of Anat 218:386-401.

Paulsen M, Legewie S, Eils R, Karaulanov E, Niehrs C. 2011. Negative feedback in the bone morphogenetic protein 4 (BMP4) synexpression group governs its dynamic signaling range and canalizes development. PNAS 108:10202-10207.

Pearson OM, Lieberman DE. 2004. The aging of Wolff's "Law": ontogeny and responses to mechanical loading in cortical bone. Yearb Phys Anthropol 47:63-99.

Pigliucci M. 2001. Characters and environment. In: Wagner GP, editor. The Character Concept in Evolutionary Biology. San Diego: Academic Press. p 363-388.

Poe S. 2004. A test for patterns of modularity in sequences of developmental events. Evolution 58:1852-1855.

Polly, DP. 2008. Adaptive zones and the pinniped ankle: a three-dimensional quantitative analysis of carnivoran tarsal evolution. In: Sargis EJ, Dagosto M, editors. Mammalian Evolutionary Morphology: A Tribute to Fredrick S. Szalay. Dordrecht: Springer. p 167-196.

Prud'homme B, Gompel N, Carroll SB. 2007. Emerging principles of regulatory evolution. PNAS 104:8605-8612.

Raff RA. 1996. The Shape of Life. Chicago: University of Chicago Press.

Rafferty KL, Ruff CB. 1994. Articular structure and function in Hylobates, Colobus, and Papio. Am J Phys Anthropol 94:395-408.

Ravosa MJ, Kunwar R, Stock SR, Stack MS. 2007. Pushing the limit: masticatory stress and adaptive plasticity in mammalian craniomandibular joints. J Exp Biol 210:628-641.

Reichard UH, Barelli C. 2008. Life history and reproductive strategies of Khao Yai Hylobates lar: implications for social evolution in apes. Int J Primatol 29:823-844.

Remis M. 1995. Effects of body size and social context on the arboreal activities of lowland gorillas in the Central African Republic. Amer J Phys Anth 97:413-433.

Retallack GJ. 2001. Soils of the Past. Malden, MA: Blackwell Science.

Retallack GJ. 2007. Paleosols. In: Henke W, Tatersall I, editors. Handbook of Paleoanthropology 1. Berlin: Springer. p 383-408.

Robbins MM, Bermejo M, Cipolletta C, Magliocca F, Parnell RJ, Stokes E. 2004. Social structure and life-history patterns in western gorillas (Gorilla gorilla gorilla). Amer J Primatol 64:145-159.

Rodman PS. 1979. Skeletal differentiation of Macaca fascicularis and Macaca nemestrina in relation to arboreal and terrestrial quadrapedalism. Amer J Phys Anth 51:51-62.

Rohlf FJ. 1999. NTSY Spc 2.2 Exeter Software. Online at www.exetersoftware.com

Rohlf FJ. 2006. A comment on phylogenetic correction. Evolution 60(7):1509-1515.

Rohlf FJ, Corti M. 2000. Use of two-block partial least-squares to study covariation of shape. Sys Biol 49(4):740-753.

Rohlf FJ, Slice D. 1990. Extensions of the Procrustes method for the optimal superposition of landmarks. Sys Zool 39:40-59.

Ross C. 1998. Primate life histories. Evol Anthropol 6:54-63.

Ruff C. 1988. Hindlimb articular surface allometry in Hominoidea and Macaca, with comparison to diaphyseal scaling. J Hum Evol 17:687-714.

Ruff CB. 2002. Long bone articular and diaphyseal structure in Old World monkeys and apes. I: Locomotor effects. Am J Phys Anthropol 119:305-342.

Sarmiento EE. 1988. Anatomy of the hominoid wrist joint: its evolutionary and functional implications. Int J Primatol 9:281-345.

Sarrafian SK, Kelikian AS. 2011. Development of the foot and ankle: osteology. In: Kelikian AS, editor. Sarrafian's Anatomy of the Ankle, 3rd ed. Philadelphia: Wolters Kluwer. p 3-119.

SAS. 2006. SAS 9.1. Cary, NC: SAS Institute.

Schaefer K, Bookstein FL. 2009. Does geometric morphometrics serve the needs of plasticity research. J Biosci 34(4):589-599.

Scheuer L. 2004. The Juvenile Skeleton. New York: Elsevier Academic Press.

Scheuer L, Black S. 2000. Developmental Juvenile Osteology. New York: Elsevier Academic Press.

Schultz AH. 1930. The skeleton of the trunk and limbs of higher primates. Hum Biol 2:303-438.

Schultz AH. 1935. Eruption and decay of the permanent teeth in primates. Amer J Phys Anth 19:489-581.

Schultz AH. 1960. Age changes in primates and their modification in man. In Tanner JM, editor. Human Growth. Oxford: Pergamon Press.

Schwenk K. 2001. Functional units and their evolution. In: Wagner GP, editor. The Character Concept in Evolutionary Biology. San Diego: Academic Press. p 165-198.

Shubin N, Tabin C, Carroll S. 2009. Deep homology and the origins of evolutionary novelty. Nature 457:818-823.

Singleton M. 2012. Postnatal cranial development in papionin primates: an alternative model for hominin evolutionary development. Evol Biol 39:499-520.

Singleton M, McNulty KP, Frost SR, Soderberg J, Guthrie EH. 2010. Bringing up baby: developmental simulation of the adult cranial morphology of Rungwecebus Kipunji. Anat Rec 293:388-401.

Slice DE. 1998. Morpheus et al. Ecology and Evolution. Stony Brook: State University of New York.

Smith BH. 1994. Sequence of emergence of the permanent teeth in Macaca, Pan, Homo, and Australopithecus: its evolutionary significance. Amer J Hum Biol 6:61-76.

Smith BH. 2000. "Schultz's rule" and the evolution of tooth emergence and replacement in primates and ungulates. In: Teaford MF, Smith MM, Ferguson MWJ, editors. Development, Function and Evolution of Teeth. Cambridge: Cambridge University Press. p 212-227.

Smith RJ, Jungers WL. 1997. Body mass in comparative primatology. J Hum Evol 32:523-559.

Smith TM, Smith BH, Reid DJ, Siedel H, Vigilant L, Hublin JJ, Boesch C. 2010. Dental development of the Tai forest chimpanzees revisited. J Hum Evol 58:363-373.

Sokal RR, Rohlf FJ. 1995. Biometry. San Francisco: W. H. Freeman.

Stefani G, Slack FJ. 2008. Small non-coding RNAs in animal development. Nature Reviews 9:219-230.

Stempel J, Fritsch H, Pfaller K, Blumer MJF. 2011. Development of articular cartilage and the metaphyseal growth plate: the localization of TRAP cells, VEGF, and endostatin. J Anat 218:608-618.

Strasser E. 1989. Form, Function and Allometry of the Cercopithecoid Foot. Thesis, the City University of New York.

Strasser E. 1992. Hindlimb proportions, allometry, and biomechanics in Old World monkeys (primates, Cercopithecidae). Am J Phys Anthropol 87(2):187-213.

Streeter GL. 1942. Developmental horizons in human embryos. Contrib Embryol Monograph 30(197).

Susman RL. 1984. The Pigmy Chimpanzee. New York: Plenum Press.

Swindler DR. 2002. Primate Dentition. Cambridge: Cambridge University Press.

Thompson DW. 1917. On Growth and Form. Cambridge: Cambridge University Press.

Thompson DW. 1942. On Growth and Form, 2nd ed. Cambridge: Cambridge University Press.

Thorpe SKS, Crompton RH. 2006. Orangutan positional behavior and the nature of arboreal locomotion in Hominoidea. Amer J Phys Anth 131:384-401.

Thorpe SKS, Holder RL, Crompton RH. 2007. Origin of human bipedalism as an adaptation for locomotion on flexible branches. Science 316:1328-1331.

True JR, Haag EC. 2001. Developmental system drift and flexibility in evolutionary trajectories. Evol Devel 3(2):109-119.

Turley K, Frost SR. in press. Shape and presentation of the catarrhine talus: a geometric morphometric analysis. Anat Rec.

Turley K, Henderson E, Frost S. 2009. Astragalus proximal facet shape: differences in articular morphology among closely related hominoid taxa. Am J Phys Anthropol (Supplement) 48:258.

Turley K, Henderson EH, Frost SR. 2008. Distal tibial shape and presentation reflect the type of substrate. Am J Phys Anthropol (Supplement) 46:210.

Turley K, Henderson EH, Frost SR. 2011. Geometric morphometric analysis of tibial shape and presentation among catarrhine taxa. Anat Rec 294:217-230.

Turley K, Midttveit E, Guthrie EH, Frost S. 2010. Astragalar shape: differences and similarities in articular morphology among diverse catarrhine taxa. Am J Phys Anthropol (Supplement) 50:231.

Vancata V. 1991. The roots of hominid bipedality. In: Coppens Y, Senut B, editors. Origine(s) de la Bipedie chez les Hominides. Paris: Cathiers de Paleoanthroplogie, Editions du CNRS. p 143-158.

Wagner GP. 2001. The Character Concept in Evolutionary Biology. New York: Academic Press.

Wagner GP, Schwenk K. 2000. Evolutionarily stable configurations: functional integration and the evolution of phenotypic stability. In: Hecht MK, MacIntyre RJ, Clegg MT, editors. Evolutionary Biology. New York: Plenum Press. p 155-217.

Walker AC, Pickford M. 1983. New postcranial fossils of Proconsul africanus and Proconsul nyanzae. In: Ciochon RL, Corruccini RS, editors. New Interpretations of Ape and Human Ancestry. New York: Plenum Press. p 325-351.

Watson JD, editor. 2005. Darwin: The Indelible Stamp. Philadelphia: Running Press Book Publishers.

Wells JP, Turnquist JE. 2001. Ontogeny of locomotion in Rhesus Macaques (Macaca mulatta): II. Postural and locomotor behavior and habitat use in a free-ranging colony. Amer J Phys Anth 115:80-94.

West-Eberhard MJ. 2003. Developmental Plasticity and Evolution. Oxford: Oxford University Press.

West-Eberhard MJ. 2005. Developmental plasticity and the origin of species differences. PNAS 102:6543-6549.

White FJ. 1992. Activity budgets, feeding behavior, and habitat use of pygmy chimpanzees in Lomako, Zaire. Amer J Prim 26:215-223.

White TD, Folkens PA. 2000. Human Osteology, 2nd ed. New York: Academic Press.

Whitehead PF, Jolly C. 2000. Old World Monkeys. Cambridge: Cambridge University Press.

Wiley DF. 2006. Landmark Editor. Davis: University of California.

Winkler LA. 1996. Appearance of ossification centers in the lower arm, wrist, lower leg, and ankle in immature orangutans and chimpanzees with an assessment of the relationship of ossification to dental development. Amer J Phys Anth 99:191-203.

Wood B, Aiello L, Wood C, Key C. 1998. A technique for establishing the identity of "isolated" fossil hominin limb bones. J Anat 193:61-72.

Wood-Jones F. 1929. Man's Place Among the Mammals. London: Longmans.

Wu Q, Chen Q. 2000. Mechanoregulation of chondrocyte proliferation, maturation, and hypertrophy: ion-channel dependent transduction of matrix deformation signals. Exp Cell Res 256:383-391.

Wunderlich RE, Jungers WL. 2009. Manual digital pressures during knuckle-walking in chimpanzees (Pan troglodytes). Amer J Phys Anthropol 139:394-403.

Wynarsky GT, Greenwald AE. 1983. Mathematical model of the human ankle joint. J Biomech 16:241-251.

Xing J, Witherspoon DJ, Ray DA, Batzer MA, Jorde LB. 2007. Mobile DNA elements in primate and human evolution. Yearb Phys Anthropol 50:2-19.

Young NM. 2008. A comparison of the ontogeny of shape variation in the anthropoid scapula: functional and phylogenetic signal. Am J Phys Anthropol 136:247-264.

Young NM, Hallgrimsson B. 2005. Serial homology and the evolution of mammalian limb covariation structure. Evolution 59:2691-2704.

Young RL, Badyaev AV. 2007. Evolution of ontogeny: linking epigenetic remodeling and genetic adaptation in skeletal structures. Integ Comp Biol 47:234-244.

Zakany J, Kmita M, Duboule D. 2004. A dual role for Hox genes in limb anterior-posterior asymmetry. Science 304(5677):1669-1672.

Zhao M, Harris SE, Horn D, Geng Z, Nishimura R, Mundy GR, Chen D. 2002. Bone morphogenetic protein receptor signaling is necessary for normal murine postnatal bone formation. J Cell Biol 157:1046-1060.

Zollikofer CPE, Ponce de Leon MS. 2005. Virtual Reconstructions. New York: Wiley.

Zoricic S, Maric I, Bobinac D, Vukicevic S. 2003. Expression of bone morphogenetic proteins and cartilage derived morphogenetic proteins during osteophyte formation in humans. J Anat 202:269-277.